

REVIEWER 1

General comments

The authors investigated snow Hg dynamics in the interior arctic tundra at Toolik, Alaska. They compared their results to a temperate snowpack in the Rocky Mountain, Colorado and conclude that photochemical Hg(0) losses from the snowpack in models should be adjusted and treated differently in arctic and temperate snowpacks. I think that this research provides some very interesting results and the manuscript is fairly well written. However, to my opinion, it lacks a thorough comparison to other studies performed in polar regions and a discussion on instrumental limitations. I think that the manuscript will be appropriate for publication in The Cryosphere after the authors address the major comments discussed below.

Major comments

The conclusion of the manuscript (see above) derives from two main observations. Firstly, low concentrations of Hgtot and Hgdiss were measured in surface snow. Secondly, the photochemical formation of Hg(0)gas in the snowpack was largely absent.

1. I am quite surprised by the very low Hgtot concentrations in surface snow samples reported in this study, especially during depletion events. This raises concern about the potential influence of drifting snow. While the authors admit that the Toolik snowpack is subject to significant drifts and changes in snowpack height, there is no discussion on potential consequences and uncertainties.

We added more discussions about that. See below for more details. However, since we did not observe Hg concentration trend in snowpacks with depths or differences between lake and tundra snowpacks, we largely focus our discussion on the importance of spatial redistribution on snowpack Hg pool sizes.

2. While I agree that the photochemical formation of Hg(0)gas in the snowpack is most likely low compared to a temperate snowpack, I would like to see a comparison to other studies performed in polar regions. To me, the Toolik snowpack is more similar to a polar than a temperate snowpack (e.g., given permanent darkness/sunlight periods).

We added additional comparisons and discussions with respect to other polar snowpack (see below).

However, we maintain our discussion and comparison to temperate snowpack as well to highlight the dramatic difference between temperate and arctic snowpacks.

3. Additionally, there is no discussion on instrumental/analytical uncertainties. I would for instance very much like to know how the results collected with the two Tekran instruments compare. I expect a 10-20 % difference and wonder if the conclusions remain valid taking that analytical uncertainty into account. I also wonder whether the upper inlet in the snowpack was too far from the surface in spring, explaining why the authors did not observe any photochemical production of Hg(0)gas in the upper layers.

Please note that the Tekran used for the snowpack tower had one inlet line in the atmosphere which allowed us to adjust the two Tekrans used in this study based on atmospheric measurements (see detailed comment below). So, the differences between atmospheric and snowpack Hg concentrations cannot be explained by instrument variability.

The uppermost inlet in snow was always ≤ 10 cm from the atmosphere (note that was the spacing between snow inlets). Also, the absolute inlet depth (from the top of the snowpack) is variable based on the snowpack height. We added a discussion point that a possible reason for not detecting Hg^0_{gas} production may be that if this process was limited to a few cm in the top snow, our measurements would have missed this. We also determined using a webcam and snowpack sticks that the upper snowpack inlet was on average 7 cm from the atmosphere during the Apr. 2016's AMDE, 5 cm in Mar. 2016, and 6 cm in Mar. 2015 (i.e., during for the three biggest AMDEs). Also, we added that when using the exactly same measurement system, detecting Hg^0_{gas} enhancements in temperate snowpack (Fain et al., 2013) apparently were not problematic using this system.

The following line by line comments should be useful to fully comprehend and address the major comments.

Line by line comments

Page 2, lines 21-22: "In the Arctic and Antarctic, Hg cycling also is affected by atmospheric Hg depletion events (AMDEs) which are observed primarily in the springtime along coastal locations (Dommergue et al., 2010; Schroeder et al., 1998; Steffen et al., 2008)." The authors should also cite Angot et al. (2016a), latest review paper about

mercury in polar regions which includes a discussion on the occurrence and frequency of AMDEs in recent years.

Thanks for this reference. We added it.

Page 2, line 28: Typo; McMurod should be McMurdo.

Done, thanks!

Page 4, lines 6-8: "Atmospheric air sampling was performed using the top snow tower air inlet (. . .), as well as on a nearby micrometeorological tower at a height of 3.6 m above ground." How do the results compare? Did you collect data with two different Tekran instruments? If so, it would be an easy way to answer the following comment.

We collected data from two different Tekran instruments. The first one was connected to the micrometeorological tower (data not used in this paper, but in Obrist et al., 2017) and the soil wells (used in this paper). The second one was connected to the snow tower (snowpack measurement by 0, 10, 20, 30, and 40-cm inlets, as well as atmospheric levels measured at the top inlet of the snowpack (110-cm above ground, hence always located in the atmosphere). For this study, we hence always compared the snow data to atmospheric data using the same Tekran analyzer. For further comparisons, we were also able to adjust atmospheric measurements of the Tekran connected to the snow tower with atmospheric gradients: (we found on average 7% of differences, which could be adjusted to eliminate this difference). We added some information in the text to clarify this on page 4 lines 14-19.

Page 4, lines 10-11: "Gaseous Hg(0) concentrations were measured using two Tekran 2537B analyzers, one for interstitial snow air measurements and the other shared for soil gas and atmospheric measurements." Did you check how the results from the two instruments compare? What is the associated uncertainty? According to several

studies, the analytical uncertainty is about 10-20 % (e.g., Slemr et al., 2015) and this should be taken into account when comparing data acquired with different instruments. See major comments.

See responses above.

Page 4, line 12: "Air sampling was alternated between different snowpack heights every 5 min so that a full sequence of air extraction from the snowpack (six inlet heights) was achieved every 30 minutes." If I understood correctly, you just collected one data point per inlet height. Could there be any significant sampling-induced snowpack ventilation influencing the results?

We apologize that there was a mistake in this description. We clarified that snow tower measurements were based on switching heights every 10-min corresponding to two individuals of 5-min measurements per inlet (to avoid Tekran trap bias), resulting in 1-hour measurements per full gradient. The reviewer raises an important point, that is if and to what degree the active sampling of air from the snowpack induces artificial ventilation and dilution of the natural gas profile. The dual inlet sampling at a given depth, the 90° rotation of inlets at adjacent depths, and the only intermittent sampling (10 min every 1 h) were all selected to minimize this effect. The higher resolution trace gas (CO₂, O₃) were used to assess this artifact. Concentration changes within the 10-min interval were relatively minor (<10–20%) which suggests that mostly air from within the vicinity of the inlets was sampled. We have thoroughly evaluated this in other previous descriptions of this snowpack air sampling approach and refer the reviewer to those publications for a more in depth assessment (Seok et al., 2009). Moreover, our continuous and automatic sampling (i.e., resulting in 24 full snowpack profiles each day when data coverage is complete), limits any systematic bias that would be introduced by ventilation.

Page 4, line 27: "The top 3 cm of the snowpack was collected in triplicate."

1. What was the approximate distance between the replicates? According to lines 3-5 on page 6, the Toolik snowpack is subject to significant drifts and changes in snowpack height. Did you take that into account when interpreting the transect data? See major comments.

The triplicate samples were collected within a distance of 5 m (we added this in the text). We do not focus our discussion on surface snow patterns (since there was no significant difference to snowpack-averaged data with the exception of active AMDEs periods), so we did not further evaluate/discuss how drifts in surface snow may affect results.

2. According to lines 30-31 on page 5, average data are shown as mean \pm standard deviation. Were the replicate surface snow samples pooled together for analysis, similarly to snowpit samples? If so, what does the standard deviation reported in Table S2 stand for?

Surface snow samples were analyzed separately. Surface snow SD is based on the triplicates (n=3) while snowpack SD is based on the two replicate pits (n=2). The two snowpack samples pooled together were collected from the same pit, but from different walls. We added this information in the Table S2 caption and clarified this in the methods (from page 4 line 25).

Page 5, lines 7-9: "The detection limits, determined as 3-times the standard deviation of blank samples, averaged 0.08 ng/L. For statistic purpose, values below the detection limit (DL) were included as 0.5xDL. Recoveries, determined by 5 ng/L standards analyzed every 10 samples, averaged between 93 and 107 %." If I understood correctly, the analytical uncertainty is of 7 % at 5 ng/L. Given that most of the concentrations you analyzed are < 1.0 ng/L, did you check what the analytical uncertainty at that concentration is? I expect it to be much higher (>50%). Additionally, is the analytical uncertainty the same for Hgtot and Hgdiss? I am asking because you say later (page 13, lines 1-2) that Hgtot concentrations were much more variable than Hgdiss concentrations.

This is an excellent point. We indeed determined analyzer performance using recoveries of 5 ng L⁻¹ samples every 10 samples, and report a recovery between 93 and 107% for these samples. We did not assess the stability of the analyzer specifically at concentrations <1.0 ng L⁻¹, and this could be more variable. However, it is unlikely that higher variability in Hgtot can be explained by this since concentrations are higher in Hgtot than Hgdiss.

Page 6, lines 24-25: "The transect between Toolik and the Arctic Ocean performed in March 2016 showed snowpack height ranging between 30 and 66 cm". How can you explain the difference? Could it be due to drifting snow? If so, how can you compare Hg concentrations at various depths and locations? See major comment.

We believe (and clarified) that such differences reflect a high degree of variability in snowpack distribution across the area, but our dataset is not dense enough (or frequent enough) to explain differences in depth across locations in this study. We state, however, that we observed that snow height is higher at Toolik (between 40 and 50 cm) compared to coastal sites (<30 cm). Secondly, we state that highest snow height was observed where the vegetation was composed of shrubs which may have facilitated snow accumulation.

We also focused our spatial discussion on pool size of Hg stored in the snowpack because a detailed comparison of depth patterns would require a frequent and detailed observations of snowpack drifts which is not possible in our study. We clarified this point.

Page 7, line 3: "compared to the literature from temperate snowpacks". It seems to me that your reference is the study by Fain et al. (2013) in Colorado. "compared to the literature from a temperate snowpack" would be more appropriate here. Additionally, while I understand why you compare your results to those obtained in the Rocky Mountain (same instrumental setup and so on), I would like to see a more thorough comparison to other studies performed in polar regions (e.g., Angot et al., 2016b; Steffen et al., 2014).

We perform a detailed comparison to Fain et al. (2013) because that study used the same instrumental setup. However, we added a sentence for comparing Hg⁰_{gas} data to other polar regions (see page 8, lines 3-7).

Page 7, lines 10-12: "The Hg(0)gas measurements consistently showed strong concentration gradients in the atmosphere-snowpack-soil continuum with highest concentrations in the atmosphere (on average, 1.18 and 1.09 ng/m³, respectively) and lowest concentrations in soils (mostly below the detection limits for both years, i.e., <0.05 ng/m³)."

1. Could you please add the standard deviations?

Done!

2. Is this gradient significant given the large error bars in the snowpack (see Fig. 4)?

We clarified that the high error bars shown in Fig. 4 are mainly due to the temporal variability. The gradient is well defined for each given measurement sequence (see Fig. 1 in Obrist et al., 2017).

3. It's just a detail, but I think that the detection limit for the Tekran 2537 is 0.10 ng/m³.

Thanks for this remark, indeed, it is $<0.10 \text{ ng m}^{-3}$ for the Tekran 2537. We corrected that.

Page 7, lines 23-25, referring to AMDEs: “During one of these periods shown in Figure S2, $\text{Hg(0)}_{\text{gas}}$ concentrations in the snowpack showed variable $\text{Hg(0)}_{\text{gas}}$ levels generally following $\text{Hg(0)}_{\text{gas}}$ concentration changes in the atmosphere above”.

1. What do you mean by “generally following”? Is there a correlation between concentrations in the atmosphere and upper layers of the snowpack?

Hg^0_{gas} concentration variations in the upper layers (as well as for deeper layers) are linked to the Hg^0_{gas} concentration variations in the atmosphere (due to the snowpack diffusivity). We clarify this point in the manuscript (page 8, lines 27-31).

2. Could you please add the following data on Figure S2?

a) O₃ in the atmosphere b) Snow height (is the inlet at 20 cm above the ground far from the surface?) c) Hg_{tot} in surface snow samples d) Hg(II) concentrations in the atmosphere (the data do exist according to Obrist et al. (2017)).

O₃ and Hg^{II} concentrations were added in the figure. The snow height was between 25 and 28 cm, i.e., 5 to 8 cm far from the surface (information added in the caption). Hg_{tot} concentrations in surface snow samples were $1.00 \pm 0.07 \text{ ng L}^{-1}$ for Mar. 25th and $1.46 \pm 0.16 \text{ ng L}^{-1}$ for Apr. 2nd (only concentrations that we have, available in Table S2).

3. How can you explain the peaks at 10 cm above the ground (e.g., daytime on Mar 28th, 29th and 30th)? Was the temperature in the snowpack or the sample line stable? Could it be Hg(II) released from the sample line and analyzed as Hg(0) ?

In general, we found similar diurnal patterns in the atmosphere as well as in all snowpack levels. We attribute such diurnal variability to differences in daytime and nighttime boundary layer mixing. However, we cannot specifically explain why inlet depth at 10 cm was more variable during this time. In general, atmospheric Hg^0_{gas} concentrations, which then also affect snowpack concentrations, are most variable during these periods of AMDEs.

4. According to table S2 you collected surface snow samples during the AMDE. I am very surprised by the very low concentration (1.46 ng/L). This is rather unusual during a depletion event. How does it compare to other studies (e.g., Steffen et al., 2014)? If we do a back of the envelope calculation based on Hg(0) and Hg(II) concentrations in the atmosphere, what should be the concentration in surface snow to have a coherent Hg budget? With 1.46 ng/L in surface snow and $\sim 0.4 \text{ ng/m}^3$ of Hg(II) according to Obrist et al. (2017), I have the feeling that there is Hg missing in the budget. If so, a) How reliable are the Hg(II) measurements? What is the analytical uncertainty? Is an underestimation of Hg(II) concentration conceivable? b) Since Toolik snowpack is subject to significant drifts and changes in snowpack height, are you 100 % sure that you collected surface snow samples? If you collected deeper layers due to drifting snow that could explain the unusually low concentrations during the depletion event.

Indeed, the concentrations are low compared to Steffen et al. (2014) data. We revised this discussion and now state that the coarse resolution of our snow sampling campaign during AMDEs is not sufficient to closely track the fate of Hg deposition and subsequent Hg reemissions during AMDEs. So, while we feel that the reviewer's points are excellent, we strongly think a mass balance approach is above what we are comfortable to address in this study with a very coarse snow sampling activities during AMDEs. However, if we were to perform a back-of the envelope mass balance, it would amount to the following: First, please note that during the weeks of the most intense AMDEs (last week of March and first week of April), we observed highly variable daily average atmospheric Hg^{II} concentrations, ranging between non-detectable levels to a daily average of 310 pg m^{-3} based on the dataset presented in Obrist et al. (2017) (Extended Data Figure 2). Hence, peak Hg^{II} concentrations of $\sim 400 \text{ pg m}^{-3}$ as the reviewer refers were only observed during very few hourly measurements and cannot be applied over long time. In fact, we estimated a total Hg^{II} deposition of between 0.8 and $2.8 \text{ } \mu\text{g m}^{-2} \text{ a}^{-1}$ (based on a deposition velocity of 1.5 cm s^{-1}), of which most of this occurred during periods of AMDEs. At the same time, measured Hg^0_{gas} fluxes (re-emissions) showed a similar magnitude of Hg^0_{gas} re-emissions, e.g., of $1.5 \text{ } \mu\text{g m}^{-2}$ in ~ 20 day during AMDEs (Figure 1 of Obrist et al., 2017). Hence, we believe in fact that re-emission of Hg^0_{gas} after AMDEs largely accounted for the estimated Hg^{II} deposition, a finding we support with stable Hg isotope measurements in Obrist et al. (2017).

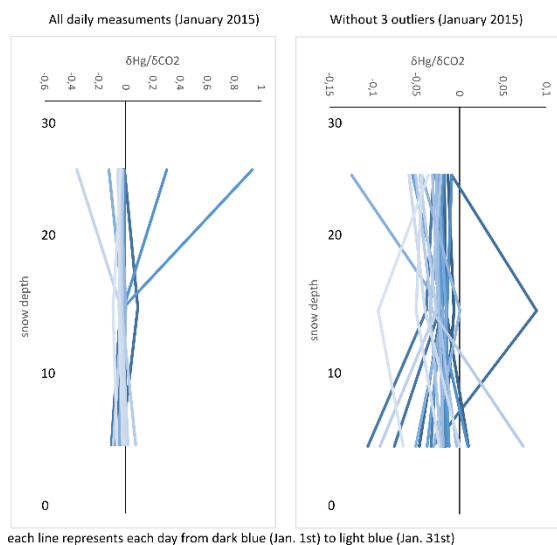
Now, looking at surface snow (3 cm, which has a water equivalent of 10 L m^{-2} considering a snow density of 0.3), an increase in snow Hg (difference of Hg_{diss} from 0.26 to $1.15 = 0.89 \text{ ng L}^{-1}$) would represent a very small input of only $\sim 9 \text{ ng m}^{-2}$ during the AMDEs. So, in fact, what would find that snow indeed only represent a very low amount of the potential Hg^{II} deposition and Hg^0_{gas} re-emission. It would be interesting to perform a high-resolution mass balance campaign to address this issue further during AMDEs.

Page 7, lines 32-34: “This pattern was consistent for two independent soil profiles measured at this site, one mainly representing an organic soil profile and one profile dominated by mineral soil horizons”. I do not understand this sentence. Was the experimentation carried out at two different locations with different soil composition? There is no mention of this in the Materials and Methods section.

We clarified that of our soil measurements, we had measurements in different soils types (present within 5 m), some were more organic soils a some were more mineral soils.

Page 8, lines 25-27: “Analysis of $\delta \text{Hg}/\delta \text{CO}_2$ ratios showed no statistically significant differences from the top to the bottom of the snowpack”. It seems like the authors used the mean concentration at each height to calculate the $\delta \text{Hg}/\delta \text{CO}_2$ ratios. Given the quite large error bars for $\text{Hg}(0)_{\text{gas}}$ in the snowpack (Fig. 4), it is not really surprising that such a calculation yields insignificant differences. On the contrary, Fain et al. (2013) calculated the ratio for each day. Did you try to do it this way?

Actually, the ratios presented in boxplots of the Fig. 4 were in fact calculated from daily Hg^0_{gas} and CO_2 measurements, as performed by Fain et al. (2013). See below the detail on the individual days. On the left panel, each dataline represents each day (from darker to lighter). On the right panel, the same plot without 3 outliers. No apparent trend was observed. What we have done in Fig. 4 was to apply boxplot for each snow height difference (0 to 10, 10 to 20, and 20 to 30 cm).



Page 9, lines 7-10: “No consistent temporal trends in Hg_{tot} or Hg_{diss} were observed with increasing duration of winter in both seasons, and no correlations were observed with air temperature (red line). One noticeable period of enhanced surface snow Hg concentrations was April 2016 when both Hg_{tot} and Hg_{diss} concentrations exceeded 1 ng/L .”

1. Is there an anti-correlation between Hg_{tot} and $\text{Hg}(0)$ in the atmosphere?

No, there is no anti-correlation between Hg_{tot} and Hg^0_{gas} , nor for Hg_{diss} and Hg^0_{gas} , during most of the time. One exception was during AMDE where we observed low Hg^0_{gas} and higher snow Hg concentrations.

2. See previous comments regarding the magnitude of the concentrations. How do a maximum of 1 ng/L compare with other studies performed in polar regions?

We indicated that snowpack $\text{Hg}_{\text{tot}}/\text{Hg}_{\text{diss}}$ measured in literature were between 0.14 and 820 ng L^{-1} . This range mostly includes Hg_{tot} concentrations (and so, potentially higher concentrations) when no filtration was applied. We state that our observed concentrations were in the lower part of the Arctic data set: the lowest values were observed in Greenland (Ferrari et al., 2004), in Canada for Hg_{tot} (St Louis et al., 2005), and in Alaska for Hg_{diss} (Douglas & Sturm, 2004).

Page 9, line 12: “Due to the low snow height on the frozen lake.” Why is the snow height lower on the frozen lake? Drifting snow?

We assume that both drifting snow and surface roughness (brush vs ice) are responsible to the difference of snow height, as already discussed page 11, from line 4.

Page 9, lines 15-16: “Measurements of Hgtot and Hgdiss across a large North slope transect (about 200 km) in March, 2016 showed concentrations of 0.70 μC^{-1} s 0.79 and 0.24 μC^{-1} s 0.20 ng/L, respectively.” Are you referring to surface snow or to average snowpack concentrations?

We referred here to average snowpack concentrations. Surface snow sampling was not performed for the transect. We clarified that.

Page 9, lines 16-19: “Concentrations of Hgdiss of the 5 northernmost stations were statistically significantly higher compared to those measured in the 4 stations located in the interior tundra which included the Toolik site where the mean Hgdiss concentrations were 0.33 and 0.11 ng/L for the same period, respectively”.

1. Please add the standard deviations (in the text and on Figure 7)

The standard deviations were added. The standard deviations of the Fig. 7, however, were not added since only a composite sample from both replicates of the same snow height was measured.

2. I would like to see a critical discussion of these results, notably in light of drifting snow issues and analytical uncertainty (50 % at such low concentrations?).

We discussed the influence of drifting snow in each part of the discussion (absence of vertical patter, absence of difference between the lake and tundra snowpacks...). Note that we reorganized the manuscript merging Results and Discussion.

Page 9, line 23: “similar to concentration of Hg”. Where is that discussed in the manuscript?

We clarified this sentence. Major cations and anions concentrations in snowpack were lower at Toolik compared to coastal locations, which we also observed for Hg as discussed in the previous section.

Page 11, lines 11-12: “Hg(0) concentration profiles in the arctic snowpack are inherently different to patterns observed in lower latitude snowpacks”. Now may be a good time to compare your results to other studies in polar regions (see comment page 7, line 3).

We added the comparison with other polar snowpacks, as discussed above.

Page 11, lines 23-25: “We speculate that a reason for the general lack of Hg(0)gas formation and volatilization in snow includes substrate limitation due to very low total snow Hg concentrations, several times lower compared to concentrations in temperate snowpacks.” While I agree that this is a possible explanation, I would like to see a more thorough discussion of other conceivable hypothesis, including instrumental limitations. A few ideas:

1. The comparison between your results and those by Fain et al. (2013) is based on data acquired in winter and early spring. I would expect Hg(0)gas formation and volatilization to start in spring, when the sun is back. What is the difference in UV load between Toolik and Colorado at that time of year? That could explain a lower photo-reduction in the upper layers of the snowpack at Toolik.

Indeed, the solar radiation is a little bit lower at Toolik. We clarified that solar radiation at Toolik was about 400 W m⁻² in Mar. and 600 W m⁻² in Apr. at Toolik versus ~700 W m⁻² in the end of Feb. in the Rocky Mountain (Fain et al., 2013). The solar radiation data were added in the text (page 8, lines 17-19). However, we do not believe this can explain the dramatically different behavior between these sites.

2. Atmospheric and snowpack Hg(0) concentrations were collected using two different Tekran instruments. Could a 10-20 % difference between the instruments explain why Hg(0)gas in surface snow is not higher than in ambient air (especially Figure 4c)?

See our comment above. In this study, we always compared snow and atmospheric measurements using the same Tekran instrument.

3. 85 % of photo-reduction occurs in the top two e-folding depths (King and Simpson, 2001). Fain et al. (2013) observed a diurnal cycle 0-60 cm below the surface. But the density/nature of the snowpack is most likely very different at Toolik.

a) You recorded the physical properties (e.g., density) of the snowpack. Could you compare your results to those obtained by Fain et al. (2013)? According to Durnford and Dastoor (2011), the range of chemically active depths may be explained by physical differences in the snowpacks.

b) The e-folding depth is about 5 cm at Alert (King and Simpson, 2001) while Poulain et al. (2004) reported that photo-reduction occurred in the first 3 cm of snow. I am worried that the upper inlet in the snowpack (the one at 40 cm above the ground, Fig. 4c) might be too far from the surface. This is more obvious on Fig. 3 if you compare the distance between the upper inlet and the surface in your case and in Fain et al. (2013).

We added the measurement depths of the surface snow inlet which was between 5 and 7 cm. We also discuss the possibility that our surface measurements may have missed Hg^0_{gas} production. However, at the same point, we point out that in Fain et al. (2013), we used the same measurement system and that Hg^0_{gas} concentration enhancements in that study were well measurable (with concentrations up to 8 ng m^{-3} and detectable to a depth of $>90 \text{ cm}$).

4. What about the occurrence of fresh snow at Toolik vs. Colorado? Fresh snow provides a new reservoir of photoreducible Hg(II) and highest surface snow Hg(0) levels are linked to the deposition of new snow (Faïn et al., 2013).

We performed plot as done in Fig. 5 in Faïn et al. (2013) but no relationships were observed.

Page 12, lines 1-2: “This illustrates that the Hg(0) gas uptake occurs in soils rather than in the snowpack.” The way the ratios are plotted, I am not sure I understand why you can conclude that uptake occurs in soils rather than in the snowpack.

We clarified the results as follows: the constant ratios and the fact that CO_2 is largely non-reactive in snowpack indicates that Hg^0_{gas} also was not subject to snowpack chemical reactions. The constant, and negative ratios, between CO_2 and Hg^0_{gas} ratios are hence indicative that both profiles are affected by underlying soil processes, i.e., soil sources for CO_2 and soil sinks (for H^0_{gas}).

Page 12, line 10-11: “which we attribute to higher variability in upper snowpack concentrations due to variable atmospheric Hg(0) gas levels”. Isn’t it in contradiction with error bars (Fig. 4 and 5)? I actually don’t understand why (Fig 5) a ratio based on highly variable concentrations (e.g., 0 cm) can be less variable than a ratio based on less variable concentrations (e.g., upper inlet). Am I missing something?

You are correct. we cannot only attribute the high variability to the Hg^0_{gas} atmospheric fluctuation. We think that the source of variability is due much lower concentration differences between 20 and 30 cm inlets for both CO_2 and Hg^0_{gas} which cause increases variabilities in ratios. We modified the text (page 10, lines 15-17).

Page 12, line 23: “relatively weak and infrequent AMDEs”. I quibble but the AMDE reported on Fig. S2 does not look weak to me. About the frequency, how many AMDEs did you observe? You can use a 1.00 ng/m^3 threshold to calculate the frequency of occurrence (Angot et al., 2016a; Cobbett et al., 2007; Steffen et al., 2005).

We changed this to infrequent and generally weaker AMDEs. We think it is important to note that the frequency and magnitude of AMDEs indeed is lower than those along the coast. While we see several occasions with air masses with Hg^0_{gas} levels below 1.0 ng m^{-3} (4 to 5 per year), it is very rare to find stronger depletions (e.g., one per year with concentrations $<0.5 \text{ ng m}^{-3}$). This is dramatically different to studies along the coast where Hg^0_{gas} frequently drops below detection for pronounced time periods.

Page 12, line 31-32: “Total Hg concentrations in all snow samples collected were always much higher than Hg_{diss} levels”. Can we really say that concentrations are “much higher” given the range observed (0-1 ng/L)? By the way, I don’t see anywhere Hg_{tot} concentrations from the transect.

Done, we removed “much”.

Page 13, line 10: “(. . .) and few studies include inland sites such as Toolik”. What is the range of concentrations at these inland sites? Which studies are you referring to?

We clarified that in Douglas & Sturm (2004), snowpack Hg_{diss} concentrations were between 0.5 and 1.7 ng L^{-1} for the interior sites. While our values are even lower, they are not that different from Douglas and Sturm (2004).

Page 14, line 27: “Fresh surface snow”. There is no mention of the fact that you collected fresh surface snow in the Materials and Methods Section.

We removed “fresh” and only keep “surface” (i.e., top 3 cm).

Figure 2: Why don't you report the standard deviation for each green bar?

The absence of standard deviation may be due to either narrow differences between the two replicates (i.e., two snow pits), or different snowpack height between the two snow pits (top measurements of Jan. 2015 and Mar. 2016 for example, illustrating the spatial heterogeneity). See Table S2 for more detail about standard deviation values.

Figure 4: What does “soil: organic/mineral” refer to?

This information is now added in the site description in ‘Materials and methods’ (page 4, lines 8-9).

Figure 7: Please add standard deviations.

As described above, the two samplings were pooled together to constitute a composite sample. Only one sample was analyzed per layer and per site.

Figure 8: I really like this Figure but aren't the various concentrations (<DL, 0.25, 0.50) in the range of the analytical uncertainty?

No, values of 0.25 ng L⁻¹ and 0.5 ng L⁻¹ are significantly above the detection limit of our method (i.e., above 3 × standard deviation of blank samples).

Figure 9: The colors are really difficult to read. Can you use something else than shades of blue? Maybe a gradient from blue to red.

Done

References

- Douglas, T. A. and Sturm, M.: Arctic haze, mercury and the chemical composition of snow across northwestern Alaska, *Atmos. Environ.*, 38(6), 805–820, doi:10.1016/j.atmosenv.2003.10.042, 2004.
- Faïn, X., Helmig, D., Hueber, J., Obrist, D. and Williams, M. W.: Mercury dynamics in the Rocky Mountain, Colorado, snowpack, *Biogeosciences*, 10(6), 3793–3807, doi:10.5194/bg-10-3793-2013, 2013.
- Ferrari, C. P., Dommergue, A., Boutron, C. F., Jitaru, P. and Adams, F. C.: Profiles of mercury in the snow pack at Station Nord, Greenland shortly after polar sunrise, *Geophys. Res. Lett.*, 31(3), L03401, doi:10.1029/2003GL018961, 2004.
- Obrist, D., Agnan, Y., Jiskra, M., Olson, C. L., Colegrove, D. P., Hueber, J., Moore, C. W., Sonke, J. E. and Helmig, D.: Tundra uptake of atmospheric elemental mercury drives Arctic mercury pollution, *Nature*, 547(7662), 201–204, doi:10.1038/nature22997, 2017.
- Seok, B., Helmig, D., Williams, M. W., Liptzin, D., Chowanski, K. and Hueber, J.: An automated system for continuous measurements of trace gas fluxes through snow: an evaluation of the gas diffusion method at a subalpine forest site, Niwot Ridge, Colorado, *Biogeochemistry*, 95(1), 95–113, doi:10.1007/s10533-009-9302-3, 2009.
- St. Louis, V. L., Sharp, M. J., Steffen, A., May, A., Barker, J., Kirk, J. L., Kelly, D. J. A., Arnott, S. E., Keatley, B. and Smol, J. P.: Some sources and sinks of monomethyl and inorganic mercury on Ellesmere Island in the Canadian high Arctic, *Environ. Sci. Technol.*, 39(8), 2686–2701, doi:10.1021/es049326o, 2005.

REVIEWER 2

General comments

The manuscript describes a detailed study of Hg in air, snow and soil at an Arctic site, which unlike almost all previous studies is a significant distance from the coast. Given that vast amounts of tundra are inland this study begins to fill in some of the gaps in our knowledge of Hg cycling in these remote regions. Of particular interest are the differences seen between the processes seen at this site when compared to coastal sites. The fact that tundra soils are a sink for atmospheric elemental Hg has important repercussions for future multimedia modelling studies and hints at the potential remobilization of large amounts of Hg from Arctic soils in a warming climate. This should be emphasised more in the Abstract and the Conclusions, in the Abstract particularly the comment on this is brief and hidden in the middle.

Thank you for your comment. We agree with you that the fact that Arctic tundra soils constitute a sink of Hg⁰_{gas} is an interesting finding for the global understanding of Arctic Hg cycling. This is, however, not the

focus of this paper since we already published that in a previous study (Obrist et al., 2017). We slightly edited both the abstract and conclusion in order to highlight and clarify this point.

The manuscript is however rather long-winded. I think that both the Results and the Discussion section could be shortened significantly, and quite usefully (from the reader's point of view) combined. Just as an example, the discussion of the major ions and the O and H isotope signatures, repeats parts of the pertinent results section. Conversely the results section rather leaves the reader with a sense of 'and what do these results imply?', which is only answered six pages later. I would recommend combining these sections as it will most likely lead naturally to a more concise and less prolix article. If some of the detail in the methods section has already been published perhaps it could be shortened by including more references, if not maybe some of the detail could be moved to the Supplementary material.

We reorganized the manuscript by merging Results and Discussions.

The previous reviewer has comprehensively addressed a number of technical issues, and for me only a few real problems remain.

1. The issue of blowing snow, and where the snow that is being sampled at Toolik comes from.

Indeed, the entire snowpack is subject to important movements that generate uncertainties mentioned by the first reviewer and limiting the observation of trend in the snowpacks. We mention this in regard to vertical Hg concentration patterns, in response to the comments of reviewer 1.

2. The fact that the paper is interesting and adds an important contribution to polar Hg research but is unfortunately not very well presented and at times rather heavy going.

We hope that the key messages are now better presented in this reorganized manuscript version.

3. The importance of atmospheric elemental Hg effectively being sequestered (for the moment) by tundra soils, is not emphasised sufficiently from my point of view.

We previously mentioned the influence of tundra soil in Arctic Hg cycling in Obrist et al., 2017 and highlighted this in the abstract and conclusions.

Mercury in the Arctic tundra snowpack: temporal and spatial concentration patterns and trace-gas exchanges

Yannick Agnan^{1,2}, Thomas A. Douglas³, Detlev Helmig⁴, Jacques Hueber⁴, Daniel Obrist^{5,2}

¹Sorbonne Université, CNRS, EPHE, UMR Metis, F-75252, Paris, France

²Division of Atmospheric Sciences, Desert Research Institute, Reno, Nevada 89523, USA

³US Army Cold Regions Research and Engineering Laboratory, PO Box 35170, Fort Wainwright, Alaska 99709, USA

⁴Institute of Arctic and Alpine Research, University of Colorado, Boulder, Colorado 80309, USA

⁵Department of Environmental, Earth, and Atmospheric Sciences, University of Massachusetts, Lowell, MA 01854, USA

Correspondence to: Yannick Agnan (yannick.agnan@biogeochimie.fr) and Daniel Obrist (daniel_obrist@uml.edu)

Abstract. In the Arctic, the snowpack forms the major interface between atmospheric and terrestrial cycling of mercury (Hg), a global pollutant. We investigated Hg dynamics in an interior arctic tundra snowpack in northern Alaska during two snow seasons. Using a snow tower system to monitor Hg trace gas exchange, we observed consistent concentration declines of gaseous elemental Hg (Hg^0_{gas}) from the atmosphere to the snowpack to soils. The snowpack itself was unlikely a direct sink for atmospheric Hg^0_{gas} . In addition, there was no evidence of photochemical reduction of Hg^{II} to Hg^0_{gas} in the tundra snowpack, with the exception of short periods during late winter in the uppermost snow layer. The patterns in this interior arctic snowpack hence differ substantially from observations in arctic coastal and temperate snowpacks. We consistently measured low concentrations of both total and dissolved Hg in snowpack throughout the two seasons. Chemical tracers showed that Hg was mainly associated with local mineral dust and regional marine sea spray inputs. Mass balance calculations show that the snowpack represents a small reservoir of Hg, resulting in low inputs during snowmelt. Taken together, the results from this study suggest that interior arctic snowpacks are negligible sources of Hg in the Arctic.

1 Introduction

Mercury (Hg) is a neurotoxic pollutant of worldwide importance that is transported over long distances in the atmosphere as gaseous elemental Hg (Hg^0_{gas}), and thus reaches remote environments (Cobbett et al., 2007; Driscoll et al., 2013; Sprovieri et al., 2010). In the Arctic, modern atmospheric Hg deposition has increased about three-fold from pre-industrialized background levels (Fitzgerald et al., 2005), similar to increases observed in temperate locations, although other studies suggest much stronger increases (e.g., Enrico et al., 2017). The increase in Hg loading has led to vulnerability of polar ecosystems to Hg contamination due to detrimental impacts to wildlife and humans, in particular through biomagnification processes across trophic levels (Atwell et al., 1998).

Representing about 26% of the global land surface area, polar regions are unique environments with specific physical, chemical, and biological processes affecting pollutant cycles including that of Hg (Douglas et al., 2012). In particular, most of

the northern latitudes are covered by a laterally continuous snowpack during long periods of the year. In the Alaskan tundra, the surface snow cover is present about two thirds of the year (Cherry et al., 2014). The snowpack hence forms a critical interface between the arctic atmosphere, tundra ecosystems, and underlying tundra soils. Trace gas exchanges between the atmosphere and the tundra are modulated by sinks and sources below and within snowpack, by snow diffusivity, snow height, and snow porosity (Dominé and Shepson, 2002; Lalonde et al., 2002; Monson et al., 2006). The snowpack accumulates nutrients, pollutants, and impurities that are deposited by snowfall and dry deposition processes, all of which can subsequently be transported to underlying ecosystems during snowmelt (Bergin et al., 1995; Uematsu et al., 2000).

The snowpack plays an important role for the cycling of Hg as well, including for atmospheric deposition, photochemical redox reactions, and associated phase changes between solid and gaseous Hg that can volatilize Hg to the atmosphere (Douglas et al., 2008, 2012; Faïn et al., 2013; Mann et al., 2014; Steffen et al., 2013). In particular, temperate and arctic studies have shown that the snowpack can serve as sink or source of Hg^0_{gas} , whereby photochemical reduction of snow-bound Hg^{II} can produce Hg^0_{gas} , and oxidation processes can reversely scavenge atmospheric Hg^0_{gas} in snow (Faïn et al., 2013; Lalonde et al., 2002; Mann et al., 2011). Photochemical reactions occur primarily in the top 10 cm of the snowpack, where sunlight radiation transmits and is absorbed and scattered by snow crystals (Faïn et al., 2007; King and Simpson, 2001). The degree of photochemical production of Hg^0_{gas} and subsequent atmospheric re-volatilization from the snowpack can be significant, as shown in temperate snowpacks with strong recurring daytime atmospheric emissions of Hg^0_{gas} throughout the winter season (Faïn et al., 2013). In global models, snowpack Hg^0_{gas} emissions can account for ~50% of all snowpack Hg (Corbitt et al., 2011). The reverse process—oxidation of Hg^0_{gas} to Hg^{II} —, has also been proposed to occur in the dark snowpack deeper in the snow profile (Faïn et al., 2007, 2013; Mann et al., 2015), resulting in concentration declines of Hg^0_{gas} with depth in the snowpack. To our knowledge, no direct in situ measurement of snowpack Hg^0_{gas} dynamics, however, is available in the field in the interior arctic snowpack.

In the Arctic and Antarctic, Hg cycling is also affected by atmospheric Hg depletion events (AMDEs), which are observed primarily in the springtime along coastal locations (Angot et al., 2016a; Dommergue et al., 2010; Schroeder et al., 1998; Steffen et al., 2008). During AMDEs, atmospheric Hg^0_{gas} concentrations fluctuate strongly due to atmospheric conversion of Hg^0_{gas} to oxidized Hg^{II} . Because Hg^{II} is subject to faster deposition (Schroeder and Munthe, 1998; Selin, 2009), AMDEs result in Hg temporarily deposited from the atmosphere to the arctic ecosystems. AMDEs are considered to be initiated by halogens (Brooks et al., 2008; Obrist et al., 2011; Steffen et al., 2008), such as bromine and chlorine radicals released from sea salt by photochemical processes (Simpson et al., 2007). AMDEs have been mainly observed along the coasts, e.g., at Barrow in Alaska (Douglas et al., 2008), Alert in Canada (Steffen et al., 2002), Ny-Ålesund in Svalbard (Ferrari et al., 2008), McMurdo in Antarctica (Brooks et al., 2008), as well as directly over the sea ice (Moore et al., 2014; Nerentorp Mastromonaco et al., 2016). The impacts of AMDEs at inland sites is reduced with increasing distance from the coast (Douglas and Sturm, 2004; Obrist et al., 2017; Van Dam et al., 2013).

The objectives of this study were to characterize Hg dynamics in the inland arctic snowpack at Toolik Field Station, and along a 170-km transect between this site and the arctic coast. For the first time, we comprehensively linked trace gas fluxes of Hg^0_{gas}

in interstitial snow air with the seasonal development of total Hg (Hg_{tot}) and dissolved Hg (Hg_{diss}) bound in the snowpack to assess conversions between volatile and solid Hg in the arctic snowpack. We specifically aimed to assess: (1) temporal and vertical Hg^0_{gas} patterns to quantify exchanges of Hg^0_{gas} in the atmosphere–snowpack–soil continuum; (2) impacts of springtime AMDEs on snowpack Hg deposition to and emission from the inland arctic snowpack; (3) temporal and vertical concentration and mass patterns of the snowpack Hg_{tot} and Hg_{diss} , to estimate Hg deposition throughout the snow accumulation period and pool of Hg available through snow melt; and (4) relationships of snow Hg concentrations with major ion concentrations and oxygen and hydrogen stable isotopes in precipitation to determine potential origins of Hg contained in the snowpack.

2 Materials and methods

2.1 Study site

Measurements were mainly performed at Toolik Field Station (Alaska, USA) over two full snow cover seasons from October 2014 to May 2016. The research station is located on the north slopes of the Brooks Range (68° 38' N, 149° 36' W) at an elevation of 720 m a.s.l., approximately 200 km south of the Arctic Ocean (Fig. 1, orange bullet). The area is characterized by gently sloping hills comprised of poorly drained silty loams underlain by continuous permafrost 250–300 m deep (Barker et al., 2014). Lithology is characterized by glacial till over Cretaceous sedimentary substrates (shale, claystone, siltstone, and sandstone; Alaska Division of Oil and Gas, 2008). The ecotype is classified as an acidic tussock tundra (Shaver and Chapin, 1991) with vegetation composed of scrubby plants (e.g., *Cassiope tetragona* (L.) D. Don, *Arctostaphylos alpinus* (L.) Spreng.), shrubs (e.g., *Betula nana* L., *Salix pulchra* Cham.), tussock grasses (*Carex*), and a variety of mosses and lichens. The mean annual air temperature is −8.5 °C, and mean annual precipitation is 312 mm (Cherry et al., 2014). In the two measurement years, the tundra was covered by snow for 236 and 248 days (i.e., 65 and 68% of the year) in the 2014–2015 and 2015–2016 seasons, respectively.

Snowpack sampling was also performed along a transect between Toolik and the Arctic Ocean in March 2016 (Fig. 1, yellow bullets). Detailed geographical characteristics of the sample sites are given in Table S1. A total of eight study sites were sampled from south (500 m a.s.l.) to north (20 m a.s.l.). All the sampled sites were characterized by similar ecosystems and lithology (including undifferentiated volcanic Upper Tertiary beds to the north) as described above for the Toolik area.

2.2 Trace gas in the atmosphere, interstitial snow air, and soil pores

We continuously sampled and analyzed interstitial air of the tundra snowpack at Toolik using a snow tower (Fig. S1) as described in detail by Seok et al. (2009) and Fäin et al. (2013). In summary, a snow tower consists of an air inlet manifold placed in the snowpack, so sampling of trace gases can be remotely alternated between various snow depths for undisturbed sampling of interstitial snow air throughout an entire snow season. The snow tower used at Toolik consisted of six 60 cm aluminum cross arms mounted at heights of 0, 10, 20, 30, 40, and 110 cm above the ground surface. Gas inlets were mounted to each cross arm allowing vertical sampling of snow interstitial air for analysis for multiple trace gases, including Hg^0_{gas} , CO_2 ,

and O₃. Each cross arm supported a pair of air inlets fitted with 25 mm syringe filters with 1 µm glass fiber membranes (Pall Life Sciences, Ann Arbor, MI, USA). Perfluoroalkoxy Teflon® tubing with equal lengths (35 m) were directed in a heated conduit to solenoid valves in the laboratory that allowed for sequential sampling of trace gases at the six different snowpack heights. The snow tower was deployed over the tundra in August of each year prior to the onset of snowfall. When the snow tower was subsequently covered by the accumulating snowpack, this set-up allowed sequentially continuous sampling of snow interstitial air without any disturbance. Inlets were sampled sequentially, 10 min at a time (i.e., averages of two individual measurements of 5 min), resulting in a 60-min sampling cycle. Corresponding trace gas sampling was performed below the snowpack in tundra soils at depths of 10, 20, and 40 cm using Teflon® soil trace gas wells (Obrist et al., 2014, 2017). Both organic and mineral soil profiles were considered in this study, distant of 5 m as described in Obrist et al. (2017). Atmospheric air sampling was performed using the top snow tower air inlets which always were above the developing snowpack, as well as on a nearby micrometeorological tower at a height of 3.6 m above ground. All interstitial snow, soil pore, and atmospheric inlets were connected by Teflon® tubing and solenoid valves to trace gas monitors in a nearby (10–30 m distance) field laboratory that were operated year-round.

Gaseous Hg⁰ concentrations were measured using two Tekran 2537B analyzers (Tekran Instruments Corporation, Toronto, ON, Canada), one shared for interstitial snow air and atmospheric measurements, and the other shared for soil gas and atmospheric measurements. The discrepancy in Hg⁰_{gas} measurements observed between the two Tekran instruments along the two seasons was on average 7%; concentration data showed here were adjusted. Air sampling was alternated between different snowpack heights every 5 min so that a full sequence of air extraction from the snowpack (six inlet heights) was achieved every 30 min. Interstitial snow, soil pore, and atmospheric measurements continued through the entire winter with only small-time periods of interruptions due to power failures or other technical problems. Additional trace gases were measured along with Hg⁰_{gas}, including concentrations of CO₂ using a LI-840A (LI-COR Inc., Lincoln, NE, USA).

2.3 Snow sampling and physical and chemical characterization

2.3.1 Snow sampling

At Toolik, we characterized Hg in the snowpack both over the undisturbed tundra and the adjacent frozen Toolik Lake (within 200 m of the tundra location). Two snow pits were sampled on five dates between October and May in the 2014–2015 season, and on four dates between December and June in 2015–2016. For each pit, we vertically excavated snow samples using a stainless-steel snow cutter (RIP 1 cutter 1000 cc), clean latex gloves, and trace metal Nasco Whirl-Pak® (The Aristotle Corporation, Stamford, CT, USA) HDPE plastic bags. We sampled at 10 cm-layer increments from the top to the bottom of the snowpack. Samples from two perpendicular walls of the pit were each pooled together per layer for analysis. Snow height, density, and temperature were measured for each layer, and frozen snow samples were stored in a cooler before transferring to a –20 °C freezer. Snow water equivalent (SWE), which represents the amount of water stored in the snowpack, was calculated using snow density measurements in incremental 10 cm-layers, multiplied by snow height. Additional sampling of

surface snow was performed over the tundra for a total of 17 sampling dates. The top 3 cm of the snowpack was collected in triplicate within a distance of 5 m into Nasco Whirl-Pak® plastic bags using clean latex gloves. Sampling along the south to north transect was performed over two days in March 2016.

2.3.2 Chemical analyses

5 In the laboratory, we melted snow samples overnight in the Nasco Whirl-Pak® bags at room temperature in the dark, and melted snow samples were subsequently analyzed for Hg. A fraction of snowmelt was directly transferred to 50 mL polypropylene tubes (Falcon®, Corning Incorporated, Corning, NY, USA) for analysis of Hg_{tot} . For Hg_{diss} , snowmelt water was filtered using 0.45 μm Acrodisc® filter with polyethersulfone membrane (Pall Corporation, Port Washington, NY, USA) into 50 mL Falcon® polypropylene tubes. In addition, filtered meltwater was used in 60 mL high-density polyethylene tubes
10 (VWR®, Radnor, PA, USA) for determination of major cations, anions, and stable isotopes (^2H and ^{18}O). Total Hg and Hg_{diss} concentrations were determined using Tekran 2600 cold-vapor atomic fluorescence spectrometry (Tekran Instruments Corporation, Toronto, ON, Canada) using a bromine monochloride (BrCl) digestion and reduction by stannous chloride (SnCl_2) following EPA method 1631 (US EPA, 2002). The detection limits (DL), determined as 3-times the standard deviation of blank samples, averaged 0.08 ng L^{-1} . For statistic purpose, values below the DL were included as $0.5 \times \text{DL}$. Analyzer
15 performance was determined by 5 ng L^{-1} standards analyzed every 10 samples, and recovery averaged between 93 and 107%. Laboratory and field blanks were conducted, and we evaluated any potential metal contamination of the stainless-steel snow cutter by analyzing Milli-Q water in contact with the snow cutter; all these blank determinations were bellow detection limits. Major cation and anion concentrations were quantified at the U.S. Army Cold Regions Research and Engineering Laboratory's (CRREL) Alaska Geochemistry Laboratory on Fort Wainwright, Alaska, with a Dionex ICS-3000 ion chromatograph. An AS-
20 19 anion column and a CS-12A cation column (Dionex Corporation Sunnyvale, California) were used, each with a 10 μL injection volume. A gradient method using potassium hydroxide (20 to 35 $\mu\text{mol L}^{-1}$) was used for anion analyses, while cation analyses used methane sulfonic acid eluent with a concentration of 25 $\mu\text{mol L}^{-1}$ in isocratic mode. The flow rate was 1 mL min^{-1} and the operating temperature was 30 °C. The ion chromatograph was calibrated using standards with a range from 0.5 to 50 mg L^{-1} . Repeat analyses of calibration standards from 0.5 to 50 mg L^{-1} yielded a precision of $\pm 5\%$. Peaks were
25 identified using Chromeleon (Dionex) and verified visually. Stable isotopes of oxygen and hydrogen were also measured at CRREL Alaska using Wavelength-Scanned Cavity Ringdown Spectroscopy on a Picarro L2120i (Sunnyvale, California). Standards and samples were injected into the analyzer for seven separate analyses. Results from the first four injections were not used to calculate the stable isotope values to eliminate internal system memory. The mean value from the final three sample injections was used to calculate the mean and standard deviation
30 value for each sample. Values are reported in standard per mil notation. Repeated analyses of five internal laboratory standards representing a range of values spanning the samples analyzed and analyses of SMOW, GISP, and SLAP standards (International Atomic Energy Agency) were used to calibrate the analytical results. Based on thousands of these standards analyses and of sample duplicate analyses we estimate the precision is $\pm 0.2\%$ for $\delta^{18}\text{O}$ and $\pm 0.5\%$ for $\delta^2\text{H}$.

2.4 Data processing and statistical analyses

We performed all data processing and statistical analyses with RStudio 1.1.383 (RStudio Inc., Boston, Massachusetts, USA) using R 3.4.2 (R Foundation for Statistical Computing, Vienna, Austria). Averaged data and variance in figures and tables are shown as mean \pm standard deviation. Significant differences were determined with the Kruskal-Wallis test ($\alpha = 0.05$). We performed plots with *ggplot2*, *ggtern*, and *lattice* R packages, and used normality (eq L⁻¹) for the ternary diagram. Geographical maps were prepared using Quantum GIS 2.18 (Quantum GIS Development Team, 2017).

3 Results and discussion

3.1 Snowpack development and snowpack physics

Due to high wind conditions in the Arctic tundra (Cherry et al., 2014), the physical development of the snowpack and its depth and the thickness of wind slab layers at Toolik were subject to significant drifts and changes in snowpack height, and were hence highly variable spatially and temporally throughout the winter season. The average snow height over the tundra site (shown in gray bars in Fig. 2) was continuously measured in both winters using a camera set to record daily pictures and using reference snow stakes placed in the snowpack. In the 2014–2015 season, the average snowpack height was 37 cm, with a standard deviation of 12 cm and a maximum depth of 60 cm. In the 2015–2016 season, the snowpack was almost half of that of the previous year, with an average snowpack height of 19 cm, a standard deviation of 7 cm, and a maximum depth of 35 cm. Based on snow pit measurements in the 2014–2015 season, we observed an increase of snow density with time, from an average of 0.18 g cm⁻³ in October to 0.26 g cm⁻³ in March (blue lines in Fig. 2). No clear temporal pattern was observed in the 2015–2016 season when average snow density; it ranged between 0.28 and 0.30 g cm⁻³. Results showed similar temporal evolution as snow heights, with maximum SWE observed in March in both snow seasons of 158 and 116 mm, respectively.

Snowpack temperatures were highly variable throughout the seasons and also strongly differed vertically within the snowpack (red lines in Fig. 2). Temperatures ranged from -34 to 0 °C in the top of the snowpack and from -21 to -1 °C in the bottom of the snowpack; temperatures showed strong increases from the top to the bottom of the snowpack, illustrating the important insulating function that the snowpack has in the cold Arctic winter and spring months. Minimum snowpack temperatures were recorded during the January 26th 2015 sampling event when air temperatures were -40 °C.

The snowpack over the adjacent frozen lake showed an average density of 0.23 g cm⁻³ and temperatures ranged between -18 and 0 °C. The snow height over Toolik Lake was much lower than that over the tundra, with snow heights consistently <15 cm for both seasons. The maximum SWE calculated above the lake was 40 and 42 mm for the two snow seasons, respectively.

The transect between Toolik and the Arctic Ocean performed in March 2016 showed snowpack height ranging between 30 and 66 cm. The maximum height was observed at one site located 55 km from the Arctic Ocean where presence of dense shrubs up to 40 cm height induced accumulation of local drifting snow due to high roughness. Snow density (between 0.19 and 0.26 g cm⁻³) and temperatures (between -20 and -10 °C) followed the same trends as observed at Toolik with decreasing

density and increasing temperatures with snowpack thickness. The calculated SWE averaged 104 mm and ranged between 70 and 164 mm.

3.2 Gaseous Hg^0 in the atmosphere–snowpack–soil continuum

3.2.1 Gaseous Hg^0 concentration profiles

5 Gaseous Hg^0 concentrations were measured at Toolik over two years in the atmosphere, in snowpack interstitial air at up to five inlet heights, and in soil pore air in the tundra ecosystem. Data coverage was 183 and 207 days for the 2014–2015 and 2015–2016 seasons, respectively, with only few periods when system failures resulted in lack of data. A continuous temporal record of the Hg^0_{gas} concentration profile in the snowpack is presented in Fig. 3a for the 2014–2015 season, i.e., when the snowpack was deeper compared to the 2015–2016 season, and compared to a similar record from a temperate snowpack based on published data (Fig. 3b; Faïn et al., 2013; note different y-scale of figure panels). In addition, full time-averaged atmosphere–snowpack–soil Hg^0_{gas} diffusion profiles are shown for the entire two winter seasons: 2014–2015 (Fig. 4a–c) and 2015–2016 (Fig. 4d–f). Gaseous Hg^0 concentrations were averaged for each season for three different periods, i.e., November to December (representing early winter and full darkness), January to February (representing mid-winter and full darkness), and March to April (when sunlight emerged and when occasional AMDEs were active). Note that standard deviations indicate natural fluctuations in Hg^0_{gas} concentrations as observed in Obrist et al. (2017).

15 The Hg^0_{gas} measurements consistently showed strong concentration gradients in the atmosphere–snowpack–soil continuum with highest concentrations in the atmosphere (on average, 1.18 ± 0.13 and $1.09 \pm 0.13 \text{ ng m}^{-3}$, respectively) and lowest concentrations in soils (often below detection limits of 0.10 ng m^{-3}). This pattern was consistent over two independent soil profiles measured at this site, one mainly consisting of organic soils and one soil profile dominated by mineral soil horizons.

20 Hg^0_{gas} concentrations in the snowpack were between concentration in the atmosphere and in soils, and showed pronounced patterns of decreasing concentrations from the top to the bottom of the snow profile. In the first year, Hg^0_{gas} concentrations decreased from the top snowpack inlet (i.e., 40 cm above the ground; average Hg^0_{gas} concentration of 1.18 ng m^{-3}) to the lower snowpack sampling heights (30, 20, and 10 cm above the ground; average Hg^0_{gas} concentrations of 1.11, 1.00, and 0.76 ng m^{-3} , respectively), and showed the lowest Hg^0_{gas} concentrations at the soil–snowpack interface (0 cm: 0.53 ng m^{-3}). Due to a much shallower snowpack in the 2015–2016 season and an absence of measurements at 0 cm height due to line freezing of the lowest inlet, the profile of Hg^0_{gas} was less pronounced compared to 2014–2015. However, we similarly found a Hg^0_{gas} decline from upper to lower snowpack heights (e.g., Hg^0_{gas} concentrations of 1.09 ng m^{-3} in the atmosphere, 1.02 ng m^{-3} at 20 cm, and 0.88 ng m^{-3} at 10 cm height above ground). In a previous paper, we reported a small rate of continuous Hg^0_{gas} deposition from the atmosphere to the tundra—measured by a micrometeorological tower—during much of the snow-covered season, with the exception of short time periods in spring when AMDEs occurred at Toolik (Obrist et al., 2017). Here, we show that these flux measurements are supported by consistent Hg^0_{gas} concentration gradients that existed through both seasons and that showed that snowpack Hg^0_{gas} concentrations were consistently lower than atmospheric levels above. In addition, snowpack Hg^0_{gas}

30

declined with depth in the snowpack and were lowest in the underlying soil, showing evidence of a consistent Hg^0_{gas} concentration gradient from the atmosphere to surface snow to tundra soils.

The top of the snowpack (ranging between 2 and 12 cm depth below the atmosphere depending on snow depth) generally showed highest Hg^0_{gas} concentrations close to concentrations measured in the atmosphere. This pattern is inconsistent with other arctic snowpack measurements that showed atmospheric Hg^0_{gas} concentrations higher than those in snowpack (Angot et al., 2016b; Steffen et al., 2014). Indeed, the uppermost snowpack Hg^0_{gas} concentrations can reach 3-times the atmospheric levels in the interior Antarctic regions (Angot et al., 2016b). It also differed to patterns observed in lower latitude snowpacks: in the Rocky Mountains, for example, the upper snowpack showed strong enrichments of Hg^0_{gas} throughout most of the winter (i.e., up to 6-times higher concentrations than in the atmosphere; Fig. 3b, Faïn et al., 2013). Such Hg^0_{gas} concentration enrichments were attributed to strong photochemically initiated reduction of snow-bound Hg^{II} to Hg^0_{gas} (Lalonde et al., 2002). The implications of Hg^0_{gas} production is that subsequent volatilization of the Hg^0_{gas} from the porous snowpack to the atmosphere can alleviate atmospheric deposition loads, and it is estimated that globally 50% of snow-bound Hg is volatilized back to the atmosphere prior to snowmelt (Corbitt et al., 2011). Our trace gas concentration measurements showed that Hg^0_{gas} re-volatilization does not occur in this interior tundra snowpack during most of the winter. An absence of direct solar radiation likely explains the lack of photochemical Hg^0_{gas} formation and volatilization between December through mid-January. Yet, springtime is a photochemically active period in the arctic when strong Hg^0_{gas} volatilization from snow has been reported further north along the Arctic Ocean coast (Brooks et al., 2006; Kirk et al., 2006). Even in late spring, when abundant solar radiation is present ($400\text{--}600 \text{ W m}^{-2}$), however, Hg^0_{gas} volatilization losses were rare and largely limited to periods of active AMDEs. We speculate that a reason for the general lack of Hg^0_{gas} formation and volatilization in snow includes substrate limitation due to low snow Hg_{tot} concentrations (Fig. 2). An alternative possibility may be that our sampling setup (between 5 and 7 cm below the surface during the three main AMDEs) may have limited our ability to detect and observe photo-reduction processes that may occur only in the upper few cm of the snowpack surface (King and Simpson, 2001; Poulain et al., 2004). However, using the same measurement system, Hg^0_{gas} concentration enhancements in temperate snowpacks were large (up to 8 ng m^{-3}) and detectable up to a depth of $>90 \text{ cm}$ from the snowpack surface (Fig. 3b). Unlike in Faïn et al. (2013), we also did not observe Hg^0_{gas} formation after fresh snowfall, although it also is important to note that snowfall amounts at Toolik were much lower than in temperate snowpack.

During March and April, snowpack Hg^0_{gas} concentrations were highly variable (Figs. 4c and f) following Hg^0_{gas} concentration changes in the atmosphere above, indicating an apparently high snowpack diffusivity (Fig. S2). During these time periods, snowpack Hg^0_{gas} concentrations in the top snowpack at times exceeded concentrations in the atmosphere above (less than 5% of the time), and these occurrences were mainly related to periods of AMDEs when Hg^0_{gas} depletion occurred in the overlying atmosphere. Our measurements of Hg^0_{gas} showed that early spring was the only time period when we observed small rates of Hg^0_{gas} formation in the uppermost snowpack layer, suggesting some photochemical reduction and re-volatilization of Hg^0_{gas} after AMDE-Hg deposition. However, Hg^0_{gas} production was small, limited in time, and no photochemical Hg^0_{gas} production or re-emission was observed in deeper snow layers, suggesting that the process was limited to the snowpack surface. These

patterns in March and April were also consistent with flux measurements when we observed periods of net Hg^0_{gas} emission from the tundra ecosystem to the atmosphere (Obrist et al., 2017), in support of the typical Hg dynamics often reported during AMDEs (Hg^{II} deposition followed by photochemical reduction and Hg^0_{gas} re-emission; Ferrari et al., 2005). We propose that, in addition to relatively infrequent and generally weaker AMDE activity, rapid photochemical re-emission losses of Hg following AMDEs render these events relatively unimportant as a deposition source of Hg in this interior arctic tundra site. We provided support for this notion using stable Hg isotope analysis in soils from this site in Obrist et al. (2017), which showed that atmospheric Hg^0_{gas} is the dominant Hg source to the interior tundra snowpack accounting for over 70% of Hg present.

3.2.2 Snowpack diffusivity of trace gases

A key question pertaining to the wintertime snowpack Hg^0_{gas} concentration profiles and measured deposition is if the observed Hg^0_{gas} deposition and concentration declines in the snowpack are driven by Hg^0_{gas} sinks in the snowpack or by Hg^0_{gas} uptake by underlying tundra soils. Sinks of Hg^0_{gas} in the snowpack have been observed in a few studies (Dommergue et al., 2003; Faïn et al., 2008, 2013) and have been attributed to dark oxidation of Hg^0_{gas} to divalent, non-volatile Hg^{II} , possibly including oxidation by halogen species, O_3 , or related to NO_x chemistry. To address this question, we compared the ratios of Hg^0_{gas} to CO_2 gradients in the snowpack to determine commonality or differences between sinks and sources of both gases. Because CO_2 in the atmosphere is relatively stable in winter and soils are the only wintertime source, CO_2 can be used to assess how the snowpack affects diffusion and advective exchange processes between soils and the atmosphere. Comparing Hg^0_{gas} to CO_2 allows assessment of whether Hg^0_{gas} concentrations in the snowpack are driven by processes in the underlying soils (i.e., similar to CO_2) or if in-snowpack chemistry affects Hg^0_{gas} concentration profiles. The gas diffusion model, based on Fick's first law of diffusion, is defined as follows, Eq. (1):

$$F = -D \left(\frac{\delta C}{\delta z} \right) \quad (1)$$

where F is the molecular flux in the snowpack airspace ($\text{mol m}^{-2} \text{s}^{-1}$), D is the diffusivity in the snowpack airspace ($\text{m}^2 \text{s}^{-1}$), and $\delta C/\delta z$ is the gas concentration gradient in the snowpack integrated in the snow depth (mol m^{-4}).

Since diffusivity is determined by both snowpack porosity and tortuosity—both of which are poorly known and not directly measured—, we used the flux ratios between Hg^0_{gas} and CO_2 to determine if both gases show similar flux behavior across the snowpack (Faïn et al., 2013), Eq. (2):

$$\frac{F_{\text{Hg}^0_{\text{gas}}}}{F_{\text{CO}_2}} = \frac{D_{\text{Hg}^0_{\text{gas}}}}{D_{\text{CO}_2}} \times \frac{\Delta_{\text{Hg}^0_{\text{gas}}}}{\Delta_{\text{CO}_2}} \quad (2)$$

where $\Delta_{\text{Hg}^0_{\text{gas}}}$ and Δ_{CO_2} are the $\delta C/\delta z$ gradients for both Hg^0_{gas} and CO_2 , respectively. Assuming similar gas diffusivity for both Hg^0_{gas} and CO_2 , the ratio of concentration gradients of the two gases ($\Delta_{\text{Hg}^0_{\text{gas}}}/\Delta_{\text{CO}_2}$) gives direct information about their respective flux ratios between different snowpack trace gas inlets. Please note that these fluxes are in the opposite direction.

We focused our analysis of Hg^0_{gas} and CO_2 concentration gradients at Toolik for the month of January 2015, when the snow height was among the highest (approximately 40 cm), and when strong decreases in interstitial Hg^0_{gas} concentrations from

the top to the bottom of the snowpack were present. At this time, soils still were a relatively active source of CO₂ to the snowpack (Fig. 5), facilitating a comparison to the soil CO₂ source. In contrast to Hg⁰_{gas} (Fig. 5a), profiles for CO₂ showed strong increases in concentrations with increasing depth in the snowpack (Fig. 5b). Highest CO₂ concentrations were present in the soil (up to 5000 μmol mol⁻¹, data not shown), and these patterns are consistent with an expected source of soils for CO₂ and diffusive and advective mixing of CO₂ produced in snow through the snowpack with the atmosphere (Liptzin et al., 2009; Oechel et al., 1997). Analysis of $\Delta_{Hg^0_{gas}}/\Delta_{CO_2}$ ratios showed no statistically significant differences from the top to the bottom of the snowpack, as evidenced from calculated gradients between 0 to 10 cm, 10 to 20 cm, and 20 to 30 cm heights (Fig. 5c). The constant and negative ratios between CO₂ and Hg⁰_{gas} and the fact that CO₂ is largely non-reactive in snowpack hence indicates that Hg⁰_{gas} also was not subject to snowpack chemical reactions; both profiles are affected by underlying soil processes, i.e., soil sources for CO₂ and soil sinks (for Hg⁰_{gas}). These wintertime atmosphere–snowpack–soil Hg⁰_{gas} concentration profiles at Toolik were also consistent with a measured net deposition of Hg⁰_{gas} throughout winter using flux measurements (Figs. 2 and 4; Obrist et al., 2017). Both net flux measurements, combined with snowpack Hg⁰_{gas} concentration profiles, hence suggest that a soil Hg⁰_{gas} sink was active throughout the Arctic winter, notably under very cold wintertime soil temperatures as low as −15 °C. Such soil Hg⁰_{gas} sinks were previously reported to occur in temperate soils (Obrist et al., 2014), although the mechanisms for the Hg⁰_{gas} sinks are currently not clear. It is notable that $\Delta_{Hg^0_{gas}}/\Delta_{CO_2}$ ratios in the upper snowpack (i.e., between 20 and 30 cm height) were more variable compared to lower snowpack heights, which we attribute to much smaller concentrations differences for both CO₂ and Hg⁰_{gas} between these inlets.

3.3 Snowbound mercury in the interior arctic snowpack

3.3.1 Spatial patterns

Snow samples were analyzed at Toolik for Hg_{tot} and Hg_{diss} (Fig. 2 and Table S1). Concentrations in snowpack collected over the tundra averaged 0.70 ± 0.98 ng L⁻¹ for Hg_{tot} concentrations and 0.17 ± 0.10 ng L⁻¹ for Hg_{diss} concentrations (both seasons, average of entire snowpack height). Total Hg concentrations were always higher than Hg_{diss} levels, likely due to impurities and deposition of Hg associated with plant detritus or soil dust, and showed higher variability in Hg_{tot} concentrations compared to Hg_{diss}. We thus focused our discussions on Hg_{diss} data. Measurements performed at Toolik showed very low levels compared to many other high latitude studies, with Hg_{diss} concentrations averaging 0.17 ng L⁻¹, and ranging between 0.08 and 1.15 ng L⁻¹. This is generally lower than Hg concentrations in interior Arctic sites reported by Douglas and Sturm (2004) (i.e., Hg_{diss} concentrations between 0.5 and 1.7 ng L⁻¹) and at the low end of concentrations found in Arctic studies along the coastal zone (0.14–820 ng L⁻¹, for both Hg_{diss} and Hg_{tot}; Douglas et al., 2005; Douglas and Sturm, 2004; Ferrari et al., 2004, 2005; Kirk et al., 2006; Nerentorp Mastromonaco et al., 2016; St. Louis et al., 2005; Steffen et al., 2002). The low concentrations we measured result in very small pool sizes of Hg_{diss} stored in the snowpack during wintertime compared to temperate studies (Pearson et al., 2015). At Toolik, snowpack pool sizes amounted to 26.9 and 19.7 ng m⁻² during peak snowpack and prior to the onset of snowmelt in 2014–2015 and 2015–2016, respectively.

The snowpack sampled over the adjacent frozen lake showed Hg_{tot} and Hg_{diss} concentrations of 0.80 ± 0.61 and $0.15 \pm 0.08 \text{ ng L}^{-1}$, respectively (Table S1). These values were not statistically different from concentrations measured in the tundra snowpack. Snowpack Hg_{diss} loads on the frozen lake were lower ($6.2 \pm 0.2 \text{ ng m}^{-2}$), i.e., only about 1/4, compared to snowpack Hg_{diss} load on the adjacent tundra ($23.3 \pm 5.0 \text{ ng m}^{-2}$). Three reasons may explain the large difference between lake and tundra snowpack Hg loads: (1) the lake did not accumulate the snowpack on open water prior to the lake surface freezing in the early fall (Sturm and Liston, 2003); (2) low surface roughness over the lake likely prevent settling of snowfall and facilitate remobilization of snow by wind transport (Essery et al., 1999; Essery and Pomeroy, 2004); and (3) the lake ice is warmer than the tundra soil resulting in higher sublimation over the lake. The implications of the latter process is a reduction of direct atmospheric deposition over Arctic lakes, and is consistent with studies that estimated that annual Hg contribution to Arctic lakes via direct wet deposition is small, generally less than 20% of total deposition (Fitzgerald et al., 2005, 2014). Spatial redistribution of snow across the tundra landscape further implies that both wet deposition and snow accumulation rates are variable, leading to spatial heterogeneity of snowmelt Hg inputs.

Most Arctic studies of snowpack Hg have been performed close to the coast (i.e., Alert and Barrow), and few studies include inland sites such as Toolik (Douglas and Sturm, 2004). In our study, measurements of Hg_{tot} and Hg_{diss} in the snowpack across a large North slope transect (about 170 km from Toolik to the Arctic Coast) in March, 2016 showed concentrations of 0.70 ± 0.79 and $0.24 \pm 0.20 \text{ ng L}^{-1}$, respectively (Fig. 6 and Table S3). Concentrations in Hg_{diss} of the five northernmost locations (<100 km distance from the Arctic Ocean) were statistically significantly ($p < 0.05$, Kruskal-Wallis test) higher compared to those measured at the four stations located in the interior tundra (>100 km), which included the Toolik site where mean Hg_{diss} concentrations were 0.33 ± 0.22 and $0.11 \pm 0.07 \text{ ng L}^{-1}$ for the same period, respectively. These patterns are consistent with previous observations in Alaska in springtime that suggested an ocean influence leading to higher Hg deposition, possibly linked to the presence of halogens (Douglas and Sturm, 2004; Landers et al., 1995; Snyder-Conn et al., 1997). We propose that low snowpack Hg concentrations (<0.5 ng L^{-1} for Hg_{diss}) are common in inland northern Alaska areas, and that the interior arctic snowpacks exhibit lower levels compared to coastal locations that are subjected to more significant ocean influences and impacts by AMDEs.

3.3.2 Seasonal patterns

Surface snow that was collected throughout the season can serve as an estimate for atmospheric wet deposition Hg concentrations and loads (Faïn et al., 2011). Concentrations of Hg_{tot} and Hg_{diss} in the surface snow layer (top 3 cm only) averaged $0.53 \pm 0.39 \text{ ng L}^{-1}$ and $0.26 \pm 0.26 \text{ ng L}^{-1}$, respectively (Fig. 7 and Table S1), which were not statistically significantly different compared to that of full snow pits or bottom snow layers. Both, low concentrations measured in surface snow, as well as low pool sizes as discussed above, suggest low wet deposition rates during winter at our inland arctic sites. However, estimation of deposition loads using snow collection can be compromised by quick re-volatilization losses of Hg from fresh snowfall (within the first few hours, e.g., Faïn et al., 2013), or snowmelt losses, but we do not consider these processes to be important at this site. The low Hg_{diss} concentrations measured in surface snow ($0.26 \pm 0.26 \text{ ng L}^{-1}$) are lower

than the 10th percentile of wet deposition Hg concentrations reported for Kodiak Island in Alaska during the same time period (National Atmospheric Deposition Program, 2017). Also, snowfall Hg_{diss} concentrations measured at Alert were between 100 and 200-times higher than in our measurements (A. Steffen, personal communication). Using median concentrations in the surface snow multiplied by the amount of wet deposition for each snow-covered season, we estimated the Hg_{diss} load annually deposited by snowfall to 41.3 and 15.3 ng m⁻² in the 2014–2015 and 2015–2016 winters, respectively. This is 1/100 of values recently provided from a coastal location 400 km northwest of our study site (Douglas et al., 2017) and 1/200 of long-term measurements from Alert between 1998 and 2010 (A. Steffen, personal communication).

Little temporal variation in snowpack Hg concentrations was observed between the early season snowpack evolving mainly under darkness and the late-season snowpack exposed to solar radiation (Figs. 2 and 6), although some temporal differences were evident during March and April when AMDEs were present in the region. Snowpack Hg_{diss} concentrations averaged 0.16 ng L⁻¹ both during the completely dark period (i.e., December and January) and after March 1st. Such patterns support measurements of Hg⁰_{gas} throughout the winter that indicated the snowpack to be a relatively inert matrix with little redox processes affecting Hg concentrations (oxidation of Hg⁰_{gas} or reduction of Hg^{II}). An apparent trend in surface snow, however, emerged during springtime, when both Hg_{tot} and Hg_{diss} concentrations exceeded 1 ng L⁻¹ (i.e., 4-times the average values observed through the rest of the season; Fig. 7). This was a period when AMDEs occurred at this site, as evident by depletions of atmospheric Hg⁰_{gas} with formation and deposition of oxidized atmospheric Hg^{II} (Obrist et al., 2017; Van Dam et al., 2013). Surface snow Hg concentration enhancements during AMDEs are commonly reported in polar regions, with at times Hg concentration enhancements up to 100-times the base concentration in the Arctic (Lalonde et al., 2002; Lindberg et al., 1998; Nerentorp Mastromonaco et al., 2016; Poulain et al., 2004; Steffen et al., 2002). The presence of AMDEs generally results in increased deposition of Hg to snow and ice surfaces, yet such additional deposition often is short-lived due to the photochemical re-emission of Hg⁰_{gas} (Kirk et al., 2006). In our study, we did not have sufficient temporal resolution of snow sampling during the period of AMDEs to closely track the fate of Hg deposition during AMDEs and subsequent re-emissions. However, we find that snow Hg enhancements during AMDEs were much lower than at coastal sites (e.g., Steffen et al., 2014), but a coarse temporal sampling could just have missed peak snow Hg levels at this site. We also found that after AMDEs, snow Hg_{diss} in surface snow declined to levels as was observed prior to AMDEs, and no concentration enhancements were observed in deeper in the snowpack. This is consistent with observations of net Hg⁰_{gas} volatilization during that time. The fact that we found no lasting impact of AMDEs on snow Hg concentrations, which also were supported by stable Hg isotope analysis (Obrist et al., 2017), may be due to the large distance to the coast from our study site and the scarcity of AMDEs—and O₃ depletion events—that occur at this inland arctic location (Van Dam et al., 2013).

Concentrations of Hg_{diss} measured in the snowpacks at Toolik did not show consistent vertical patterns (Fig. 2). Indeed, the upper snowpack Hg_{diss} concentrations were not significantly different from those in the deeper layers, which is in contrast to patterns observed in arctic snowpacks (Ferrari et al., 2004), as well as in alpine ones (Faïn et al., 2011), where strong concentration enhancements (i.e., more than 2-times the average snowpack concentrations) were observed in the top 3 cm of the snowpack. Seasonal measurements at Toolik indicate a generic lack of atmospheric gaseous Hg^{II} during most of the year

and very low amounts of total Hg^{II} deposition, i.e., wet, aerosols, plus gaseous Hg^{II} (Obrist et al., 2017). The lack of significant Hg^{II} dry deposition would prevent a Hg enhancement in surface snow, and also is consistent with the low pool sizes of Hg in this tundra snowpack. Further support of this notion also includes that snow collected at the surface throughout the arctic winter and spring was not statistically different from snow Hg concentrations contained in the entire snowpack (0.26 ± 0.26 vs $0.17 \pm 0.10 \text{ ng L}^{-1}$, respectively). Yet, another factor to explain a lack of depth gradients in snow Hg concentrations may include that snow layers can be continuously mixed and redistributed by wind gust (e.g., wind speed of Toolik were $>5 \text{ m s}^{-1}$ 12% of the time) across the landscape in the Arctic (Cherry et al., 2014).

3.4 Origin of mercury in the interior arctic snowpack

3.4.1 Cation and anion concentrations

Major cations (Ca^{2+} , K^{+} , Mg^{2+} , Na^{+} , and NH_4^{+}) and anions (Cl^{-} , NO_3^{-} , and SO_4^{2-}) were measured in snowpack and surface snow samples at Toolik to assess the chemical composition and potential origins for Hg in the snowpack (Table 1). Concentrations of these compounds were comparable to other inland Alaskan sites and, similar to concentrations of Hg, were lower than data reported from several arctic coastal locations (de Caritat et al., 2005; Douglas and Sturm, 2004). Surface snow samples (top 3 cm) generally showed somewhat higher Cl^{-} and Na^{+} concentrations and lower Mg^{2+} and K^{+} concentrations than samples collected across the entire snowpack height, although only Mg^{2+} and Na^{+} were significantly different ($p < 0.005$ and $p < 0.05$, respectively). Comparison between tundra and lake snowpack locations showed no statistical differences in elemental concentrations.

Spearman correlation coefficient (ρ) between Hg_{diss} and major ion concentrations were calculated for tundra and lake snowpack samples and surface snow collected over the tundra (Table 2). Using a correlation matrix, three groups of correlated major ions could be determined in the snowpack over the tundra: (1) NH_4^{+} and SO_4^{2-} ; (2) Ca^{2+} , Mg^{2+} , and NO_3^{-} ; (3) Cl^{-} , K^{+} , and Na^{+} . In the tundra snowpack, Hg_{diss} was not statistically significantly ($-0.22 < \rho < 0.11$) correlated to any of these major ion groups when considering the entire depth of the tundra snowpack. Relationships, however, were present in surface snow over the tundra where Hg_{diss} was correlated (ρ up to 0.80) with Ca^{2+} , Cl^{-} , and K^{+} , indicating that Hg_{diss} may have originated from a mix of natural sources possibly linked to both mineral dust (Ca^{2+}) and sea spray (Cl^{-}). The lack of strong correlation between Hg_{diss} and Na^{+} ($\rho = 0.30$) in surface snow samples may indicate that a part of Cl^{-} originated from mineral dust as CaCl_2 . A minor influence of sea salt was consistent with coastal observations that showed the highest Hg concentrations close to the Arctic Ocean related particularly to active bromine chemistry (Fig. 6; Douglas and Sturm, 2004). In addition, local or regional dust from rock and soil weathering contributed to the wintertime Hg deposition, particularly at interior sites close to the Brooks Range where higher snow pH reported were from mineral dust that contained carbonates (Douglas and Sturm, 2004). Indeed, the mountain influence was dominant during the two snow-covered seasons at Toolik where 50% of snow events and 80% of dry periods (i.e., periods without snowfall, 90% of the time) came from the south (i.e., Brooks Range). An additional group of correlated elements was identified in surface snow samples over the tundra: NH_4^{+} , NO_3^{-} , and SO_4^{2-} . Note that the low number

of lake snowpack samples (≤ 12) did not allow us to perform a meaningful correlation matrix analyses for lake snowpack samples.

To further visualize the relationships between analytes, we plotted a ternary diagram using three end-members according to Garbarino et al. (2002), Krnavek et al. (2012), Poulain et al. (2004), and Toom-Saunty and Barrie (2002) (Fig. 8). We considered Ca^{2+} as one end-member to represent a potential crustal signature, a second end-member with Cl^- as a sea salt signature, and a third end-member with SO_4^{2-} as a potential anthropogenic signature, i.e., from regional or long-range transport. Since sea salt SO_4^{2-} represented on average less than 1.2% of total SO_4^{2-} according to the calculation of Norman et al. (1999), we consider SO_4^{2-} not indicative of an ocean source. The different snow types (surface snow over the tundra, tundra snowpack, and lake snowpack) are presented with different colors in Fig. 8, and Hg_{diss} concentrations are represented by different symbol sizes. Relative concentrations of Cl^- (i.e., sea salt influence) showed statistically significant differences between snow samples collected over the tundra and those collected over the frozen lake (on average, 14 and 24% of proportion based on normality data, respectively; $p < 0.05$). However, no statistically significant differences were observed for relative concentrations of Ca^{2+} and SO_4^{2-} between tundra and lake locations. In general, snow surface samples showed low SO_4^{2-} and Cl^- relative concentrations ($< 30\%$) compared to integrated snowpack samples. Overall, Hg_{diss} concentrations were weakly correlated, except according to the SO_4^{2-} relative concentrations: Hg_{diss} concentrations averaged 0.10 and 0.17 ng L^{-1} for $> 30\%$ and $< 30\%$ of SO_4^{2-} , respectively ($p < 0.005$). These patterns indicate that anthropogenic influences from combustion processes were minor or absent for snow Hg deposition. In fact, Alaska generally showed the lowest SO_4^{2-} concentrations among arctic sites (de Caritat et al., 2005). Norman et al. (1999) also reported relatively small contributions of anthropogenic SO_4^{2-} in snow at Alert (Canada). From this, we propose that the Hg sources in the arctic snowpack is mainly derived from local lithological erosion, and that Arctic Ocean sources are minor contributions. However, this is not likely the case of Hg_{gas}^0 in tundra soils which mainly derived from global sources (Obrist et al., 2017). It should be noted that the proximity of Toolik with a busy road in the Arctic (the Dalton Highway) may influenced our measurements, but this is difficult to evaluate.

The lack of consistent statistically significant associations between major ions and Hg_{diss} across the entire snowpack depth (Table 2a) further suggest that initial snowfall Hg content was maintained and largely unaltered after deposition, with no clear accumulation or depletion zones as found in other snowpacks (Ferrari et al., 2005; Poulain et al., 2004; Steffen et al., 2014). We found a small relative enrichment of alkaline earth elements in snowpack samples compared to surface snow, which indicates some additional contributions of local mineral dust, yet this did not result in a measurable increase in snowpack Hg levels. Hence, we suggest no significant additional deposition of Hg (e.g., by dry deposition of gaseous or particulate Hg) to exposed older snow consistent with the lack of correlation to pollution tracers (SO_4^{2-} and NO_3^-). We also suggest an absence or minor importance of re-emission losses or elution losses from snow melt as occurs in temperate snowpacks (discussed in Faïn et al. (2013) and Pearson et al. (2015)). Elution losses are unlikely, given that no temperatures above freezing were present in the Arctic until May, and atmospheric re-emissions losses of volatile Hg_{gas}^0 were not important in this arctic snowpack for most of the season as discussed above.

3.4.2 Stable oxygen and hydrogen isotope signatures

Oxygen (^{18}O) and hydrogen (^2H) isotopes are frequently used as tracers for precipitation sources (Gat, 2010). The stable isotope signatures in surface snow samples collected at Toolik are presented in a $\delta^2\text{H}$ vs $\delta^{18}\text{O}$ diagram for different ranges of Hg_{diss} concentrations and different sampling dates (Fig. 9a). All the samples were distributed close to the global meteoritic water line (Craig, 1961). Despite a large variability in values (from -18.3 to -41.3‰ for $\delta^{18}\text{O}$ and from -140 to -314‰ for $\delta^2\text{H}$), samples collected on the same date were relatively close (mean standard deviation of 0.88 and 6.5‰, respectively). No clear relationships were observed between isotope signatures and Hg_{diss} concentrations (with size scale in Fig. 9) across the entire spectrum of values. However, samples with high Hg_{diss} concentrations (e.g., the three highest measured in April 2nd, 2016) and low Hg_{diss} concentrations (e.g., samples below the detection limit in December 5th, 2015) were found clustered together at similar $\delta^{18}\text{O}$ and $\delta^2\text{H}$ values. The $\delta^{18}\text{O}$ values were also plotted against air temperatures (T_{air}) during the snowfall events (Fig. 9b). A statistically significant linear relationship was found between the two variables ($r^2 = 0.50$) with the lowest $\delta^{18}\text{O}$ values being measured during the coldest temperatures. Neither the origin of precipitation as shown by the wide range of stable isotope ratios, nor the physical conditions that often cause isotopic variation in precipitation (e.g., air temperatures that explain up to 50% of isotopic values via mass effects; Siegenthaler and Oeschger, 1980), shaped the Hg concentrations measured in the snowpack.

4 Conclusions

In this study, we investigated snow Hg dynamics in the interior arctic tundra at Toolik Field Station, Alaska, simultaneously analyzing Hg in: (1) the gas-phase (Hg^0_{gas}) of the atmosphere, interstitial snowpack, and soil pores; and (2) in the solid phase in snow (Hg_{tot} and Hg_{diss}). Gaseous Hg^0 in the atmosphere–snowpack–soil continuum showed consistent concentration patterns throughout most of the snow season with the arctic tundra soil serving as a continuous sink for Hg^0_{gas} , important to consider in Arctic Hg cycling. To our surprise, photochemical formation of Hg^0_{gas} in the snowpack was largely absent and played a minor role in the interior tundra largely limited to periods of active AMDEs. These observations are in contrast with strong photochemical formation of Hg^0_{gas} in surface snow observed at temperate sites and along the arctic coast, resulting in significant photochemical losses of Hg^0_{gas} from these snowpacks. This calls for a regional adjustment of photochemical Hg^0_{gas} losses from the snowpack in models, which should have different treatment for the arctic snowpack compared to temperate snowpacks. Small Hg_{diss} enhancements were temporarily observed in surface snow during springtime, when AMDEs were present, reflecting the typical sequence of Hg deposition to the top snowpack followed by fast photochemical volatilization losses of Hg^0_{gas} during that time. At this interior arctic site, AMDEs, however, resulted in negligible deposition loads. Low concentrations of both Hg_{tot} and Hg_{diss} were measured in the snowpack across this northern Alaska region, resulting in a small reservoir of Hg stored in this snowpack available for potential mobilization during snowmelt ($<30 \text{ ng m}^{-2}$ for Hg_{diss}). These low values suggest that wet Hg deposition via snow is not a major source of Hg to this interior arctic site, a notion we previously supported by direct measurements and stable Hg isotopes that showed that two thirds of the Hg source are derived from Hg^0_{gas}

deposition. Multielement analysis of surface snow (top 3 cm) indicated that arctic snowpack Hg originated from a mix of diffuse and likely natural sources, including local mineral dust (associated with Ca^{2+} and Mg^{2+}) and, to a lesser extent, regional marine sea spray (associated with Cl^- and Na^+).

Acknowledgements

- 5 We thank Toolik Field Station staff for their support in this project over two years, especially Jeb Timm, Joe Franish, and Faye Ethridge, for helping with snow collection. We also thank Martin Jiskra (Geosciences Environnement Toulouse) and Christine Olson (DRI) for their field support, Christopher Pearson, Olivia Dillon, and Jacob Hoberg (DRI) for their support with laboratory analyses, and Dominique Colegrove and Tim Molnar (University of Colorado) for helping with field work and data processing. We finally thank Alexandra Steffen for providing mercury snow data from Alert. Funding was provided by the
- 10 U.S. National Science Foundation (NSF) under award (#PLR 1304305) and cooperative agreement from National Aeronautics and Space Administration (NASA EPSCoR NNX14AN24A).

References

- Alaska Division of Oil and Gas: Regional geology of the north slope of Alaska, 2008.
- 15 Angot, H., Dastoor, A., De Simone, F., Gårdfeldt, K., Gencarelli, C. N., Hedgecock, I. M., Langer, S., Magand, O., Mastromonaco, M. N., Nordstrøm, C., Pfaffhuber, K. A., Pirrone, N., Ryjkov, A., Selin, N. E., Skov, H., Song, S., Sprovieri, F., Steffen, A., Toyota, K., Travníkov, O., Yang, X. and Dommergue, A.: Chemical cycling and deposition of atmospheric mercury in polar regions: review of recent measurements and comparison with models, *Atmospheric Chem. Phys.*, 16(16), 10735–10763, doi:10.5194/acp-16-10735-2016, 2016a.
- 20 Angot, H., Magand, O., Helmig, D., Ricaud, P., Quennehen, B., Gallée, H., Del Guasta, M., Sprovieri, F., Pirrone, N., Savarino, J. and Dommergue, A.: New insights into the atmospheric mercury cycling in central Antarctica and implications on a continental scale, *Atmospheric Chem. Phys.*, 16(13), 8249–8264, doi:10.5194/acp-16-8249-2016, 2016b.
- Atwell, L., Hobson, K. A. and Welch, H. E.: Biomagnification and bioaccumulation of mercury in an arctic marine food web: insights from stable nitrogen isotope analysis, *Can. J. Fish. Aquat. Sci.*, 55(5), 1114–1121, doi:10.1139/f98-001, 1998.
- 25 Barker, A. J., Douglas, T. A., Jacobson, A. D., McClelland, J. W., Ilgen, A. G., Khosh, M. S., Lehn, G. O. and Trainor, T. P.: Late season mobilization of trace metals in two small Alaskan arctic watersheds as a proxy for landscape scale permafrost active layer dynamics, *Chem. Geol.*, 381, 180–193, doi:10.1016/j.chemgeo.2014.05.012, 2014.
- Bergin, M. H., Jaffrezo, J.-L., Davidson, C. I., Dibb, J. E., Pandis, S. N., Hillamo, R., Maenhaut, W., Kuhns, H. D. and Makela, T.: The contributions of snow, fog, and dry deposition to the summer flux of anions and cations at Summit, Greenland, *J. Geophys. Res. Atmospheres*, 100(D8), 16275–16288, doi:10.1029/95JD01267, 1995.
- 30 Brooks, S., Lindberg, S., Southworth, G. and Arimoto, R.: Springtime atmospheric mercury speciation in the McMurdo, Antarctica coastal region, *Atmos. Environ.*, 42(12), 2885–2893, doi:10.1016/j.atmosenv.2007.06.038, 2008.

- Brooks, S. B., Saiz-Lopez, A., Skov, H., Lindberg, S. E., Plane, J. M. C. and Goodsite, M. E.: The mass balance of mercury in the springtime arctic environment, *Geophys. Res. Lett.*, 33(L13812), doi:10.1029/2005GL025525, 2006.
- de Caritat, P., Hall, G., Gislason, S., Belsey, W., Braun, M., Goloubeva, N. I., Olsen, H. K., Scheie, J. O. and Vaive, J. E.: Chemical composition of arctic snow: concentration levels and regional distribution of major elements, *Sci. Total Environ.*, 336(1), 183–199, doi:10.1016/j.scitotenv.2004.05.031, 2005.
- Cherry, J. E., Déry, S. J., Cheng, Y., Stieglitz, M., Jacobs, A. S. and Pan, F.: Climate and hydrometeorology of the Toolik Lake region and the Kuparuk River basin, in Alaska’s changing arctic: ecological consequences for tundra, streams, and lakes, edited by J. E. Hobbie and G. W. Kling, pp. 21–60, Oxford University Press, New York., 2014.
- Cobbett, F. D., Steffen, A., Lawson, G. and van Heyst, B. J.: GEM fluxes and atmospheric mercury concentrations (GEM, RGM and Hg_p) in the Canadian Arctic at Alert, Nunavut, Canada (February–June 2005), *Atmos. Environ.*, 41(31), 6527–6543, doi:10.1016/j.atmosenv.2007.04.033, 2007.
- Corbitt, E. S., Jacob, D. J., Holmes, C. D., Streets, D. G. and Sunderland, E. M.: Global source-receptor relationships for mercury deposition under present-day and 2050 emissions scenarios, *Environ. Sci. Technol.*, 45(24), 10477–10484, doi:10.1021/es202496y, 2011.
- Craig, H.: Isotopic variations in meteoric waters, *Science*, 133(3465), 1702–1703, doi:10.1126/science.133.3465.1702, 1961.
- Dominé, F. and Shepson, P. B.: Air-snow interactions and atmospheric chemistry, *Science*, 297(5586), 1506–1510, doi:10.1126/science.1074610, 2002.
- Dommergue, A., Ferrari, C. P., Poissant, L., Gauchard, P.-A. and Boutron, C. F.: Diurnal cycles of gaseous mercury within the snowpack at Kuujjuarapik/Whapmagoostui, Québec, Canada, *Environ. Sci. Technol.*, 37(15), 3289–3297, doi:10.1021/es026242b, 2003.
- Dommergue, A., Sprovieri, F., Pirrone, N., Ebinghaus, R., Brooks, S., Courteaud, J. and Ferrari, C. P.: Overview of mercury measurements in the Antarctic troposphere, *Atmospheric Chem. Phys.*, 10(7), 3309–3319, doi:10.5194/acp-10-3309-2010, 2010.
- Douglas, T. A. and Sturm, M.: Arctic haze, mercury and the chemical composition of snow across northwestern Alaska, *Atmos. Environ.*, 38(6), 805–820, doi:10.1016/j.atmosenv.2003.10.042, 2004.
- Douglas, T. A., Sturm, M., Simpson, W. R., Brooks, S., Lindberg, S. E. and Perovich, D. K.: Elevated mercury measured in snow and frost flowers near Arctic sea ice leads, *Geophys. Res. Lett.*, 32(4), L04502, doi:10.1029/2004GL022132, 2005.
- Douglas, T. A., Sturm, M., Simpson, W. R., Blum, J. D., Alvarez-Aviles, L., Keeler, G. J., Perovich, D. K., Biswas, A. and Johnson, K.: Influence of snow and ice crystal formation and accumulation on mercury deposition to the Arctic, *Environ. Sci. Technol.*, 42(5), 1542–1551, doi:10.1021/es070502d, 2008.
- Douglas, T. A., Loseto, L. L., Macdonald, R. W., Outridge, P., Dommergue, A., Poulain, A., Amyot, M., Barkay, T., Berg, T., Chételat, J., Constant, P., Evans, M., Ferrari, C., Gantner, N., Johnson, M. S., Kirk, J., Kroer, N., Larose, C., Lean, D., Nielsen, T. G., Poissant, L., Rognerud, S., Skov, H., Sørensen, S., Wang, F., Wilson, S. and Zdanowicz, C. M.: The fate of mercury in arctic terrestrial and aquatic ecosystems, a review, *Environ. Chem.*, 9(4), 321–355, doi:10.1071/EN11140, 2012.
- Douglas, T. A., Sturm, M., Blum, J. D., Polashenski, C., Stuefer, S., Hiemstra, C., Steffen, A., Filhol, S. and Prevost, R.: A pulse of mercury and major ions in snowmelt runoff from a small arctic Alaska watershed, *Environ. Sci. Technol.*, 51(19), 11145–11155, doi:10.1021/acs.est.7b03683, 2017.

- Driscoll, C. T., Mason, R. P., Chan, H. M., Jacob, D. J. and Pirrone, N.: Mercury as a global pollutant: sources, pathways, and effects, *Environ. Sci. Technol.*, 47(10), 4967–4983, doi:10.1021/es305071v, 2013.
- Enrico, M., Le Roux, G., Heimbürger, L.-E., Van Beek, P., Souhaut, M., Chmieleff, J. and Sonke, J. E.: Holocene atmospheric mercury levels reconstructed from peat bog mercury stable isotopes, *Environ. Sci. Technol.*, 51(11), 5899–5906, doi:10.1021/acs.est.6b05804, 2017.
- Essery, R. and Pomeroy, J.: Vegetation and topographic control of wind-blown snow distributions in distributed and aggregated simulations for an arctic tundra basin, *J. Hydrometeorol.*, 5(5), 735–744, doi:10.1175/1525-7541(2004)005<0735:VATCOW>2.0.CO;2, 2004.
- Essery, R., Li, L. and Pomeroy, J.: A distributed model of blowing snow over complex terrain, *Hydrol. Process.*, 13(1415), 2423–2438, doi:10.1002/(SICI)1099-1085(199910)13:14/15<2423::AID-HYP853>3.0.CO;2-U, 1999.
- Fäin, X., Grangeon, S., Bahlmann, E., Fritsche, J., Obrist, D., Dommergue, A., Ferrari, C. P., Cairns, W., Ebinghaus, R., Barbante, C., Cescon, P. and Boutron, C.: Diurnal production of gaseous mercury in the alpine snowpack before snowmelt, *J. Geophys. Res.*, 112(D21311), doi:10.1029/2007JD008520, 2007.
- Fäin, X., Ferrari, C. P., Dommergue, A., Albert, M., Battle, M., Arnaud, L., Barnola, J.-M., Cairns, W., Barbante, C. and Boutron, C.: Mercury in the snow and firn at Summit Station, Central Greenland, and implications for the study of past atmospheric mercury levels, *Atmos Chem Phys*, 8(13), 3441–3457, doi:10.5194/acp-8-3441-2008, 2008.
- Fäin, X., Obrist, D., Pierce, A., Barth, C., Gustin, M. S. and Boyle, D. P.: Whole-watershed mercury balance at Sagehen Creek, Sierra Nevada, CA, *Geochim. Cosmochim. Acta*, 75(9), 2379–2392, doi:10.1016/j.gca.2011.01.041, 2011.
- Fäin, X., Helmig, D., Hueber, J., Obrist, D. and Williams, M. W.: Mercury dynamics in the Rocky Mountain, Colorado, snowpack, *Biogeosciences*, 10(6), 3793–3807, doi:10.5194/bg-10-3793-2013, 2013.
- Ferrari, C. P., Dommergue, A., Boutron, C. F., Jitaru, P. and Adams, F. C.: Profiles of mercury in the snow pack at Station Nord, Greenland shortly after polar sunrise, *Geophys. Res. Lett.*, 31(3), L03401, doi:10.1029/2003GL018961, 2004.
- Ferrari, C. P., Gauchard, P.-A., Aspö, K., Dommergue, A., Magand, O., Bahlmann, E., Nagorski, S., Temme, C., Ebinghaus, R., Steffen, A., Banic, C., Berg, T., Planchon, F., Barbante, C., Cescon, P. and Boutron, C. F.: Snow-to-air exchanges of mercury in an Arctic seasonal snow pack in Ny-Ålesund, Svalbard, *Atmos. Environ.*, 39(39), 7633–7645, doi:10.1016/j.atmosenv.2005.06.058, 2005.
- Ferrari, C. P., Padova, C., Fäin, X., Gauchard, P.-A., Dommergue, A., Aspö, K., Berg, T., Cairns, W., Barbante, C., Cescon, P., Kaleschke, L., Richter, A., Wittrock, F. and Boutron, C.: Atmospheric mercury depletion event study in Ny-Ålesund (Svalbard) in spring 2005. Deposition and transformation of Hg in surface snow during springtime, *Sci. Total Environ.*, 397(1–3), 167–177, doi:10.1016/j.scitotenv.2008.01.064, 2008.
- Fitzgerald, W. F., Engstrom, D. R., Lamborg, C. H., Tseng, C.-M., Balcom, P. H. and Hammerschmidt, C. R.: Modern and historic atmospheric mercury fluxes in Northern Alaska: global sources and arctic depletion, *Environ. Sci. Technol.*, 39(2), 557–568, doi:10.1021/es049128x, 2005.
- Fitzgerald, W. F., Hammerschmidt, C. R., Engstrom, D. R., Balcom, P. H., Lamborg, C. H. and Tseng, C.-M.: Mercury in the Alaskan arctic, in *Alaska’s changing arctic: ecological consequences for tundra, streams, and lakes*, edited by J. E. Hobbie and G. W. Kling, pp. 287–302, Oxford University Press, New York., 2014.

- Garbarino, J. R., Snyder-Conn, E., Leiker, T. J. and Hoffman, G. L.: Contaminants in Arctic snow collected over Northwest Alaskan sea ice, *Water. Air. Soil Pollut.*, 139(1–4), 183–214, doi:10.1023/A:1015808008298, 2002.
- Gat, J. R.: *Isotope hydrology: a study of the water cycle*, World Scientific, London., 2010.
- 5 King, M. D. and Simpson, W. R.: Extinction of UV radiation in arctic snow at Alert, Canada (82°N), *J. Geophys. Res. Atmospheres*, 106(D12), 12499–12507, doi:10.1029/2001JD900006, 2001.
- Kirk, J. L., St. Louis, V. L. and Sharp, M. J.: Rapid reduction and reemission of mercury deposited into snowpacks during atmospheric mercury depletion events at Churchill, Manitoba, Canada, *Environ. Sci. Technol.*, 40(24), 7590–7596, doi:10.1021/es061299+, 2006.
- 10 Krnavek, L., Simpson, W. R., Carlson, D., Domine, F., Douglas, T. A. and Sturm, M.: The chemical composition of surface snow in the Arctic: Examining marine, terrestrial, and atmospheric influences, *Atmos. Environ.*, 50(Supplement C), 349–359, doi:10.1016/j.atmosenv.2011.11.033, 2012.
- Lalonde, J. D., Poulain, A. J. and Amyot, M.: The role of mercury redox reactions in snow on snow-to-air mercury transfer, *Environ. Sci. Technol.*, 36(2), 174–178, doi:10.1021/es010786g, 2002.
- 15 Landers, D. H., Ford, J., Gubala, C., Monetti, M., Lasorsa, B. K. and Martinson, J.: Mercury in vegetation and lake sediments from the U.S. Arctic, *Water. Air. Soil Pollut.*, 80(1–4), 591–601, doi:10.1007/BF01189711, 1995.
- Lindberg, S. E., Hanson, P. J., Meyers, T. P. and Kim, K.-H.: Air/surface exchange of mercury vapor over forests—the need for a reassessment of continental biogenic emissions, *Atmos. Environ.*, 32(5), 895–908, doi:10.1016/S1352-2310(97)00173-8, 1998.
- 20 Liptzin, D., Williams, M. W., Helmig, D., Seok, B., Filippa, G., Chowanski, K. and Hueber, J.: Process-level controls on CO₂ fluxes from a seasonally snow-covered subalpine meadow soil, Niwot Ridge, Colorado, *Biogeochemistry*, 95(1), 151–166, doi:10.1007/s10533-009-9303-2, 2009.
- Mann, E., Meyer, T., Mitchell, C. P. J. and Wania, F.: Mercury fate in ageing and melting snow: development and testing of a controlled laboratory system, *J. Environ. Monit.*, 13(10), 2695–2702, doi:10.1039/C1EM10297D, 2011.
- 25 Mann, E., Ziegler, S., Mallory, M. and O’Driscoll, N.: Mercury photochemistry in snow and implications for arctic ecosystems, *Environ. Rev.*, 22(4), 331–345, doi:10.1139/er-2014-0006, 2014.
- Mann, E. A., Mallory, M. L., Ziegler, S. E., Tordon, R. and O’Driscoll, N. J.: Mercury in Arctic snow: quantifying the kinetics of photochemical oxidation and reduction, *Sci. Total Environ.*, 509–510, 115–132, doi:10.1016/j.scitotenv.2014.07.056, 2015.
- 30 Monson, R. K., Burns, S. P., Williams, M. W., Delany, A. C., Weintraub, M. and Lipson, D. A.: The contribution of beneath-snow soil respiration to total ecosystem respiration in a high-elevation, subalpine forest, *Glob. Biogeochem. Cycles*, 20(GB3030), doi:10.1029/2005GB002684, 2006.
- Moore, C. W., Obrist, D., Steffen, A., Staebler, R. M., Douglas, T. A., Richter, A. and Nghiem, S. V.: Convective forcing of mercury and ozone in the Arctic boundary layer induced by leads in sea ice, *Nature*, 506(7486), 81–84, doi:10.1038/nature12924, 2014.
- 35 National Atmospheric Deposition Program: (NRSP-3), NADP Program Office, Illinois State Water Survey, University of Illinois, Champaign, IL 61820., 2017.

- Nerentorp Mastromonaco, M., Gårdfeldt, K., Jourdain, B., Abrahamsson, K., Granfors, A., Ahnoff, M., Dommergue, A., Méjean, G. and Jacobi, H.-W.: Antarctic winter mercury and ozone depletion events over sea ice, *Atmos. Environ.*, 129, 125–132, doi:10.1016/j.atmosenv.2016.01.023, 2016.
- 5 Norman, A. L., Barrie, L. A., Toom-Saunty, D., Sirois, A., Krouse, H. R., Li, S. M. and Sharma, S.: Sources of aerosol sulphate at Alert: apportionment using stable isotopes, *J. Geophys. Res. Atmospheres*, 104(D9), 11619–11631, doi:10.1029/1999JD900078, 1999.
- Obrist, D., Tas, E., Peleg, M., Matveev, V., Faïn, X., Asaf, D. and Luria, M.: Bromine-induced oxidation of mercury in the mid-latitude atmosphere, *Nat. Geosci.*, 4(1), 22–26, doi:10.1038/ngeo1018, 2011.
- 10 Obrist, D., Pokharel, A. K. and Moore, C.: Vertical profile measurements of soil air suggest immobilization of gaseous elemental mercury in mineral soil, *Environ. Sci. Technol.*, 48(4), 2242–2252, doi:10.1021/es4048297, 2014.
- Obrist, D., Agnan, Y., Jiskra, M., Olson, C. L., Colegrove, D. P., Hueber, J., Moore, C. W., Sonke, J. E. and Helmig, D.: Tundra uptake of atmospheric elemental mercury drives Arctic mercury pollution, *Nature*, 547(7662), 201–204, doi:10.1038/nature22997, 2017.
- 15 Oechel, W. C., Vourlitis, G. and Hastings, S. J.: Cold season CO₂ emission from arctic soils, *Glob. Biogeochem. Cycles*, 11(2), 163–172, doi:10.1029/96GB03035, 1997.
- Pearson, C., Schumer, R., Trustman, B. D., Rittger, K., Johnson, D. W. and Obrist, D.: Nutrient and mercury deposition and storage in an alpine snowpack of the Sierra Nevada, USA, *Biogeosciences*, 12(12), 3665–3680, doi:10.5194/bg-12-3665-2015, 2015.
- 20 Poulain, A. J., Lalonde, J. D., Amyot, M., Shead, J. A., Raofie, F. and Ariya, P. A.: Redox transformations of mercury in an Arctic snowpack at springtime, *Atmos. Environ.*, 38(39), 6763–6774, doi:10.1016/j.atmosenv.2004.09.013, 2004.
- Schroeder, W. H. and Munthe, J.: Atmospheric mercury—An overview, *Atmos. Environ.*, 32(5), 809–822, doi:10.1016/S1352-2310(97)00293-8, 1998.
- Schroeder, W. H., Anlauf, K. G., Barrie, L. A., Lu, J. Y., Steffen, A., Schneeberger, D. R. and Berg, T.: Arctic springtime depletion of mercury, *Nature*, 394, 331–332, doi:10.1038/28530, 1998.
- 25 Selin, N. E.: Global biogeochemical cycling of mercury: a review, *Annu. Rev. Environ. Resour.*, 34(1), 43–63, doi:10.1146/annurev.enviro.051308.084314, 2009.
- Seok, B., Helmig, D., Williams, M. W., Liptzin, D., Chowanski, K. and Hueber, J.: An automated system for continuous measurements of trace gas fluxes through snow: an evaluation of the gas diffusion method at a subalpine forest site, Niwot Ridge, Colorado, *Biogeochemistry*, 95(1), 95–113, doi:10.1007/s10533-009-9302-3, 2009.
- 30 Shaver, G. R. and Chapin, F. S.: Production: biomass relationships and element cycling in contrasting arctic vegetation types, *Ecol. Monogr.*, 61(1), 1–31, doi:10.2307/1942997, 1991.
- Siegenthaler, U. and Oeschger, H.: Correlation of ¹⁸O in precipitation with temperature and altitude, *Nature*, 285(5763), 314–317, doi:10.1038/285314a0, 1980.
- 35 Simpson, W. R., von Glasow, R., Riedel, K., Anderson, P., Ariya, P., Bottenheim, J., Burrows, J., Carpenter, L. J., Frieß, U., Goodsite, M. E., Heard, D., Hutterli, M., Jacobi, H.-W., Kaleschke, L., Neff, B., Plane, J., Platt, U., Richter, A., Roscoe, H.,

- Sander, R., Shepson, P., Sodeau, J., Steffen, A., Wagner, T. and Wolff, E.: Halogens and their role in polar boundary-layer ozone depletion, *Atmos Chem Phys*, 7(16), 4375–4418, doi:10.5194/acp-7-4375-2007, 2007.
- Snyder-Conn, E., Garbarino, J. R., Hoffman, G. L. and Oelkers, A.: Soluble trace elements and total mercury in arctic alaskan snow, *Arctic*, 50(3), 201–215, 1997.
- 5 Sprovieri, F., Pirrone, N., Ebinghaus, R., Kock, H. and Dommergue, A.: A review of worldwide atmospheric mercury measurements, *Atmospheric Chem. Phys.*, 10(17), 8245–8265, doi:10.5194/acp-10-8245-2010, 2010.
- St. Louis, V. L., Sharp, M. J., Steffen, A., May, A., Barker, J., Kirk, J. L., Kelly, D. J. A., Arnott, S. E., Keatley, B. and Smol, J. P.: Some sources and sinks of monomethyl and inorganic mercury on Ellesmere Island in the Canadian high Arctic, *Environ. Sci. Technol.*, 39(8), 2686–2701, doi:10.1021/es049326o, 2005.
- 10 Steffen, A., Schroeder, W., Bottenheim, J., Narayan, J. and Fuentes, J. D.: Atmospheric mercury concentrations: measurements and profiles near snow and ice surfaces in the Canadian Arctic during Alert 2000, *Atmos. Environ.*, 36(15–16), 2653–2661, doi:10.1016/S1352-2310(02)00112-7, 2002.
- Steffen, A., Douglas, T., Amyot, M., Ariya, P., Aspmo, K., Berg, T., Bottenheim, J., Brooks, S., Cobbett, F., Dastoor, A., Dommergue, A., Ebinghaus, R., Ferrari, C., Gardfeldt, K., Goodsite, M. E., Lean, D., Poulain, A. J., Scherz, C., Skov, H., Sommar, J. and Temme, C.: A synthesis of atmospheric mercury depletion event chemistry in the atmosphere and snow, *Atmos Chem Phys*, 8(6), 1445–1482, doi:10.5194/acp-8-1445-2008, 2008.
- 15 Steffen, A., Bottenheim, J., Cole, A., Douglas, T. A., Ebinghaus, R., Friess, U., Netcheva, S., Nghiem, S., Sihler, H. and Staebler, R.: Atmospheric mercury over sea ice during the OASIS-2009 campaign, *Atmospheric Chem. Phys.*, 13(14), 7007–7021, doi:10.5194/acp-13-7007-2013, 2013.
- 20 Steffen, A., Bottenheim, J., Cole, A., Ebinghaus, R., Lawson, G. and Leaitch, W. R.: Atmospheric mercury speciation and mercury in snow over time at Alert, Canada, *Atmos Chem Phys*, 14(5), 2219–2231, doi:10.5194/acp-14-2219-2014, 2014.
- Sturm, M. and Liston, G. E.: The snow cover on lakes of the Arctic Coastal Plain of Alaska, U.S.A., *J. Glaciol.*, 49(166), 370–380, doi:10.3189/172756503781830539, 2003.
- Toom-Saunty, D. and Barrie, L. A.: Chemical composition of snowfall in the high Arctic: 1990–1994, *Atmos. Environ.*, 36(15–16), 2683–2693, doi:10.1016/S1352-2310(02)00115-2, 2002.
- 25 Uematsu, M., Kinoshita, K. and Nojiri, Y.: Scavenging of insoluble particles from the marine atmosphere over the sub-arctic north Pacific, *J. Atmospheric Chem.*, 35(2), 151–163, doi:10.1023/A:1006219028497, 2000.
- US EPA: Method 1631: Mercury in water by oxidation, purge and trap, and cold vapor atomic fluorescence spectrometry, United States Environmental Protection Agency., 2002.
- 30 Van Dam, B., Helmig, D., Burkhart, J. F., Obrist, D. and Oltmans, S. J.: Springtime boundary layer O₃ and GEM depletion at Toolik Lake, Alaska, *J. Geophys. Res. Atmospheres*, 118(8), 3382–3391, doi:10.1002/jgrd.50213, 2013.

Table 1: Mean concentration ($\mu\text{g L}^{-1}$), including standard deviation (*italics*), of cations and anions in tundra and lake snowpack and in surface snow at Toolik Field Station.

location		Mg ²⁺	Ca ²⁺	Na ⁺	K ⁺	Cl ⁻	NH ₄ ⁺	NO ₃ ⁻	SO ₄ ²⁻
tundra	surface	7.2	453.0	112.6	29.4	228.6	11.3	265.0	191.3
		6.8	<i>530.8</i>	<i>104.6</i>	<i>46.7</i>	<i>232.9</i>	3.9	<i>187.5</i>	<i>130.6</i>
	snowpack	32.1	523.5	58.5	60.8	137.5	13.2	202.8	234.0
		<i>34.7</i>	<i>452.1</i>	<i>38.9</i>	<i>102.3</i>	<i>113.1</i>	<i>5.4</i>	<i>104.5</i>	<i>131.8</i>
lake		27.8	784.1	119.1	23.1	117.5	12.8	270.5	181.2
		<i>21.8</i>	<i>403.7</i>	<i>135.9</i>	<i>28.6</i>	<i>73.4</i>	<i>2.9</i>	<i>94.0</i>	<i>78.1</i>

Table 2: Spearman’s coefficient correlations (ρ , in bold if ≥ 0.5 or ≤ -0.5) between chemical elements (dissolved Hg [Hg_{diss}] and major ions) in the tundra snowpack (a) and surface snow over the tundra (b).

a. Tundra snowpack

	Hg_{diss}	Mg^{2+}	Ca^{2+}	Na^+	K^+	Cl^-	NH_4^+	NO_3^-
SO_4^{2-}	-0.16	0.42	0.32	0.39	0.48	0.47	0.58	0.17
NO_3^-	0.07	0.74	0.83	0.55	0.33	0.59	0.03	
NH_4^+	-0.22	-0.04	0.03	0.15	0.35	0.30		
Cl^-	-0.11	0.41	0.39	0.89	0.72			
K^+	-0.10	0.34	0.33	0.70				
Na^+	0.11	0.47	0.38					
Ca^{2+}	-0.07	0.90						
Mg^{2+}	0.06							

b. Surface snow

	Hg_{diss}	Mg^{2+}	Ca^{2+}	Na^+	K^+	Cl^-	NH_4^+	NO_3^-
SO_4^{2-}	-0.08	0.54	0.14	0.16	-0.08	-0.04	0.74	0.74
NO_3^-	0.14	0.62	0.28	0.08	0.07	-0.20	0.57	
NH_4^+	-0.02	0.45	0.24	0.18	-0.08	-0.04		
Cl^-	0.63	0.35	0.69	0.82	0.86			
K^+	0.62	0.45	0.80	0.78				
Na^+	0.30	0.68	0.56					
Ca^{2+}	0.80	0.39						
Mg^{2+}	0.08							

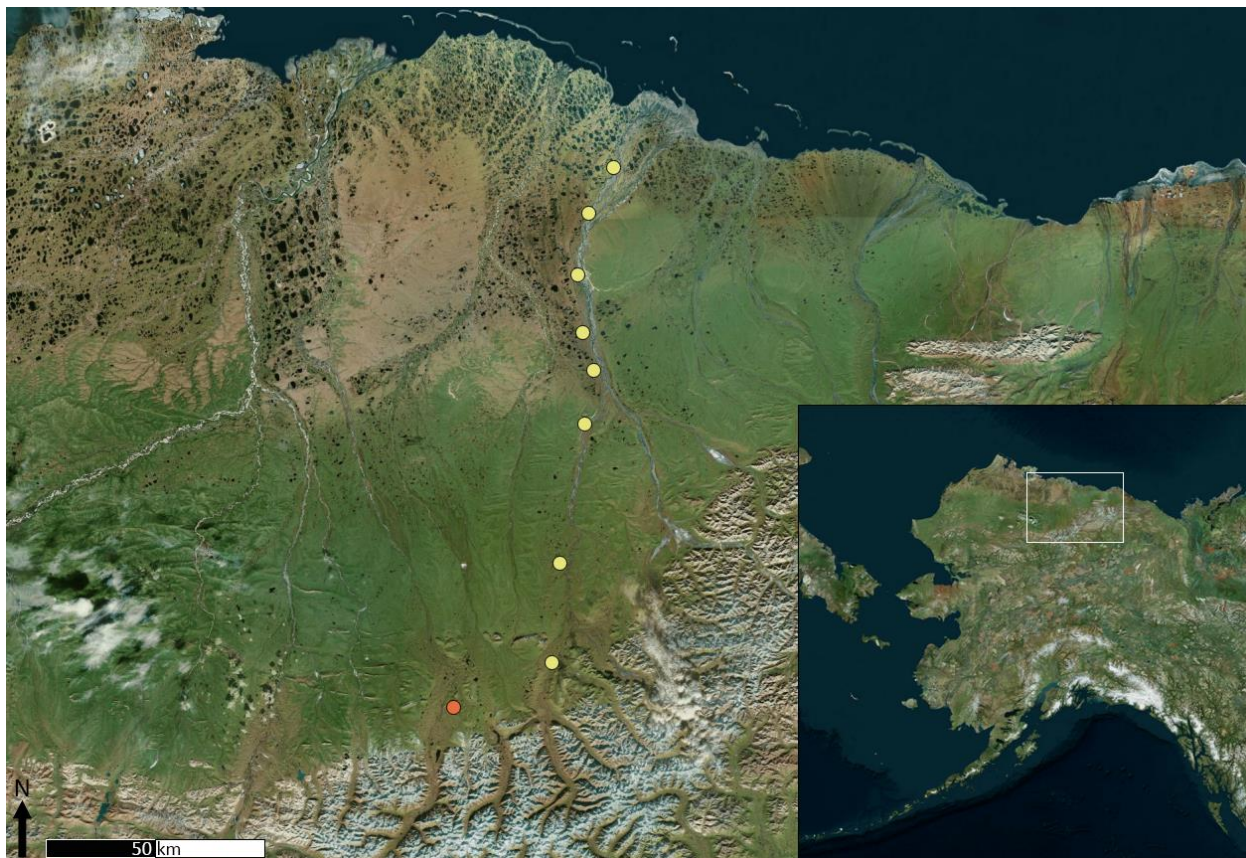


Figure 1: Study area in northern Alaska, including Toolik Field Station (orange bullet point) and the eight transect sites (yellow bullet points). Satellite images are true color images (Earthstar Geographics SIO, 2017).

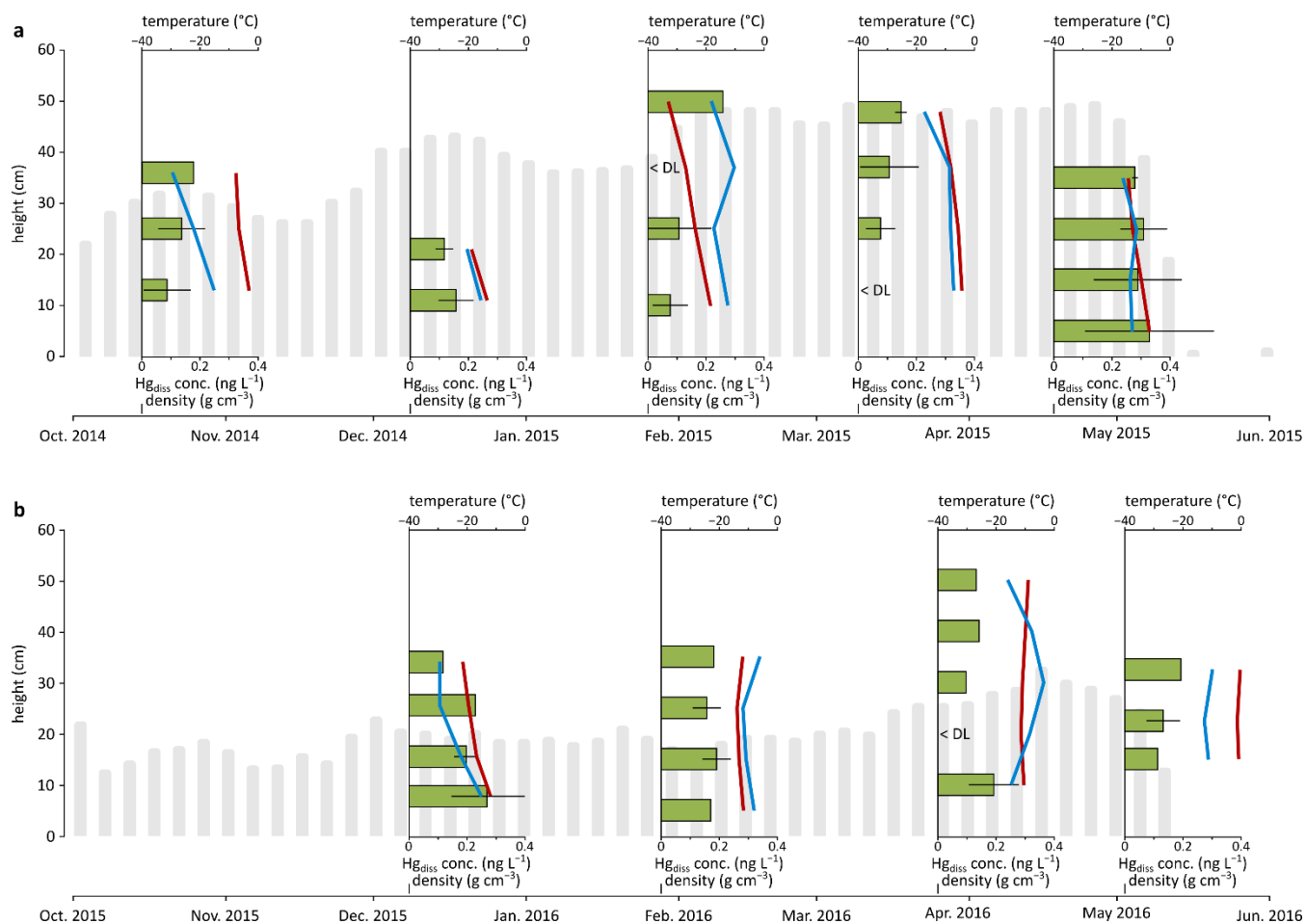


Figure 2: Snowpack temperatures (red lines) and densities (blue lines) and dissolved Hg concentrations (green bars, including mean values and standard deviations) for five snow pits in the 2014–2015 season (a) and four snow pits in the 2015–2016 season (b) over the Arctic tundra at Toolik Field Station. The gray bars illustrate the average snow heights.

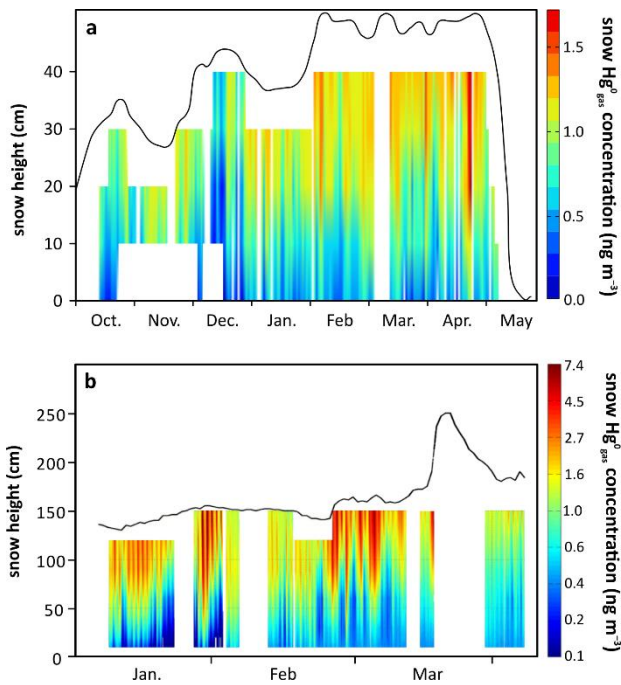


Figure 3: Gaseous Hg^0 concentration profiles in snowpack interstitial air during the snow-covered season from October 2014 to May 2015 over the Arctic tundra measured at Toolik Field Station based on continuous observations at up to five heights in the snowpack each hour, and interpolation of this data across the entire snowpack (a). For comparison, interpolated Hg^0_{gas} concentration profiles in snowpack interstitial air during the snow-covered season based on similar measurements at Niwot Ridge, Rocky Mountains, Colorado, USA, during the winter of 2009 (b) (adapted with permission; Faïn et al., 2013).

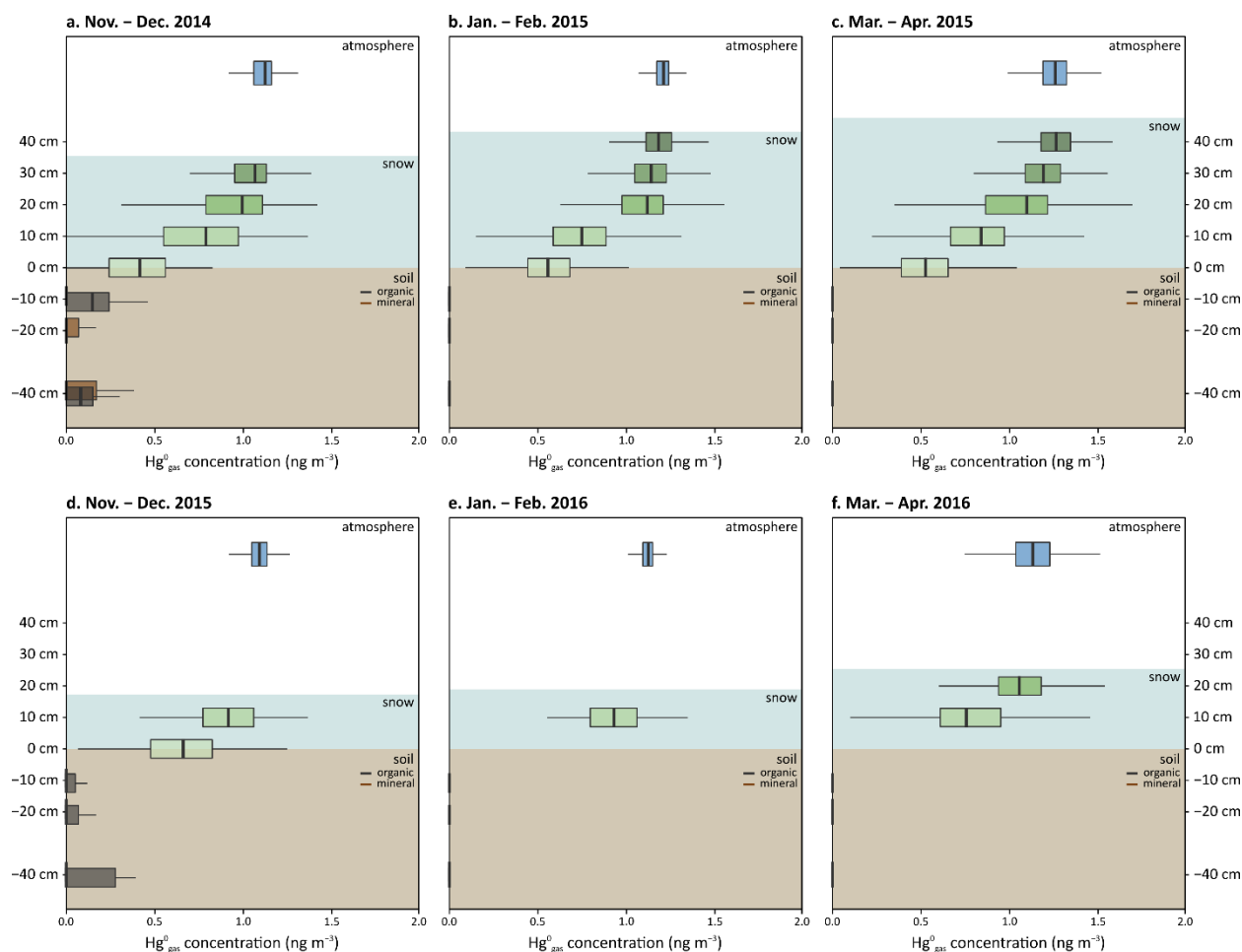


Figure 4: Hg^0_{gas} concentration profiles in the atmosphere, snowpack interstitial air, and soil interstitial air in early winter (from November to December; a and d), in winter (from January to February; b and e), and in early spring (from March to April; c and f) for 2014–2015 (top panels) and 2015–2016 (bottom panels) snow-covered periods over the arctic tundra measured at Toolik Field Station.

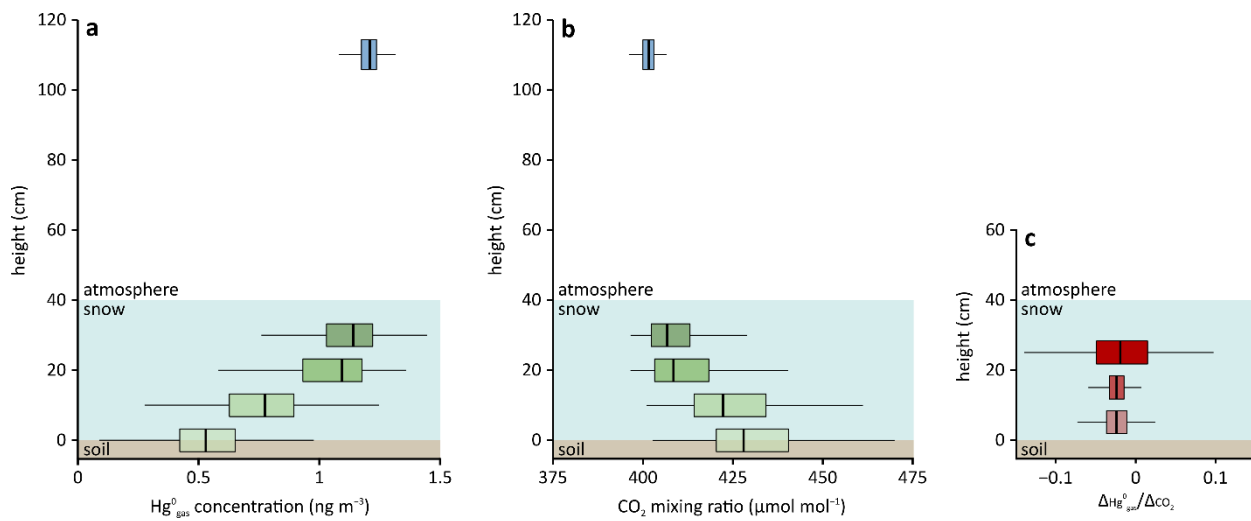


Figure 5: Snow concentration profiles for Hg^0_{gas} (a) and CO_2 (b) concentrations, and $\Delta Hg^0_{gas} / \Delta CO_2$ ratios for 0 to 10 cm, 10 to 20 cm, and 20 to 30 cm snowpack height based on daily averages (c) in January 2015 (snow height averaged 40 cm) over the arctic tundra measured at Toolik Field Station.

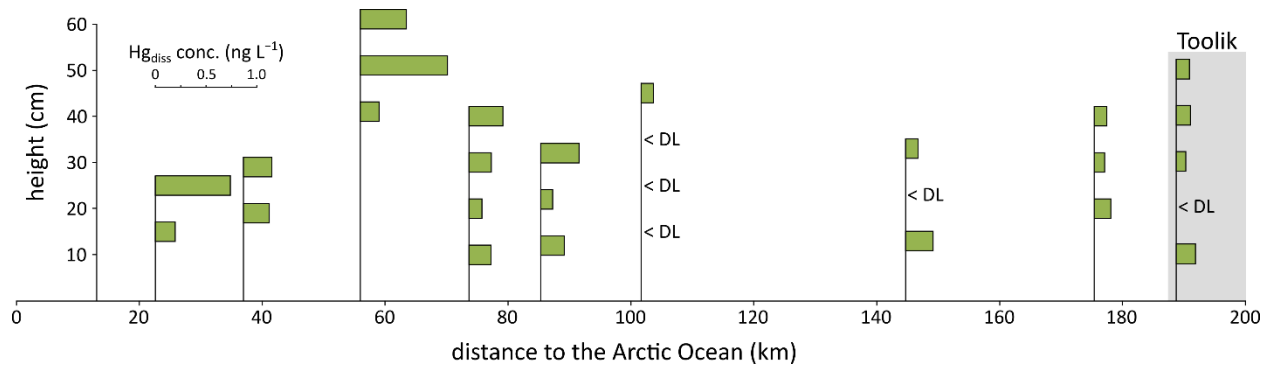


Figure 6: Spatial pattern of dissolved Hg concentrations (Hg_{diss}) in snowpack profiles across the North slope transect on March 27th–28th, 2016, and comparison with Toolik Field Station (gray box) in March 25th, 2016.

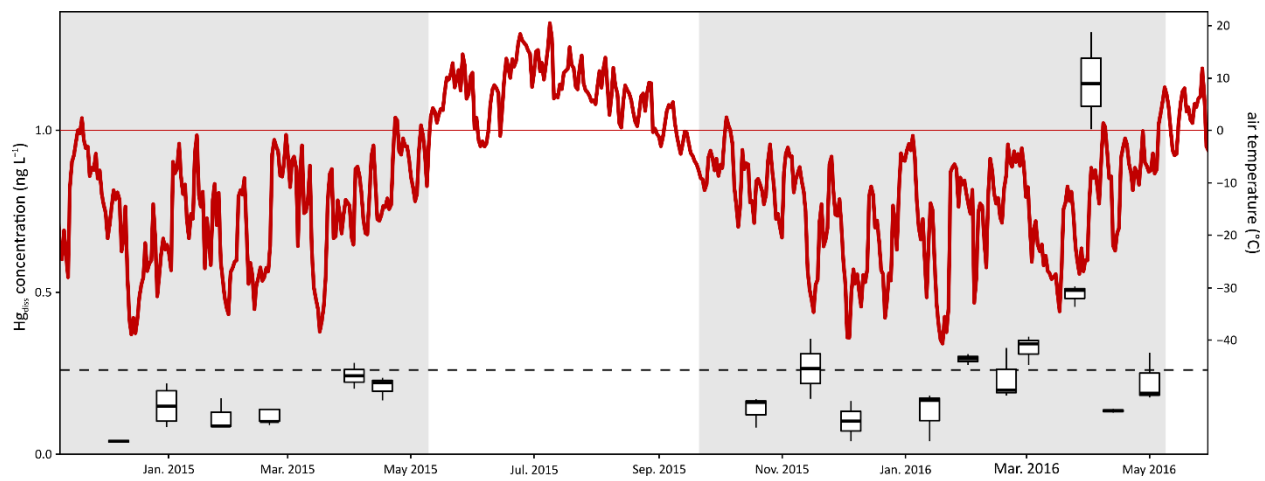


Figure 7: Temporal pattern of dissolved Hg (Hg_{diss}) concentrations in surface snow samples (top 3 cm) throughout the 2014–2015 and 2015–2016 snow-covered seasons (in grey) at Toolik Field Station. The broken line indicates the average surface snow Hg_{diss} concentration (0.26 ng L^{-1}). The red line indicates the daily average air temperature.

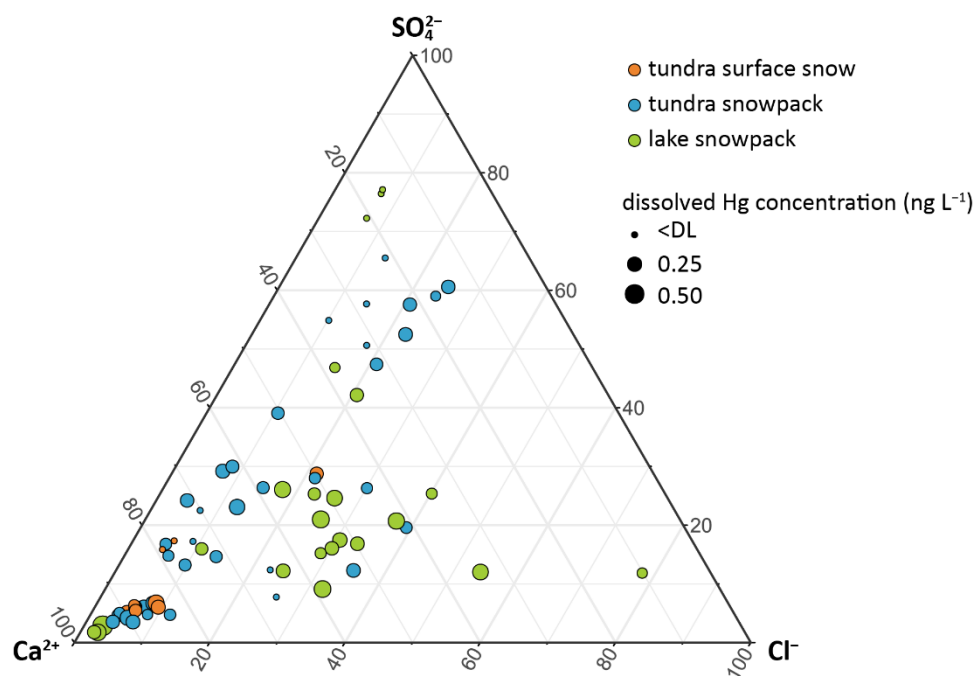


Figure 8: Ternary diagram of tundra surface snow (orange), tundra snowpack (blue), and lake snowpack (green) samples from Toolik Field Station ordered by dissolved Hg concentration between Ca^{2+} , Cl^- , and SO_4^{2-} (proportions based on meq L^{-1}).

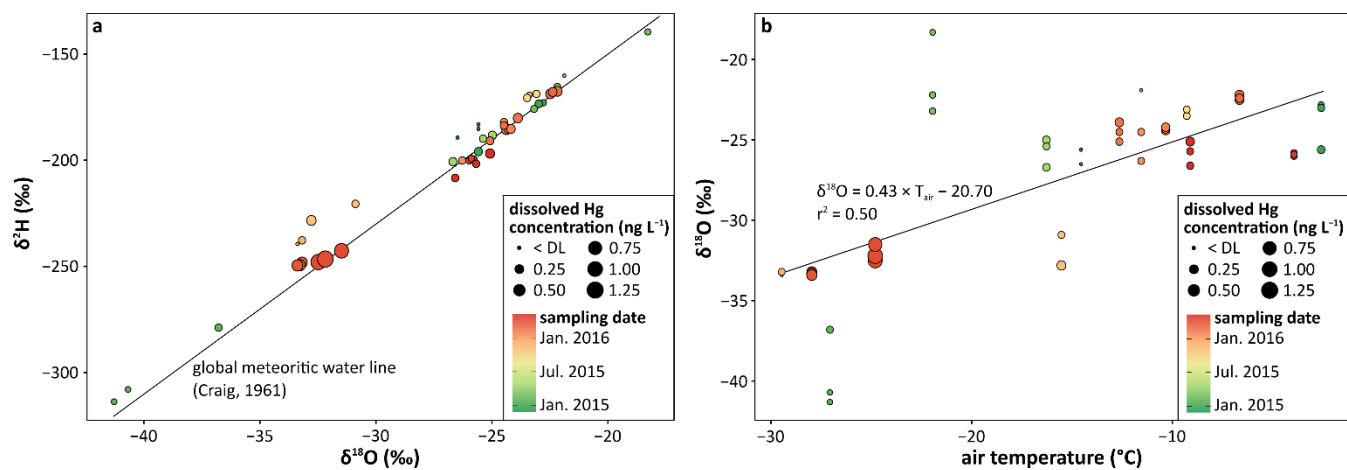


Figure 9: Dissolved Hg concentrations in surface snow samples for 2014 to 2016 in: (a) the $\delta^2\text{H}$ vs $\delta^{18}\text{O}$ diagram and (b) a plot of $\delta^{18}\text{O}$ vs air temperature (T_{air}) during the previous snowfall at Toolik Field Station.

Mercury in the Arctic tundra snowpack: temporal and spatial concentration patterns and trace-gas exchanges

Yannick Agnan^{1,2}, Thomas A. Douglas³, Detlev Helmig⁴, Jacques Hueber⁴, Daniel Obrist^{5,2}

¹Sorbonne Université, CNRS, EPHE, UMR Metis, F-75252, Paris, France

²Division of Atmospheric Sciences, Desert Research Institute, Reno, Nevada 89523, USA

³US Army Cold Regions Research and Engineering Laboratory, PO Box 35170, Fort Wainwright, Alaska 99709, USA

⁴Institute of Arctic and Alpine Research, University of Colorado, Boulder, Colorado 80309, USA

⁵Department of Environmental, Earth, and Atmospheric Sciences, University of Massachusetts, Lowell, MA 01854, USA

Correspondence to: Yannick Agnan (yannick.agnan@biogeochimie.fr) and Daniel Obrist (daniel_obrist@uml.edu)

Supplementary material:

Table S1: Geographical coordinates of transect sampling sites.....	2
Table S2: Summary total (Hg _{tot}) and dissolved Hg (Hg _{diss}) concentrations in snowpack and surface snow layers on the tundra and lake at Toolik Field Station.....	3
Table S3: Summary total (Hg _{tot}) and dissolved Hg (Hg _{diss}) concentrations in snowpack on the tundra of transect sampling sites.....	5
Figure S1: Snow tower installation over the arctic tundra at Toolik Field Station.	6
Figure S2: Hg ⁰ _{gas} concentrations (3-hours averages) in the atmosphere and snowpack interstitial air (10 and 20 cm above the ground surface), as well as Hg ^{II} and O ₃ atmospheric measurements during a week in spring 2016, including an AMDE, measured at Toolik Field Station. The snow height was between 25 and 28 cm and surface snow Hg _{tot} concentrations between 1.00 ± 0.07 (March 25 th) and 1.46 ± 0.16 ng L ⁻¹ (April 2 nd). The gray bars indicate nighttime periods.	7

Table S1: Geographical coordinates of transect sampling sites.

site	latitude	longitude	elevation (m)	distance to Dalton Highway (m)
transect 1	68.7605° N	148.8659° W	501	730
transect 2	69.0350° N	148.8258° W	400	230
transect 3	69.4212° N	148.6691° W	333	210
transect 4	69.5692° N	148.6049° W	145	560
transect 5	69.6741° N	148.7003° W	118	240
transect 6	69.8324° N	148.7555° W	84	140
transect 7	70.0031° N	148.6804° W	46	250
transect 8	70.1323° N	148.4896° W	21	250

Table S2: Summary total (Hg_{tot}) and dissolved Hg (Hg_{diss}) concentrations in snowpack and surface snow layers on the tundra and lake at Toolik Field Station.

date	location	height (cm)	Hg _{tot} (ng L ⁻¹)		Hg _{diss} (ng L ⁻¹)	
			mean	SD ^a	mean	SD ^a
Oct. 14 th 2014	tundra	36	0.22	0.04	0.18	0.00
		25	0.24	0.04	0.14	0.08
		13	0.17	0.18	0.09	0.08
Dec. 7 th 2014	tundra	surface	0.21	0.03	<DL ^b	–
		21	0.43	0.55	0.12	0.03
		11	1.06	1.30	0.16	0.06
Dec. 31 st 2014	tundra	surface	0.36	0.28	0.17	0.06
		surface	0.27	0.16	0.12	0.05
Jan. 26 th 2015	tundra	50	0.36	–	0.26	–
		37	6.23	–	<DL ^b	–
		25	0.46	0.16	0.11	0.11
		10	0.28	0.17	0.08	0.06
		lake	8	0.31	0.21	0.05
Feb. 20 th 2015	tundra	surface	0.18	0.03	0.13	0.02
		48	0.66	0.10	0.15	0.02
Mar. 8 th 2015	tundra	37	0.59	0.36	0.11	0.10
		25	0.19	0.03	0.08	0.05
		13	0.29	0.05	<DL ^b	–
		lake	11	0.74	<DL ^b	–
Apr. 3 rd 2015	tundra	surface	–	–	0.24	0.06
		surface	0.87	0.25	0.21	0.04
Apr. 17 th 2015	tundra	35	1.03	0.45	0.28	0.01
		25	0.61	0.05	0.31	0.08
		15	1.24	0.41	0.29	0.15
		5	0.91	0.62	0.33	0.22
		lake	11	1.43	0.09	0.07

^a standard deviation (n = 2 for snowpack and n = 3 for surface snow)

^b below detection limit

“–” no data

Table S2: Continued.

date	location	height (cm)	Hg _{tot} (ng L ⁻¹)		Hg _{diss} (ng L ⁻¹)	
			mean	SD ^a	mean	SD ^a
Oct. 19 th 2015	tundra	surface	0.32	0.03	0.12	0.07
Nov. 15 th 2015	tundra	surface	0.46	0.17	0.26	0.13
Dec. 5 th 2015	tundra	surface	0.19	0.01	0.10	0.09
		34	0.32	–	0.12	–
		26	0.78	–	0.23	–
		16	0.43	0.12	0.20	0.04
		8	0.37	0.08	0.27	0.13
Jan. 13 th 2016	tundra	surface	0.82	0.54	0.13	0.08
Jan. 29 th 2016	tundra	surface	0.38	0.15	0.29	0.02
		35	1.00	–	0.18	–
		25	0.69	0.75	0.16	0.05
		15	0.56	0.18	0.19	0.05
		5	0.64	–	0.17	–
	lake	5	1.63	0.63	0.24	0.06
Feb. 20 th 2016	tundra	surface	0.60	0.15	0.24	0.08
Mar. 3 rd 2016	tundra	surface	0.41	0.04	0.33	0.05
Mar. 25 th 2016	tundra	surface	1.01	0.07	0.49	0.03
		50	0.58	–	0.13	–
		40	0.85	–	0.14	–
		30	0.54	–	0.10	–
		20	0.31	0.06	<DL ^b	–
		10	0.46	0.13	0.19	0.09
	lake	13	0.41	0.16	0.17	0.02
Apr. 2 nd 2016	tundra	surface	1.46	0.16	1.15	0.15
Apr. 13 th 2016	tundra	surface	0.21	0.03	0.13	0.01
May 1 st 2016	tundra	surface	0.66	0.23	0.23	0.08
		33	0.21	0.12	0.12	0.11
		23	1.07	1.20	0.13	0.06
		15	0.43	–	0.13	–
	lake	13	0.24	0.07	0.12	0.11

^a standard deviation (n = 2 for snowpack and n = 3 for surface snow)

^b below detection limit

“–” no data

Table S3: Summary total (Hg_{tot}) and dissolved Hg (Hg_{diss}) concentrations in snowpack on the tundra of transect sampling sites.

site	height (cm)	Hg _{tot} (ng L ⁻¹)	Hg _{diss} (ng L ⁻¹)
transect 1	40	0.22	0.13
	30	0.22	0.11
	20	1.32	0.17
transect 2	33	0.27	0.13
	23	0.15	<DL ^a
	13	1.79	0.28
transect 3	45	0.25	0.13
	35	0.10	<DL ^a
	25	0.18	<DL ^a
	15	0.18	<DL ^a
transect 4	32	0.57	0.38
	22	0.38	0.13
	12	0.34	0.24
transect 5	40	0.60	0.34
	30	0.32	0.23
	20	0.36	0.14
	10	0.92	0.23
transect 6	61	0.86	0.46
	51	1.47	0.86
	41	0.54	0.19
transect 7	29	0.42	0.29
	19	0.78	0.26
transect 8	25	3.79	0.74
	15	0.73	0.20

^a below detection limit



Figure S1: Snow tower installation over the arctic tundra at Toolik Field Station.

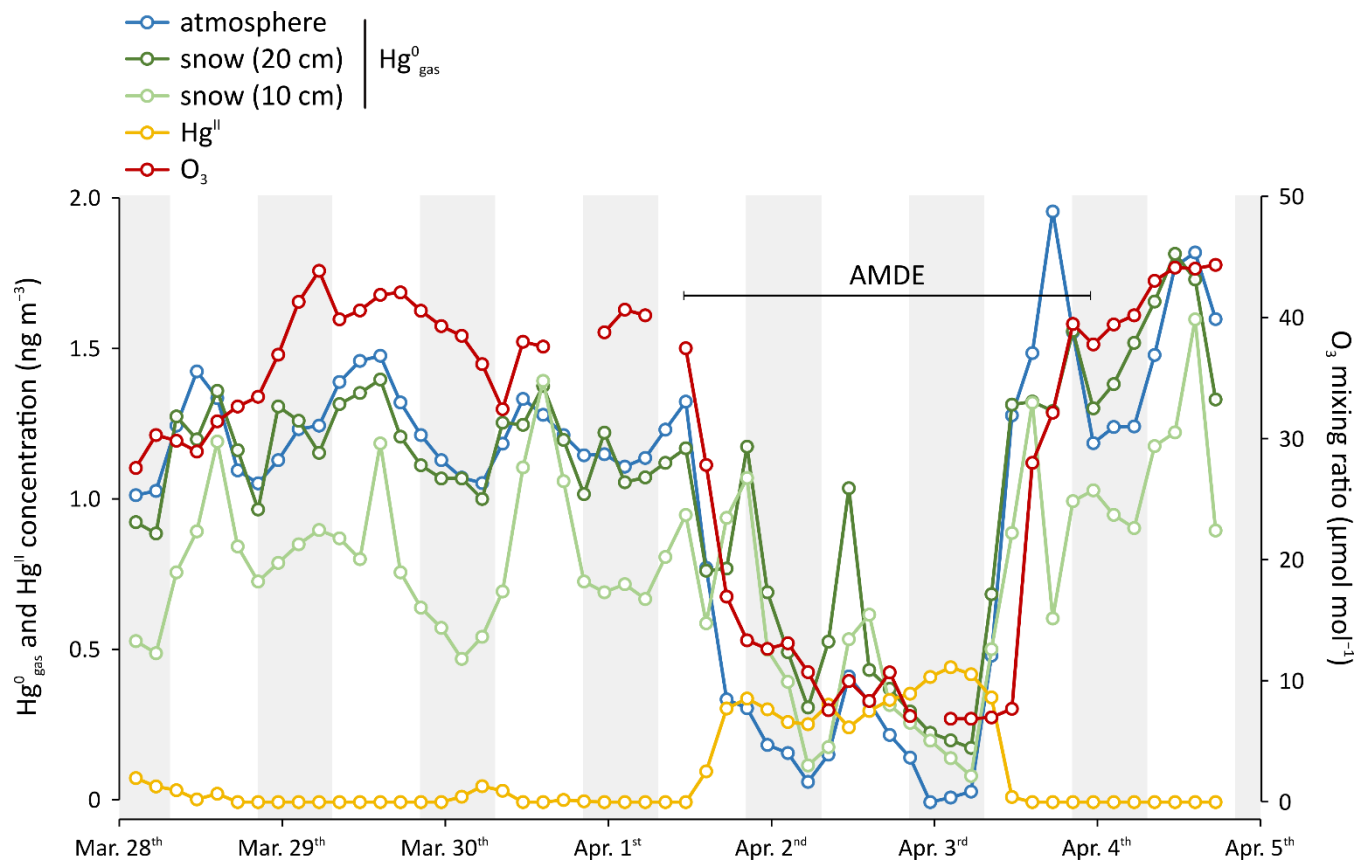


Figure S2: Hg^0_{gas} concentrations (3-hours averages) in the atmosphere and snowpack interstitial air (10 and 20 cm above the ground surface), as well as Hg^{II} and O_3 atmospheric measurements during a week in spring 2016, including an AMDE, measured at Toolik Field Station. The snow height was between 25 and 28 cm and surface snow Hg_{tot} concentrations between 1.00 ± 0.07 (March 25th) and $1.46 \pm 0.16 \text{ ng L}^{-1}$ (April 2nd). The gray bars indicate nighttime periods.

Mercury in ~~areti~~the Arctic tundra snowpack: temporal and spatial concentration patterns and trace-gas exchanges

Yannick Agnan^{1,2}, Thomas A. Douglas³, Detlev Helmig⁴, Jacques Hueber⁴, Daniel Obrist^{5,2}

~~¹Milieux Environnementaux, Transferts et Interactions dans les hydrosystèmes et les Sols (METIS), UMR 7619, Sorbonne Universités UPMC–¹Sorbonne Université, CNRS–, EPHE, 4 place Jussieu UMR Metis, F-75252, Paris, France~~

~~²Division of Atmospheric Sciences, Desert Research Institute, Reno, Nevada 89523, USA~~

~~³US Army Cold Regions Research and Engineering Laboratory, PO Box 35170, Fort Wainwright, Alaska 99709, USA~~

~~⁴Institute of Arctic and Alpine Research, University of Colorado, Boulder, Colorado 80309, USA~~

~~⁵Department of Environmental, Earth, and Atmospheric Sciences, University of Massachusetts, Lowell, MA 01854, USA~~

Correspondence to: Yannick Agnan (yannick.agnan@biogeochimie.fr) and Daniel Obrist (daniel_obrist@uml.edu)

Abstract. In the Arctic, the snowpack forms the major interface between atmospheric and terrestrial cycling of mercury (Hg) ~~eyeling.),~~ a global pollutant. ~~In this study, we~~We investigated Hg dynamics in an interior arctic tundra snowpack in northern Alaska during two snow seasons. Using a snow tower system ~~and soil wells~~ to monitor Hg trace gas exchange ~~of Hg~~, we observed consistent concentration declines of gaseous elemental Hg (Hg^0_{gas}) ~~, the volatile form of Hg,~~ from the atmosphere to the snowpack to soils. ~~This indicates~~The snowpack itself was unlikely a direct sink of for atmospheric Hg^0_{gas} ~~in tundra soils.~~ ~~There. In addition, there~~ was no evidence of photochemical reduction of Hg^{II} to Hg^0_{gas} in the tundra snowpack, ~~unlike in temperate snowpacks,~~ with the exception of short periods during late winter: ~~in the uppermost snow layer. The patterns in this interior arctic snowpack hence differ substantially from observations in arctic coastal and temperate snowpacks.~~ We consistently measured low concentrations of both total (~~Hg_{tot}~~) and dissolved (~~Hg_{diss}~~) Hg in ~~the tundra~~ snowpack throughout the two ~~years (generally <1.0 and 0.3 ng L⁻¹, respectively).~~ seasons. Chemical tracers showed that Hg was mainly associated with local mineral dust and regional marine sea spray inputs. Mass balance calculations ~~of Hg~~ show that the snowpack represents a ~~very~~ small reservoir of Hg, resulting in low inputs during snowmelt ~~(<30 ng m⁻² for Hg_{diss}).~~ The. Taken together, the results from this study suggest that interior arctic snowpacks ~~may be~~are negligible sources of Hg in the Arctic.

1 Introduction

Mercury (Hg) is a neurotoxic pollutant of worldwide importance that is transported over long distances in the atmosphere as gaseous elemental Hg (Hg^0_{gas}) ~~,~~ and thus reaches remote environments (Cobbett et al., 2007; Driscoll et al., 2013; Sprovieri et al., 2010). In the Arctic, modern atmospheric Hg deposition has increased about three-fold from ~~Hg~~ pre-industrialized background levels (Fitzgerald et al., 2005), similar to increases observed across in temperate ~~areas~~ locations, although other studies suggest much stronger increases (e.g., Enrico et al., 2017). The increase in Hg loading has led to vulnerability of polar ecosystems to Hg contamination due to detrimental impacts to wildlife and humans, in particular through biomagnification processes across trophic levels (Atwell et al., 1998).

Representing about 26% of the global land surface area, polar regions are unique environments with specific physical, chemical, and biological processes affecting pollutant cycles including that of Hg (Douglas et al., 2012). In particular, most of the northern latitudes are covered by a laterally continuous snowpack during long periods of the year. In the Alaskan tundra, the surface snow cover is present about two thirds of the year (Cherry et al., 2014). The snowpack hence forms a critical interface between the arctic atmosphere, tundra ecosystems, and underlying tundra soils. Trace gas exchanges between the atmosphere and the tundra are modulated by sinks and sources below and within snowpack, by snow diffusivity, snow height, and snow porosity (Dominé and Shepson, 2002; Lalonde et al., 2002; Monson et al., 2006). The snowpack accumulates nutrients, pollutants, and impurities that are deposited by snowfall and dry deposition processes, all of which can subsequently be transported to underlying ecosystems during snowmelt (Bergin et al., 1995; Uematsu et al., 2000).

The snowpack plays an important role for the cycling of Hg as well, including for atmospheric deposition, photochemical ~~oxidoreduction~~redox reactions, and associated phase changes between solid and gaseous Hg that can volatilize Hg to the atmosphere (Douglas et al., 2008, 2012; Faïn et al., 2013; Mann et al., 2014; Steffen et al., 2013). In particular, ~~many~~-temperate and arctic studies have shown that the snowpack can serve as ~~sinks~~sink or ~~source~~essource of Hg^0_{gas} , whereby photochemical reduction of snow-bound Hg^{II} can produce Hg^0_{gas} and oxidation processes can reversely scavenge atmospheric Hg^0_{gas} in snow (Faïn et al., 2013; Lalonde et al., 2002; Mann et al., 2011). Photochemical reactions occur primarily in the top 10 cm of the snowpack, where sunlight radiation transmits and is absorbed and scattered by snow crystals (Faïn et al., 2007; King and Simpson, 2001). The degree of photochemical production of Hg^0_{gas} and subsequent atmospheric re-volatilization from the snowpack can be ~~very~~-significant, as shown in temperate snowpacks with strong recurring daytime atmospheric emissions of Hg^0_{gas} throughout the winter season (Faïn et al., 2013). In global models, snowpack Hg^0_{gas} emissions ~~have been incorporated~~ can account for ~50% of all snowpack Hg (Corbitt et al., 2011). The reverse process—oxidation of Hg^0_{gas} to Hg^{II} —, has also been proposed to occur in the dark snowpack deeper in the snow profile (Faïn et al., 2007, 2013; Mann et al., 2015), resulting in concentration declines of Hg^0_{gas} with depth in the snowpack. To our knowledge, no direct in situ measurement of snowpack Hg^0_{gas} dynamics, however, is available in the field in the interior arctic snowpack.

In the Arctic and Antarctic, Hg cycling is also ~~is~~ affected by atmospheric Hg depletion events (AMDEs), which are observed primarily in the springtime along coastal locations (Angot et al., 2016a; Dommergue et al., 2010; Schroeder et al., 1998; Steffen et al., 2008). During AMDEs, atmospheric Hg^0_{gas} concentrations fluctuate strongly due to atmospheric conversion of Hg^0_{gas} to oxidized Hg^{II} . Because Hg^{II} is subject to faster deposition (Schroeder and Munthe, 1998; Selin, 2009), AMDEs result in ~~large amounts of~~ Hg temporarily deposited from the atmosphere to the arctic ecosystems. AMDEs are considered to be initiated by halogens (Brooks et al., 2008; Obrist et al., 2011; Steffen et al., 2008), such as bromine and chlorine radicals released from sea salt by photochemical processes (Simpson et al., 2007). AMDEs have been mainly observed along the coasts, e.g., at Barrow in Alaska (Douglas et al., 2008), Alert in Canada (Steffen et al., 2002), Ny-Ålesund in Svalbard (Ferrari et al., 2008), ~~McMurdo~~McMurdo in Antarctica (Brooks et al., 2008), as well as directly over the sea ice (Moore et al., 2014; Nerentorp Mastromonaco et al., 2016). The impacts of AMDEs at inland sites is reduced with increasing distance from the coast (Douglas and Sturm, 2004; Obrist et al., 2017; Van Dam et al., 2013).

The objectives of this study were to characterize Hg dynamics in the inland arctic snowpack at Toolik Field Station, and along a 170-km transect between this site and the arctic coast. For the first time, we comprehensively linked trace gas fluxes of Hg^0_{gas} in interstitial snow air with the seasonal development of total Hg (Hg_{tot}) and dissolved Hg (Hg_{diss}) bound in the snowpack to assess conversions between volatile and solid Hg in the arctic snowpack. We specifically aimed to assess: (1) temporal and vertical Hg^0_{gas} patterns to quantify exchanges of Hg^0_{gas} in the atmosphere–snowpack–soil continuum; (2) impacts of springtime AMDEs on snowpack Hg deposition to and emission from the inland arctic snowpack; (3) temporal and vertical concentration and mass patterns of the snowpack Hg_{tot} and Hg_{diss} , to estimate Hg deposition throughout the snow accumulation period and pool of Hg available through snow melt; and (4) relationships of snow Hg concentrations with major ion concentrations and oxygen and hydrogen stable isotopes in precipitation to determine potential origins of Hg contained in the snowpack.

2 Materials and methods

2.1 Study site

Measurements were mainly performed at Toolik Field Station (Alaska, USA) over two full snow cover seasons from October 2014 to May 2016. The research station is located on the north slopes of the Brooks Range (68° 38' N, 149° 36' W) at an elevation of 720 m a.s.l., approximately 200 km south of the Arctic Ocean (Fig. 1, orange bullet). The lithology (Fig. 1, orange bullet). The area is characterized by gently sloping hills comprised of poorly drained silty loams underlain by continuous permafrost 250–300 m deep (Barker et al., 2014). Lithology is characterized by glacial till over Cretaceous sedimentary substrates (shale, claystone, siltstone, and sandstone; Alaska Division of Oil and Gas, 2008). The ecotype is classified as an acidic tussock tundra (Shaver and Chapin, 1991) with vegetation composed of scrubby plants (e.g., *Cassiope tetragona* (L.) D. Don, *Arctostaphylos alpinus* (L.) Spreng.), shrubs (e.g., *Betula nana* L., *Salix pulchra* Cham.), tussock grasses (*Carex*), and a variety of mosses and lichens. The mean annual air temperature is -8.5°C , and mean annual precipitation is 312 mm (Cherry et al., 2014). In the two measurement years, the tundra was covered by snow for 236 and 248 days (i.e., 65 and 68% of the year) in the 2014–2015 and 2015–2016 seasons, respectively.

Snowpack sampling was also performed along a transect between Toolik and the Arctic Ocean in March 2016 (Fig. 1, (Fig. 1, yellow bullets). The full Detailed geographical details characteristics of the sample sites are given in Table S1–Table S1. A total of eight study sites were sampled from south (500 m a.s.l.) to north (20 m a.s.l.). All the sampled sites were characterized by similar ecosystems and lithology (including undifferentiated volcanic Upper Tertiary beds to the north) as described above for the Toolik area.

2.2 Trace gas in the atmosphere, interstitial snow air, and soil pores

We continuously sampled and analyzed interstitial air of the tundra snowpack at Toolik using a snow tower (Fig. S1)(Fig. S1) as described in detail by Seok et al. (2009) and Faïn et al. (2013). In summary, a snow tower consists of an air inlet manifold placed in the snowpack, so sampling of trace gases can be remotely alternated between various snow depths for undisturbed

sampling of interstitial snow air throughout an entire snow season. The snow tower used at Toolik consisted of six 60 cm aluminum cross arms mounted at heights of 0, 10, 20, 30, 40, and 110 cm above the ground surface. ~~Two trace gas~~Gas inlets were mounted to each cross arm allowing vertical sampling of snow interstitial air ~~and subsequent~~for analysis for multiple trace gases, including Hg^0_{gas} , CO_2 , and O_3 . Each cross arm ~~of the snow tower~~ supported a pair of air inlets fitted with 25 mm syringe filters with 1 μm glass fiber membranes (Pall Life Sciences, Ann Arbor, MI, USA). Perfluoroalkoxy Teflon® tubing with equal lengths (35 m) were directed ~~within~~ a heated conduit to solenoid valves in the laboratory that allowed for sequential sampling of trace gases at the six different snowpack heights. The snow tower was deployed over the tundra in August of each year prior to the onset of snowfall. When the snow tower was subsequently covered by the accumulating snowpack, this set-up allowed sequentially continuous sampling of snow interstitial air ~~from the adjacent laboratory~~ without any disturbance. Inlets were sampled sequentially, ~~5–10~~ min at a time; ~~(i.e., averages of two individual measurements of 5 min)~~, resulting in a ~~30–60~~-min sampling cycle. Corresponding trace gas sampling was performed below the snowpack in tundra soils at depths of 10, 20, and 40 cm using Teflon® soil trace gas wells (Obrist et al., 2014, 2017). ~~Both organic and mineral soil profiles were considered in this study, distant of 5 m as described in Obrist et al. (2017).~~ Atmospheric air sampling was performed using the top snow tower air ~~inlet~~inlets which always ~~was~~were above the developing snowpack, as well as on a nearby micrometeorological tower at a height of 3.6 m above ground. All interstitial snow, soil pore, and atmospheric inlets were connected by Teflon® tubing and solenoid valves to trace gas monitors in a nearby (10–30 m distance) field laboratory that were operated year-round.

Gaseous Hg^0 concentrations were measured using two Tekran 2537B analyzers (Tekran Instruments Corporation, Toronto, ON, Canada), one ~~shared~~ for interstitial snow air ~~and atmospheric~~ measurements, and the other shared for soil gas and atmospheric measurements. ~~The discrepancy in Hg^0_{gas} measurements observed between the two Tekran instruments along the two seasons was on average 7%; concentration data showed here were adjusted.~~ Air sampling was alternated between different snowpack heights every 5 min so that a full sequence of air extraction from the snowpack (six inlet heights) was achieved every 30 min. Interstitial snow, soil pore, and atmospheric measurements continued through the entire winter with only small-time periods of interruptions due to power failures or other technical problems. Additional trace gases were measured along with Hg^0_{gas} , including concentrations of CO_2 using a LI-840A (LI-COR Inc., Lincoln, NE, USA).

2.3 Snow sampling and physical and chemical characterization

2.3.1 Snow sampling

At Toolik, we characterized Hg in the snowpack both over the undisturbed tundra and the adjacent frozen Toolik Lake (within 200 m of the tundra location). ~~Snow~~Two snow pits were sampled on five dates between October and May in the 2014–2015 season, and on four dates between December and June in 2015–2016. For each pit, we vertically excavated snow samples using a stainless-steel snow cutter (RIP 1 cutter 1000 cc), clean latex gloves, and trace metal Nasco Whirl-Pak® (The Aristotle Corporation, Stamford, CT, USA) HDPE plastic bags. We sampled at 10 cm-layer increments from the top to the bottom of

the snowpack. ~~Two replicate samples~~ Samples from two perpendicular walls of the pit were each pooled together per layer for analysis. Snow height, density, and ~~temperatures~~ temperature were measured for each layer, and frozen snow samples were stored in a cooler before transferring to a -20°C freezer. Snow water equivalent (SWE), which represents the amount of water stored in the snowpack, was calculated using snow density measurements in incremental 10 cm-layers, multiplied by snow height. Additional sampling of surface snow was performed over the tundra for a total of 17 sampling dates. The top 3 cm of the snowpack was collected in triplicate within a distance of 5 m into Nasco Whirl-Pak® plastic bags using clean latex gloves. Sampling along the south to north transect was performed over two days in March 2016.

2.3.2 Chemical analyses

In the laboratory, we ~~stored~~ melted snow samples overnight in the Nasco Whirl-Pak® bags at room temperature in the dark, and melted snow samples were subsequently analyzed for Hg. A fraction of snowmelt was directly transferred to 50 mL polypropylene tubes (Falcon®, Corning Incorporated, Corning, NY, USA) for analysis of Hg_{tot} . For Hg_{diss} , snowmelt water was filtered using 0.45 μm Acrodisc® filter with polyethersulfone membrane (Pall Corporation, Port Washington, NY, USA) into 50 mL Falcon® polypropylene tubes. In addition, filtered meltwater was used in 60 mL high-density polyethylene tubes (VWR®, Radnor, PA, USA) for determination of major cations, anions, and stable isotopes (^2H and ^{18}O). ~~Hg_{tot}~~ Total Hg and Hg_{diss} concentrations were determined using Tekran 2600 cold-vapor atomic fluorescence spectrometry (Tekran Instruments Corporation, Toronto, ON, Canada) using a bromine monochloride (BrCl) digestion and reduction by stannous chloride (SnCl_2) following ~~the~~ EPA method 1631 (US EPA, 2002). The detection limits, ~~(DL)~~, determined as 3-times the standard deviation of blank samples, averaged 0.08 ng L^{-1} . For statistic purpose, values below the ~~detection limit (DL)~~ were included as $0.5 \times \text{DL}$. ~~Recoveries~~ Analyzer performance was determined by 5 ng L^{-1} standards analyzed every 10 samples, and recovery averaged between 93 and 107%. Laboratory and field blanks were conducted, and we evaluated any potential metal contamination of the stainless-steel snow cutter by analyzing Milli-Q water in contact with the snow cutter; all these blank determinations were bellow detection limits.

Major cation and anion concentrations were quantified at the U.S. Army Cold Regions Research and Engineering Laboratory's (CRREL) Alaska Geochemistry Laboratory on Fort Wainwright, Alaska, with a Dionex ICS-3000 ion chromatograph. An AS-19 anion column and a CS-12A cation column (Dionex Corporation Sunnyvale, California) were used, each with a $10\text{ }\mu\text{L}$ injection volume. A gradient method using potassium hydroxide ~~eluent ranged from (20 to 35 $\mu\text{mol L}^{-1}$ in concentration)~~ was used for anion analyses, while cation analyses used methane sulfonic acid eluent with a concentration of $25\text{ }\mu\text{mol L}^{-1}$ in isocratic mode. The flow rate was 1 mL min^{-1} and the operating temperature was 30°C . The ion chromatograph was calibrated using standards with a range ~~of values~~ from 0.5 to 50 mg L^{-1} . Repeat analyses of calibration standards from 0.5 to 50 mg L^{-1} yielded a ~~calculated~~ precision for the analyses of $\pm 5\%$. Peaks were identified using Chromeleon (Dionex) and verified visually. Stable isotopes of oxygen and hydrogen were also measured at CRREL Alaska using Wavelength-Scanned Cavity Ringdown Spectroscopy on a Picarro L2120i (Sunnyvale, California). Standards and samples were injected into the analyzer for seven separate analyses. Results from the first four injections were not used to calculate the stable isotope values to eliminate internal

system memory. The mean value from the final three sample injections was used to calculate the mean and standard deviation value for each sample. Values are reported in standard per mil notation. Repeated analyses of five internal laboratory standards representing a range of values spanning the samples analyzed and analyses of SMOW, GISP, and SLAP standards (International Atomic Energy Agency) were used to calibrate the analytical results. Based on thousands of these standards analyses and of sample duplicate analyses we estimate the precision is $\pm 0.2\text{‰}$ for $\delta^{18}\text{O}$ and $\pm 0.5\text{‰}$ for $\delta^2\text{H}$.

2.4 Data processing and statistical analyses

We performed all data processing and statistical analyses with RStudio 1.1.383 (RStudio Inc., Boston, Massachusetts, USA) using R 3.4.2 (R Foundation for Statistical Computing, Vienna, Austria). Averaged data and variance in figures and tables are shown as mean \pm standard deviation. Significant differences were determined with the Kruskal-Wallis test ($\alpha = 0.05$). We performed plots with *ggplot2*, *ggtern*, and *lattice* R packages, and used normality (eq L^{-1}) for the ternary diagram. Geographical maps were prepared using Quantum GIS 2.18 (Quantum GIS Development Team, 2017).

3 Results and discussion

3.1 Snowpack development and snowpack physics

Due to high wind conditions in the Arctic tundra (Cherry et al., 2014), the physical development of the snowpack and its depth and the thickness of wind slab layers at Toolik were subject to significant drifts and changes in snowpack height, and were hence highly variable spatially and temporally throughout the winter season. The average snow height over the tundra site (shown in gray bars in ~~Fig. 2~~Fig. 2) was continuously measured in both winters using a camera set to record daily pictures and using reference snow stakes placed in the snowpack. In the 2014–2015 season, the average snowpack height was 37 cm, with a standard deviation of 12 cm and a maximum depth of 60 cm. In the 2015–2016 season, the snowpack was almost half of that of the previous year, with an average snowpack height of 19 cm, a standard deviation of 7 cm, and a maximum depth of 35 cm.

Based on snow pit measurements in the 2014–2015 season, we observed an increase of snow density with time, from an average of 0.18 g cm^{-3} in October to 0.26 g cm^{-3} in March (blue lines in ~~Fig. 2~~Fig. 2). No clear temporal pattern was observed in the 2015–2016 season when average snow density; it ranged between 0.28 and 0.30 g cm^{-3} . ~~Snow water equivalent (SWE), which represents the amount of water stored in the snowpack, was calculated using snow density measurements in incremental 10 cm layers, multiplied by snow height.~~ Results showed similar temporal evolution as snow heights, with maximum SWE observed in March in both snow seasons of 158 and 116 mm, respectively.

Snowpack temperatures were highly variable throughout the seasons and also strongly differed vertically within the snowpack (red lines in ~~Fig. 2~~Fig. 2). Temperatures ranged from -34 to 0°C in the top of the snowpack and from -21 to -1°C in the bottom of the snowpack; temperatures ~~always~~ showed strong increases from the top to the bottom of the snowpack, illustrating

the important insulating function that the snowpack has in the cold Arctic winter and spring months. Minimum snowpack temperatures were recorded during the January 26th 2015 sampling event when air temperatures were -40°C .

The snowpack over the adjacent frozen lake showed an average density of 0.23 g cm^{-3} and temperatures ranged between -18 and 0°C . The snow height over Toolik Lake was much lower than that over the tundra, with snow heights consistently $<15\text{ cm}$ for both seasons. The maximum SWE calculated above the lake was 40 and 42 mm for the two snow seasons, respectively.

The transect between Toolik and the Arctic Ocean performed in March 2016 showed snowpack height ranging between 30 and 66 cm. The maximum height was observed at one site located 55 km from the Arctic Ocean ~~(where~~ presence of dense shrubs up to 40 cm height~~)~~. induced accumulation of local drifting snow due to high roughness. Snow density (between 0.19 and 0.26 g cm^{-3}) and temperatures (between -20 and -10°C) followed the same trends as observed at Toolik with decreasing density and increasing temperatures with snowpack thickness. The calculated SWE averaged 104 mm and ranged between 70 and 164 mm.

3.2 Hg⁰_{gas} Gaseous Hg⁰ in the atmosphere–snowpack–soil continuum

3.2.1 Hg⁰_{gas} Gaseous Hg⁰ concentration profiles

Gaseous Hg⁰ concentrations were measured at Toolik over two years in the atmosphere, in snowpack interstitial air at up to five inlet heights, and in soil pore air in the tundra ecosystem. Data coverage was 183 and 207 days for the 2014–2015 and 2015–2016 seasons, respectively, with only few periods when system failures resulted in lack of data. A continuous temporal record of the Hg⁰_{gas} concentration profile in the snowpack is presented in Fig. 3a for the 2014–2015 season, i.e., when the snowpack was deeper compared to the 2015–2016 season ~~(Fig. 3a)~~, and compared to the literature a similar record from a temperate ~~snowpacks (Fig. 3b)~~ snowpack based on published data (Fig. 3b; Faïn et al., 2013). The; note different y-scale of figure panels. In addition, full time-averaged atmosphere–snowpack–soil Hg⁰_{gas} diffusion profiles are shown for the entire two winter seasons: 2014–2015 ~~(Fig. 4a)~~ (Fig. 4a–c) and 2015–2016 ~~(Fig. 4d)~~ (Fig. 4d–f). For Fig. 4, Hg⁰_{gas} Gaseous Hg⁰ concentrations were averaged for each season for three different periods, i.e., November to December (representing early winter and full darkness), January to February (representing mid-winter and full darkness), and March to April (when sunlight emerged and when occasional AMDEs were active). Note that standard deviations indicate natural fluctuations in Hg⁰_{gas} concentrations as observed in Obrist et al. (2017).

The Hg⁰_{gas} measurements consistently showed strong concentration gradients in the atmosphere–snowpack–soil continuum with highest concentrations in the atmosphere (on average, 1.18 ± 0.13 and $1.09 \pm 0.13\text{ ng m}^{-3}$, respectively) and lowest concentrations in soils (mostly often below the detection limits for both years, i.e., <0.05 of 0.10 ng m^{-3}). This pattern was consistent over two independent soil profiles measured at this site, one mainly consisting of organic soils and one soil profile dominated by mineral soil horizons. Hg⁰_{gas} concentrations in the snowpack were in-between the two concentration in the atmosphere and in soils, and showed pronounced patterns of decreasing concentrations from the top to the bottom of the snow profile. In the first year, Hg⁰_{gas} concentrations decreased from the top snowpack inlet (i.e., 40 cm above the ground; average

Hg⁰_{gas} concentration of 1.18 ng m⁻³) to the lower snowpack sampling heights (30, 20, and 10 cm above the ground; average Hg⁰_{gas} concentrations of 1.11, 1.00, and 0.76 ng m⁻³, respectively), and showed the lowest Hg⁰_{gas} concentrations at the soil–snowpack interface (0 cm: 0.53 ng m⁻³). Due to a much shallower snowpack in the 2015–2016 season and an absence of measurements at 0 cm height due to line freezing of the lowest inlet, the profile of Hg⁰_{gas} was less pronounced compared to 2014–2015. However, we similarly found a Hg⁰_{gas} decline from upper to lower snowpack heights (e.g., Hg⁰_{gas} concentrations of 1.09 ng m⁻³ in the atmosphere, 1.02 ng m⁻³ at 20 cm, and 0.88 ng m⁻³ at 10 cm height above ground). In a previous paper, we reported a small rate of continuous Hg⁰_{gas} deposition from the atmosphere to the tundra—measured by a micrometeorological tower—during much of the snow-covered season, with the exception of short time periods in spring when AMDEs occurred at Toolik (Obrist et al., 2017). Here, we show that these flux measurements are supported by consistent Hg⁰_{gas} concentration gradients that existed through both seasons and that showed that snowpack Hg⁰_{gas} concentrations were consistently lower than atmospheric levels above. In addition, snowpack Hg⁰_{gas} declined with depth in the snowpack and were lowest in the underlying soil, showing evidence of a consistent Hg⁰_{gas} concentration gradient from the atmosphere to surface snow to tundra soils.

The top of the snowpack (ranging between 2 and 12 cm from depth below the atmosphere—depending on snow interface depth) generally showed ~~the~~ highest Hg⁰_{gas} concentrations ~~that were~~ close to ~~ambient air background~~ concentrations measured in the atmosphere. This pattern is inconsistent with other arctic snowpack measurements that showed atmospheric Hg⁰_{gas} concentrations higher than those in snowpack (Angot et al., 2016b; Steffen et al., 2014). Indeed, the uppermost snowpack Hg⁰_{gas} concentrations can reach 3-times the atmospheric levels in the interior Antarctic regions (Angot et al., 2016b). It also differed to patterns observed in lower latitude snowpacks: in the Rocky Mountains, for example, the upper snowpack showed strong enrichments of Hg⁰_{gas} throughout most of the winter (i.e., up to 6-times higher concentrations than in the atmosphere; Fig. 3b, Faïn et al., 2013). Such Hg⁰_{gas} concentration enrichments were attributed to strong photochemically initiated reduction of snow-bound Hg^{II} to Hg⁰_{gas} (Lalonde et al., 2002). The implications of Hg⁰_{gas} production is that subsequent volatilization of the Hg⁰_{gas} from the porous snowpack to the atmosphere can alleviate atmospheric deposition loads, and it is estimated that globally 50% of snow-bound Hg is volatilized back to the atmosphere prior to snowmelt (Corbitt et al., 2011). Our trace gas concentration measurements showed that Hg⁰_{gas} re-volatilization does not occur in this interior tundra snowpack during most of the winter. An absence of direct solar radiation likely explains the lack of photochemical Hg⁰_{gas} formation and volatilization between December through mid-January. Yet, springtime is a photochemically active period in the arctic when strong Hg⁰_{gas} volatilization from snow has been reported further north along the Arctic Ocean coast (Brooks et al., 2006; Kirk et al., 2006). snow season. Even in late spring, when abundant solar radiation is present (400–600 W m⁻²), however, Hg⁰_{gas} volatilization losses were rare and largely limited to periods of active AMDEs. We speculate that a reason for the general lack of Hg⁰_{gas} formation and volatilization in snow includes substrate limitation due to low snow Hg_{tot} concentrations (Fig. 2). An alternative possibility may be that our sampling setup (between 5 and 7 cm below the surface during the three main AMDEs) may have limited our ability to detect and observe photo-reduction processes that may occur only in the upper few cm of the snowpack surface (King and Simpson, 2001; Poulain et al., 2004). However, ~~this pattern changed in using the same measurement system,~~

Hg^0_{gas} concentration enhancements in temperate snowpacks were large (up to 8 ng m^{-3}) and detectable up to a depth of $>90 \text{ cm}$ from the snowpack surface (Fig. 3b). Unlike in Faïn et al. (2013), we also did not observe Hg^0_{gas} formation after fresh snowfall, although it also is important to note that snowfall amounts at Toolik were much lower than in temperate snowpack.

During March and April ~~when atmospheric, snowpack~~ Hg^0_{gas} concentrations were highly variable ~~as a result of ongoing~~ AMDEs (Fig. 4e and Fig. 4(Figs. 4c and f)). During one of these periods shown in Fig. S2, Hg^0_{gas} concentrations in the snowpack showed variable Hg^0_{gas} levels generally following Hg^0_{gas} concentration changes in the atmosphere above, indicating an apparently high snowpack diffusivity (Fig. S2). During these time periods in March and April, snowpack Hg^0_{gas} concentrations in the top snowpack at times exceeded concentrations in the atmosphere above, as shown in Fig. S2. Periods when snowpack Hg^0_{gas} concentrations exceeded concentrations in the atmosphere occurred during (less than 5% of the time), and these occurrences were mainly related to periods of AMDEs when Hg^0_{gas} depletion occurred in the overlying atmosphere. Our measurements of Hg^0_{gas} showed that early spring was the only time period when we observed small rates of Hg^0_{gas} formation in the uppermost snowpack layer, suggesting some photochemical reduction and re-volatilization of Hg^0_{gas} after AMDE-Hg deposition. However, Hg^0_{gas} production was small, limited in time, and no photochemical Hg^0_{gas} production or re-emission was observed in deeper snow layers, suggesting that the process was limited to the snowpack surface. These patterns in March and April were also consistent with flux measurements when we observed periods of net Hg^0_{gas} emission from the tundra ecosystem to the atmosphere (Obrist et al., 2017), in support of the typical Hg dynamics often reported during AMDEs (Hg^{II} deposition followed by photochemical reduction and Hg^0_{gas} re-emission; Ferrari et al., 2005). We propose that, in addition to relatively infrequent and generally weaker AMDE activity, rapid photochemical re-emission losses of Hg following AMDEs render these events relatively unimportant as a deposition source of Hg in this interior arctic tundra site. We provided support for this notion using stable Hg isotope analysis in soils from this site in Obrist et al. (2017), which showed that atmospheric Hg^0_{gas} is the dominant Hg source to the interior tundra snowpack accounting for over 70% of Hg present. Meanwhile, the soil pore air Hg^0_{gas} showed concentrations consistently below those measured in the snowpack (often below detection limits with an average concentration of 0.06 ng m^{-3}). Highest soil pore Hg^0_{gas} concentrations were measured in October and November for both years, after which soil pore Hg^0_{gas} concentrations declined and stayed mainly below the detection limits of our system ($<0.05 \text{ ng m}^{-3}$) between December and May. This pattern was consistent for two independent soil profiles measured at this site, one mainly representing an organic soil profile and one profile dominated by mineral soil horizons.

3.2.2 Snowpack diffusivity of trace gases

A key question pertaining to the wintertime snowpack Hg^0_{gas} concentration profiles and measured deposition is if the observed Hg^0_{gas} deposition and concentration declines in the snowpack are driven by Hg^0_{gas} sinks in the snowpack or by Hg^0_{gas} uptake by underlying tundra soils. Sinks of Hg^0_{gas} in the snowpack have been observed in a few studies (Dommergue et al., 2003; Faïn et al., 2008, 2013) and ~~We~~ have been attributed to dark oxidation of Hg^0_{gas} to divalent, non-volatile Hg^{II} , possibly including oxidation by halogen species, O_3 , or related to NO_x chemistry. To address this question, we compared the ratios of Hg^0_{gas} to

CO₂ gradients in the snowpack to determine commonality or differences between sinks and sources of both gases. Because CO₂ in the atmosphere is relatively stable in winter and soils are the only wintertime source, CO₂ can be used to assess how the snowpack affects diffusion and advective exchange processes between soils and the atmosphere. Comparing Hg⁰_{gas} to CO₂ allows assessment of whether Hg⁰_{gas} concentrations in the snowpack are driven by processes in the underlying soils (i.e., similar to CO₂) or if in-snowpack chemistry affects Hg⁰_{gas} concentration profiles. The gas diffusion model, based on Fick's first law of diffusion, is defined as follows, Eq. (1):

$$F = -D \left(\frac{\delta C}{\delta z} \right) \quad (1)$$

where F is the molecular flux in the snowpack airspace (mol m⁻² s⁻¹), D is the diffusivity in the snowpack airspace (m² s⁻¹), and $\delta C/\delta z$ is the gas concentration gradient in the snowpack integrated in the snow depth (mol m⁻⁴).

Since diffusivity is determined by both snowpack porosity and tortuosity—both of which are poorly known and not directly measured—, we used the flux ratios between Hg⁰_{gas} and CO₂ to determine if both gases show similar flux behavior across the snowpack (Faïn et al., 2013), Eq. (2):

$$\frac{F_{Hg^0_{gas}}}{F_{CO_2}} = \frac{D_{Hg^0_{gas}}}{D_{CO_2}} \times \frac{\Delta_{Hg^0_{gas}}}{\Delta_{CO_2}} \quad (2)$$

where $\Delta_{Hg^0_{gas}}$ and Δ_{CO_2} are the $\delta C/\delta z$ gradients for both Hg⁰_{gas} and CO₂, respectively. Assuming similar gas diffusivity for

both Hg⁰_{gas} and CO₂, the ratio of concentration gradients of the two gases ($\Delta_{Hg^0_{gas}}/\Delta_{CO_2}$) gives direct information about their respective flux ratios between different snowpack trace gas inlets. Please note that these fluxes are in the opposite direction.

We focused our analysis of Hg⁰_{gas} and CO₂ concentration gradients at Toolik for the month of January 2015, when the snow height was among the highest (approximately 40 cm), and when strong decreases in interstitial Hg⁰_{gas} concentrations from the top to the bottom of the snowpack were present. At this time, soils still were a relatively active source of CO₂ to the snowpack (Fig. 5)(Fig. 5), facilitating a comparison to the soil CO₂ source. In contrast to Hg⁰_{gas} (Fig. 5a)(Fig. 5a), profiles for CO₂ showed strong increases in concentrations with increasing depth in the snowpack (Fig. 5b)(Fig. 5b). Highest CO₂ concentrations were present in the soil (up to 5000 μmol mol⁻¹, data not shown), and these patterns are consistent with an expected source of soils for CO₂ and diffusive and advective mixing of CO₂ produced in snow through the snowpack with the atmosphere (Liptzin et al., 2009; Oechel et al., 1997). Analysis of $\Delta_{Hg^0_{gas}}/\Delta_{CO_2}$ ratios showed no statistically significant differences from the top to the bottom of the snowpack, as evidenced from calculated gradients between 0 to 10 cm, 10 to 20 cm, and 20 to 30 cm heights (Fig. 5c)(Fig. 5c).

The constant and negative ratios between CO₂ and Hg⁰_{gas} and the fact that CO₂ is largely non-reactive in snowpack hence indicates that Hg⁰_{gas} also was not subject to snowpack chemical reactions; both profiles are affected by underlying soil processes, i.e., soil sources for CO₂ and soil sinks (for Hg⁰_{gas}). These wintertime atmosphere-snowpack-soil Hg⁰_{gas} concentration profiles at Toolik were also consistent with a measured net deposition of Hg⁰_{gas} throughout winter using flux measurements (Figs. 2 and 4; Obrist et al., 2017). Both net flux measurements, combined with snowpack Hg⁰_{gas} concentration profiles, hence suggest that a soil Hg⁰_{gas} sink was active throughout the Arctic winter, notably under very cold wintertime soil

temperatures as low as -15°C . Such soil Hg_{gas}^0 sinks were previously reported to occur in temperate soils (Obrist et al., 2014), although the mechanisms for the Hg_{gas}^0 sinks are currently not clear. It is notable that $\Delta_{\text{Hg}_{\text{gas}}^0}/\Delta_{\text{CO}_2}$ ratios in the upper snowpack (i.e., between 20 and 30 cm height) were more variable compared to lower snowpack heights, which we attribute to ~~Snowpack chemistry and snowbound mercury~~. Snowpack and surface snow much smaller concentrations differences for both CO_2 and Hg_{gas}^0 between these inlets.

~~3.2.3 Total and dissolved mercury concentrations~~

3.3 Snowbound mercury in the interior arctic snowpack

3.3.1 Spatial patterns

~~Snow~~ samples were analyzed at Toolik for Hg_{tot} and Hg_{diss} (Fig. 2 and Table S1). ~~Tundra snowpack~~ (Fig. 2 and Table S1). Concentrations in snowpack collected over the tundra averaged $0.70 \pm 0.98 \text{ ng L}^{-1}$ for Hg_{tot} concentrations and $0.17 \pm 0.10 \text{ ng L}^{-1}$ for Hg_{diss} concentrations (both seasons, average of entire snowpack height). ~~Mercury content in the surface snow layer (top 3 cm only) averaged $0.53 \pm 0.39 \text{ ng L}^{-1}$ and $0.26 \pm 0.26 \text{ ng L}^{-1}$, respectively, and was not statistically significantly different compared to that of full snow pits or bottom snow layers (averaging 0.49 ± 0.48 and $0.17 \pm 0.12 \text{ ng L}^{-1}$). Total Hg and Hg_{diss} . Total Hg concentrations in the surface snow ranged from 0.18–1.46 were always higher than Hg_{diss} levels, likely due to impurities and 0.04 – 1.15 ng L^{-1} most of the time, respectively (Table S1). The temporal pattern of Hg_{diss} deposition of Hg associated with plant detritus or soil dust, and showed higher variability in Hg_{tot} concentrations of surface snow samples is reported in Fig. 6. No consistent temporal trends in Hg_{tot} or compared to Hg_{diss} . We thus focused our discussions on Hg_{diss} data. Measurements performed at Toolik showed very low levels compared to many other high latitude studies, with Hg_{diss} concentrations averaging 0.17 ng L^{-1} , and ranging between 0.08 and 1.15 ng L^{-1} . This is generally lower than Hg concentrations in interior Arctic sites reported by Douglas and Sturm (2004) (i.e., Hg_{diss} concentrations between 0.5 and 1.7 ng L^{-1}) and at the low end of concentrations found in Arctic studies along the coastal zone (0.14 – 820 ng L^{-1} , for both Hg_{diss} and Hg_{tot} ; Douglas et al., 2005; Douglas and Sturm, 2004; Ferrari et al., 2004, 2005; Kirk et al., 2006; Nerentorp Mastromonaco et al., 2016; St. Louis et al., 2005; Steffen et al., 2002). The low concentrations we measured result in very small pool sizes of Hg_{diss} stored in the snowpack during wintertime compared to temperate studies (Pearson et al., 2015). At Toolik, snowpack pool sizes amounted to 26.9 and 19.7 ng m^{-2} during peak snowpack and prior to the onset of snowmelt in 2014–2015 and 2015–2016, respectively were observed with increasing duration of winter in both seasons, and no correlations were observed with air temperatures (red line). One noticeable period of enhanced surface snow Hg concentrations was April 2016 when both Hg_{tot} and Hg_{diss} concentrations exceeded 1 ng L^{-1} , which was 4 times the average values observed through the rest of the season.~~

The snowpack sampled over the adjacent frozen lake showed Hg_{tot} and Hg_{diss} concentrations of 0.80 ± 0.61 and $0.15 \pm 0.08 \text{ ng L}^{-1}$, respectively. ~~Due to the low snow height on the frozen lake, we were able to collect only one depth sample per snow pit. Total Hg and Hg_{diss} concentrations of snow over the frozen lake (Table S1). These values~~ were not statistically

different ~~in both seasons~~ from concentrations measured in the tundra snowpack. Snowpack Hg_{diss} loads on the frozen lake were lower ($6.2 \pm 0.2 \text{ ng m}^{-2}$), i.e., only about $\frac{1}{4}$, compared to snowpack Hg_{diss} load on the adjacent tundra ($23.3 \pm 5.0 \text{ ng m}^{-2}$). Three reasons may explain the large difference between lake and tundra snowpack Hg loads: (1) the lake did not accumulate the snowpack on open water prior to the lake surface freezing in the early fall (Sturm and Liston, 2003); (2) low surface roughness over the lake likely prevent settling of snowfall and facilitate remobilization of snow by wind transport (Essery et al., 1999; Essery and Pomeroy, 2004); and (3) the lake ice is warmer than the tundra soil resulting in higher sublimation over the lake. The implications of the latter process is a reduction of direct atmospheric deposition over Arctic lakes, and is consistent with studies that estimated that annual Hg contribution to Arctic lakes via direct wet deposition is small, generally less than 20% of total deposition (Fitzgerald et al., 2005, 2014). Spatial redistribution of snow across the tundra landscape further implies that both wet deposition and snow accumulation rates are variable, leading to spatial heterogeneity of snowmelt Hg inputs.

Measurements Most Arctic studies of snowpack Hg have been performed close to the coast (i.e., Alert and Barrow), and few studies include inland sites such as Toolik (Douglas and Sturm, 2004). In our study, measurements of Hg_{tot} and Hg_{diss} in the snowpack across a large North slope transect (about ~~200~~170 km from Toolik to the Arctic Coast) in March, 2016 showed concentrations of 0.70 ± 0.79 and $0.24 \pm 0.20 \text{ ng L}^{-1}$, respectively. (Fig. 6 and Table S3). Concentrations ~~of in~~ Hg_{diss} of the five northernmost ~~stations~~locations (<100 km distance from the Arctic Ocean) were statistically significantly ($p < 0.05$, Kruskal-Wallis test) higher compared to those measured ~~in at~~ the four stations located in the interior tundra (>100 km), which included the Toolik site where ~~the~~ mean Hg_{diss} concentrations were 0.33 ± 0.22 and $0.11 \pm 0.07 \text{ ng L}^{-1}$ for the same period, respectively. These patterns are consistent with previous observations in Alaska in springtime that suggested an ocean influence leading to higher Hg deposition, possibly linked to the presence of halogens (Douglas and Sturm, 2004; Landers et al., 1995; Snyder-Conn et al., 1997). We propose that low snowpack Hg concentrations ($<0.5 \text{ ng L}^{-1}$ for Hg_{diss}) are common in inland northern Alaska areas, and that the interior arctic snowpacks exhibit lower levels compared to coastal locations that are subjected to more significant ocean influences and impacts by AMDEs.

3.3.2 Seasonal patterns

Surface snow that was collected throughout the season can serve as an estimate for atmospheric wet deposition Hg concentrations and loads (Faïn et al., 2011). Concentrations of Hg_{tot} and Hg_{diss} in the surface snow layer (top 3 cm only) averaged $0.53 \pm 0.39 \text{ ng L}^{-1}$ and $0.26 \pm 0.26 \text{ ng L}^{-1}$, respectively (Fig. 7 and Table S1), which were not statistically significantly different compared to that of full snow pits or bottom snow layers. Both, low concentrations measured in surface snow, as well as low pool sizes as discussed above, suggest low wet deposition rates during winter at our inland arctic sites. However, estimation of deposition loads using snow collection can be compromised by quick re-volatilization losses of Hg from fresh snowfall (within the first few hours, e.g., Faïn et al., 2013), or snowmelt losses, but we do not consider these processes to be important at this site. The low Hg_{diss} concentrations measured in surface snow ($0.26 \pm 0.26 \text{ ng L}^{-1}$) are lower than the 10th percentile of wet deposition Hg concentrations reported for Kodiak Island in Alaska during the same time period

(National Atmospheric Deposition Program, 2017). Also, snowfall Hg_{diss} concentrations measured at Alert were between 100 and 200-times higher than in our measurements (A. Steffen, personal communication). Using median concentrations in the surface snow multiplied by the amount of wet deposition for each snow-covered season, we estimated the Hg_{diss} load annually deposited by snowfall to 41.3 and 15.3 ng m^{-2} in the 2014–2015 and 2015–2016 winters, respectively. This is 1/100 of values recently provided from a coastal location 400 km northwest of our study site (Douglas et al., 2017) and 1/200 of long-term measurements from Alert between 1998 and 2010 (A. Steffen, personal communication).

Little temporal variation in snowpack Hg concentrations was observed between the early season snowpack evolving mainly under darkness and the late-season snowpack exposed to solar radiation (Figs. 2 and 6), although some temporal differences were evident during March and April when AMDEs were present in the region. Snowpack Hg_{diss} concentrations averaged 0.16 ng L^{-1} both during the completely dark period (i.e., December and January) and after March 1st. Such patterns support measurements of Hg^0_{gas} throughout the winter that indicated the snowpack to be a relatively inert matrix with little redox processes affecting Hg concentrations (oxidation of Hg^0_{gas} or reduction of Hg^{II}). An apparent trend in surface snow, however, emerged during springtime, when both Hg_{tot} and Hg_{diss} concentrations exceeded 1 ng L^{-1} (i.e., 4-times the average values observed through the rest of the season; Fig. 7). This was a period when AMDEs occurred at this site, as evident by depletions of atmospheric Hg^0_{gas} with formation and deposition of oxidized atmospheric Hg^{II} (Obrist et al., 2017; Van Dam et al., 2013). Surface snow Hg concentration enhancements during AMDEs are commonly reported in polar regions, with at times Hg concentration enhancements up to 100-times the base concentration in the Arctic (Lalonde et al., 2002; Lindberg et al., 1998; Nerentorp Mastromonaco et al., 2016; Poulain et al., 2004; Steffen et al., 2002). The presence of AMDEs generally results in increased deposition of Hg to snow and ice surfaces, yet such additional deposition often is short-lived due to the photochemical re-emission of Hg^0_{gas} (Kirk et al., 2006). (Fig. 7). It is noteworthy that no In our study, we did not have sufficient temporal resolution of snow sampling during the period of AMDEs to closely track the fate of Hg deposition during AMDEs and subsequent re-emissions. However, we find that snow Hg enhancements during AMDEs were much lower than at coastal sites (e.g., Steffen et al., 2014), but a coarse temporal sampling could just have missed peak snow Hg levels at this site. We also found that after AMDEs, snow Hg_{diss} in surface snow declined to levels as was observed prior to AMDEs, and no concentration enhancements were observed in deeper in the snowpack. This is consistent with observations of net Hg^0_{gas} volatilization during that time. The fact that we found no lasting impact of AMDEs on snow Hg concentrations, which also were supported by stable Hg isotope analysis (Obrist et al., 2017), may be due to the large distance to the coast from our study site and the scarcity of AMDEs—and O_3 depletion events—that occur at this inland arctic location (Van Dam et al., 2013). Concentrations of Hg_{diss} measured in the snowpacks at Toolik did not show consistent vertical patterns (Fig. 2). Indeed, the upper snowpack Hg_{diss} concentrations were not significantly different from those in the deeper layers, which is in contrast to patterns observed in arctic snowpacks (Ferrari et al., 2004), as well as in alpine ones (Fäin et al., 2011), where strong concentration enhancements (i.e., more than 2-times the average snowpack concentrations) were observed in the top 3 cm of the snowpack. Seasonal measurements at Toolik indicate a generic lack of atmospheric gaseous Hg^{II} during most of the year and very low amounts of total Hg^{II} deposition, i.e., wet, aerosols, plus gaseous Hg^{II} (Obrist et al., 2017). The lack of significant

Hg^{II} dry deposition would prevent a Hg enhancement in surface snow, and also is consistent with the low pool sizes of Hg in this tundra snowpack. Further support of this notion also includes that snow collected at the surface throughout the arctic winter and spring was not statistically different from snow Hg concentrations contained in the entire snowpack (0.26 ± 0.26 vs 0.17 ± 0.10 ng L⁻¹, respectively). Yet, another factor to explain a lack of depth gradients in snow Hg concentrations may include that snow layers can be continuously mixed and redistributed by wind gust (e.g., gradient concentrations were found in snow across the transect, wind speed of Toolik were >5 m s⁻¹ 12% of the time) across the landscape in the Arctic (Cherry et al., 2014).

3.4 Origin of mercury in the interior arctic snowpack

3.2.43.4.1 Cation and anion concentrations

Major cations (Ca²⁺, K⁺, Mg²⁺, Na⁺, and NH₄⁺) and anions (Cl⁻, NO₃⁻, and SO₄²⁻) were measured in both snowpack and surface snow samples at Toolik (Table 1) to assess the chemical composition and potential origins for Hg in the snowpack (Table 1). Concentrations of these compounds were comparable to other inland Alaskan sites and, similar to concentrations of Hg, were lower than data reported from several arctic coastal locations (de Caritat et al., 2005; Douglas and Sturm, 2004). Surface snow samples (top 3 cm) generally showed somewhat higher Cl⁻ and Na⁺ concentrations and lower Mg²⁺ and K⁺ concentrations than samples collected across the entire snowpack height, although only Mg²⁺ and Na⁺ were significantly different ($p < 0.005$ and $p < 0.05$, respectively). Comparison between tundra and lake snowpack locations showed no statistical differences in elemental concentrations.

Spearman correlation coefficient (ρ) between Hg_{diss} and major ion concentrations were calculated for tundra and lake snowpack samples and surface snow collected over the tundra (Table 2). Using a correlation matrix, three groups of correlated major ions could be determined in the snowpack over the tundra: (1) NH₄⁺ and SO₄²⁻; (2) Ca²⁺, Mg²⁺, and NO₃⁻; (3) Cl⁻, K⁺, and Na⁺. In the tundra snowpack, Hg_{diss} was not statistically significantly ($-0.22 < \rho < 0.11$) correlated to any of these major ion groups when considering the entire depth of the tundra snowpack. Relationships, however, were present in surface snow over the tundra where Hg_{diss} was correlated (ρ up to 0.80) with Ca²⁺, Cl⁻, and K⁺, indicating that Hg_{diss} may have originated from a mix of natural sources possibly linked to both mineral dust (Ca²⁺) and sea spray (Cl⁻). The lack of strong correlation between Hg_{diss} and Na⁺ ($\rho = 0.30$) in surface snow samples may indicate that a part of Cl⁻ originated from mineral dust as CaCl₂. A minor influence of sea salt was consistent with coastal observations that showed the highest Hg concentrations close to the Arctic Ocean related particularly to active bromine chemistry (Fig. 6; Douglas and Sturm, 2004). In addition, local or regional dust from rock and soil weathering contributed to the wintertime Hg deposition, particularly at interior sites close to the Brooks Range where higher snow pH reported were from mineral dust that contained carbonates (Douglas and Sturm, 2004). Indeed, the mountain influence was dominant during the two snow-covered seasons at Toolik where 50% of snow events and 80% of dry periods (i.e., periods without snowfall, 90% of the time) came from the south (i.e., Brooks Range). An additional group of correlated elements was identified in surface snow samples over the tundra: NH₄⁺, NO₃⁻, and SO₄²⁻ strongly

correlated (ρ up to 0.80) with Ca^{2+} , Cl^- , and K^+ . An additional group of correlated elements was identified in surface snow samples: NH_4^+ , NO_3^- , and SO_4^{2-} . The Note that the low number of lake snowpack samples (≤ 12) did not allow us to perform a meaningful correlation matrix analyses for lake snowpack samples.

To ~~better~~ further visualize the relationships between analytes, we plotted a ternary diagram using three end-members according to Garbarino et al. (2002), Krnavek et al. (2012), Poulain et al. (2004), and Toom-Sauntry and Barrie (2002) ~~(Fig. 8)~~. (Fig. 8).

We considered Ca^{2+} as one end-member to represent a potential crustal signature, a second end-member with Cl^- as a sea salt signature, and a third end-member with SO_4^{2-} as a potential anthropogenic signature, i.e., from regional or long-range transport.

Since sea salt SO_4^{2-} represented on average less than 1.2% of total SO_4^{2-} according to the calculation of Norman et al. (1999), we consider SO_4^{2-} not indicative of an ocean source. The different snow types (surface snow over the tundra, tundra snowpack, and lake snowpack) are presented with different colors in ~~the Figure~~ Fig. 8, and Hg_{diss} concentrations are represented by different symbol sizes. Relative ~~contributions~~ concentrations of Cl^- (i.e., sea salt influence) ~~in samples~~ showed statistically significant differences between snow samples collected over the tundra and those collected over the frozen lake ~~locations~~ (on average, 14 and 24% of proportion based on normality data, respectively; $p < 0.05$), ~~but~~. However, no statistically significant differences were observed for relative concentrations of Ca^{2+} and SO_4^{2-} between tundra and lake locations. In general, snow

surface samples showed ~~very~~ low SO_4^{2-} and Cl^- relative concentrations ($< 30\%$) compared to integrated snowpack samples.

Overall, Hg_{diss} concentrations were weakly correlated, except according to the SO_4^{2-} relative concentrations: Hg_{diss} concentrations averaged 0.10 and 0.17 ng L^{-1} for $> 30\%$ and $< 30\%$ of SO_4^{2-} , respectively ($p < 0.005$). These patterns indicate that anthropogenic influences from combustion processes were minor or absent for snow Hg deposition. In fact, Alaska generally showed the lowest SO_4^{2-} concentrations among arctic sites (de Caritat et al., 2005). Norman et al. (1999) also reported

relatively small contributions of anthropogenic SO_4^{2-} in snow at Alert (Canada). From this, we propose that the Hg sources in the arctic snowpack is mainly derived from local lithological erosion, and that Arctic Ocean sources are minor contributions.

However, this is not likely the case of Hg_{gas}^0 in tundra soils which mainly derived from global sources (Obrist et al., 2017). It should be noted that the proximity of Toolik with a busy road in the Arctic (the Dalton Highway) may influenced our measurements, but this is difficult to evaluate.

The lack of consistent statistically significant associations between major ions and Hg_{diss} across the entire snowpack depth (Table 2a) further suggest that initial snowfall Hg content was maintained and largely unaltered after deposition, with no clear accumulation or depletion zones as found in other snowpacks (Ferrari et al., 2005; Poulain et al., 2004; Steffen et al., 2014).

We found a small relative enrichment of alkaline earth elements in snowpack samples compared to surface snow, which indicates some additional contributions of local mineral dust, yet this did not result in a measurable increase in snowpack Hg

levels. Hence, we suggest no significant additional deposition of Hg (e.g., by dry deposition of gaseous or particulate Hg) to exposed older snow consistent with the lack of correlation to pollution tracers (SO_4^{2-} and NO_3^-).

We also suggest an absence or minor importance of re-emission losses or elution losses from snow melt as occurs in temperate snowpacks (discussed in Fäin et al. (2013) and Pearson et al. (2015)). Oxygen Elution losses are unlikely, given that no temperatures above freezing

were present in the Arctic until May, and atmospheric re-emissions losses of volatile Hg^0_{gas} were not important in this arctic snowpack for most of the season as discussed above.

3.2.53.4.2 Stable oxygen and hydrogen isotope signatures

Oxygen (^{18}O) and hydrogen (^2H) isotopes are frequently used as tracers for precipitation sources (Gat, 2010). The stable isotope signatures in surface snow samples collected at Toolik are presented in a $\delta^2\text{H}$ vs $\delta^{18}\text{O}$ diagram for different ranges of Hg_{diss} concentrations and different sampling dates (Fig. 9a(Fig. 9a). All the samples were distributed close to the global meteoritic water line (Craig, 1961). Despite a large variability in values (from -18.3 to -41.3‰ for $\delta^{18}\text{O}$ and from -140 to -314‰ for $\delta^2\text{H}$), samples collected on the same date were relatively close (mean standard deviation of 0.88 and 6.5‰ , respectively). No clear relationships were observed between isotope signatures and ~~dissolved Hg~~ Hg_{diss} concentrations (with size scale in Fig. 9Fig. 9) across the entire spectrum of values. However, samples with high Hg_{diss} concentrations (e.g., the three highest measured in April 2nd, 2016) and low Hg_{diss} concentrations (e.g., samples below the detection limit in December 5th, 2015) were found clustered together at similar $\delta^{18}\text{O}$ and $\delta^2\text{H}$ values. The $\delta^{18}\text{O}$ values were also plotted against air temperatures (T_{air}) during the snowfall events (Fig. 9b)(Fig. 9b). A statistically significant linear relationship was found between the two variables ($r^2 = 0.50$) with the lowest $\delta^{18}\text{O}$ values being measured during the coldest temperatures.

4 Discussions

4.1 Gas-phase mercury exchanges in the snowpack and photochemical processes

~~We continuously measured Hg^0_{gas} concentrations and diffusion patterns in the atmosphere-snowpack-soil continuum throughout the two snow seasons at Toolik (Fig. 3 and Fig. 4). The measurement of trace gas concentration patterns allows determination of the direction of atmosphere-surface exchanges as trace gas exchange must follow concentration gradients (Sommerfeld et al., 1996). In a previous paper, we reported a small rate of continuous Hg^0_{gas} deposition from the atmosphere to the tundra—measured by a micrometeorological tower—during much of the snow-covered season, with the exception of short time periods in spring during the occurrence of AMDEs at Toolik (Obrist et al., 2017). Here, we show that these flux measurements are supported by consistent Hg^0_{gas} concentration gradients that existed through both seasons and that showed that snowpack Hg^0_{gas} concentrations were consistently lower than atmospheric levels in the snowpack. In addition, snowpack Hg^0_{gas} declined with depth in the snowpack and were lowest in the underlying soil, showing evidence of a consistent Hg^0_{gas} concentration gradient from the atmosphere to surface snow to tundra soils.~~

~~It is important to mention that our Hg^0_{gas} concentration profiles in the arctic snowpack are inherently different to patterns observed in lower-latitude snowpacks. In the Rocky Mountains, for example, the upper snowpack showed strong enrichments of Hg^0_{gas} throughout most of the winter (i.e., up to 6 times higher concentrations than in the atmosphere; Fig. 3b, Fäin et al., 2013). Such Hg^0_{gas} concentration enrichments were attributed to strong photochemically initiated reduction of snow-bound Hg^{II} to Hg^0_{gas} (Lalonde et al., 2002). The implications of Hg^0_{gas} production is that subsequent volatilization of the Hg^0_{gas} from~~

the porous snowpack to the atmosphere can alleviate atmospheric deposition loads and it is estimated that globally 50% of snow-bound Hg is volatilized back to the atmosphere prior to snowmelt (Corbitt et al., 2011). Our trace gas concentration measurements showed that Hg^0_{gas} re-volatilization is missing in this interior tundra snowpack during most of the winter, and the absence of direct solar radiation likely explains the lack of photochemical Hg^0_{gas} formation and volatilization between December through mid-January. Yet, springtime is a photochemically active period in the arctic when strong Hg^0_{gas} volatilization from snow has been reported further north along the Arctic Ocean coast (Brooks et al., 2006; Kirk et al., 2006). Even in late spring, when abundant solar radiation is present, however, Hg^0_{gas} volatilization losses were rare and largely limited to periods of active AMDEs. We speculate that a reason for the general lack of Hg^0_{gas} formation and volatilization in snow includes substrate limitation due to very low total snow Hg concentrations (Fig. 2, see below), several times lower compared to concentrations in temperate snowpacks (Faïn et al., 2013).

A key question pertaining to the wintertime Hg^0_{gas} concentration profiles and measured deposition is if the observed Hg^0_{gas} deposition and concentration declines in the snowpack are driven by Hg^0_{gas} sinks in the snowpack or by Hg^0_{gas} uptake by the underlying tundra. Sinks of Hg^0_{gas} in the snowpack have been observed in a few studies (Dommergue et al., 2003; Faïn et al., 2008, 2013) and attributed to dark oxidation of Hg^0_{gas} to divalent, non-volatile Hg^{II} , possibly including oxidation by halogen species, O_3 , or related to NO_x chemistry. To address this question, CO_2 serves as a tracer for soil contributions since soils are the only active wintertime sources of CO_2 . Because the concentration gradients are directly related to the flux ratios, the consistent $\Delta_{\text{Hg}^0_{\text{gas}}}/\Delta_{\text{CO}_2}$ values through the snowpack provide evidence that the two trace gases are transported similarly through the snowpack, although in opposite direction as shown by negative ratio values (Fig. 5). This illustrates that the Hg^0_{gas} uptake occurs in soils rather than in the snowpack.

A soil Hg^0_{gas} sink was previously reported to occur in temperate soils (Obrist et al., 2014), although the mechanisms for the Hg^0_{gas} sinks are currently not clear. Our observations hence indicate that the tundra snowpack was not an active sink for atmospheric Hg^0_{gas} , but rather represented a porous and relatively unreactive matrix that reflected a strong concentration gradient between the atmosphere and tundra soils. The wintertime atmosphere-snowpack-soil Hg^0_{gas} concentration profiles at Toolik were consistent with a measured net deposition of Hg^0_{gas} throughout winter (Fig. 2 and Fig. 4; Obrist et al., 2017). Both net flux measurements and observations within the snowpack hence suggest that a soil Hg^0_{gas} sink was active throughout the Arctic winter, notably under very cold wintertime soil temperatures as low as -15°C . It is notable that $\Delta_{\text{Hg}^0_{\text{gas}}}/\Delta_{\text{CO}_2}$ ratios in the upper snowpack (i.e., between 20 and 30 cm height) were more variable compared to lower snowpack heights, which we attribute to higher variability in upper snowpack concentrations due to variable atmospheric Hg^0_{gas} levels. Strong variations of Hg^0_{gas} concentrations were observed in the atmosphere—particularly during springtime (Fig. S2)—, supporting the notion of snowpack as a highly porous matrix that is in strong diffusive and advective exchange with atmospheric trace gas concentrations (Fig. 5).

Springtime was the only period when occasional Hg^0_{gas} concentration enhancements in the uppermost snowpack were present (less than 5% of the time) while deeper snowpack Hg^0_{gas} concentrations remained at low levels (Fig. S2). Our measurements

of Hg^0_{gas} showed that during March and April was the only time when we observed small rates of Hg^0_{gas} formation in the uppermost snowpack layer, suggesting some photochemical reduction and re-volatilization of Hg^0_{gas} after AMDE-Hg deposition. However, the Hg^0_{gas} production was small, limited in time, and no photochemical Hg^0_{gas} production and re-emission was observed from deeper snow layers suggesting that the process was limited to the snowpack surface. March and April were also the only months when we observed periods of net Hg^0_{gas} flux emission from the tundra ecosystem to the atmosphere (Obrist et al., 2017), in further support of the typical Hg dynamics reported during AMDEs (Hg^{II} deposition, photochemical reduction, Hg^0_{gas} re-emission; Ferrari et al., 2005). We propose that in addition to relatively weak and infrequent AMDE activity and Hg deposition in this interior arctic tundra, rapid photochemical re-emission losses of Hg following AMDEs render these events relatively unimportant as a deposition source of Hg. We provided support for this notion using stable Hg isotope analysis in soils from this site in Obrist et al. (2017) which showed that atmospheric Hg^0_{gas} is the dominant source to the interior tundra snowpack.

4.2 Spatial and temporal patterns of snowbound mercury in the interior arctic snowpack

Concentrations of Hg_{tot} and Hg_{diss} were measured in the snowpack overlying a tundra ecosystem at Toolik, a snowpack over the adjacent frozen Toolik Lake, and the tundra snowpack along a 170 km transect between Toolik and the Arctic Ocean (Fig. 2, Fig. 7, and Table S1). Total Hg concentrations in all snow samples collected (i.e., tundra snowpack, lake snowpack, and surface snow) were always much higher than Hg_{diss} levels, likely due to impurities and deposition of Hg associated with plant detritus or soil dust. This also resulted in much higher variability of Hg_{tot} concentrations compared to Hg_{diss} concentrations. Due to the high variability in Hg_{tot} concentrations we focused our discussions on Hg_{diss} data. The measurements performed at Toolik showed low levels compared to many other high latitude studies, with Hg_{diss} concentrations averaging 0.17 ng L^{-1} and ranging between 0.08 and 1.15 ng L^{-1} , which is at the low end of concentration ranges reported in other studies mainly focused along the coastal zone (0.14 – 820 ng L^{-1} for both Hg_{diss} and Hg_{tot} ; Douglas et al., 2005; Douglas and Sturm, 2004; Ferrari et al., 2004, 2005; Kirk et al., 2006; Nerentorp Mastromonaco et al., 2016; St. Louis et al., 2005; Steffen et al., 2002). The low concentrations we measured result in very small pool sizes of Hg_{diss} stored in the snowpack during wintertime compared to temperate studies (Pearson et al., 2015). At Toolik, snowpack pool sizes amounted to 26.9 and 19.7 ng m^{-2} during peak snowpack and prior to the onset of snowmelt in 2014–2015 and 2015–2016, respectively. Most other Arctic studies were performed close to the coast (i.e., Alert and Barrow), and few studies include inland sites such as Toolik (about 200 km south of the Arctic Ocean). Measurements performed along the transect across the Alaska North Slope (from Toolik to the Arctic Coast) in March 2016 indicated Hg_{diss} concentrations decreased significantly from the Arctic Ocean coast to inland (Figure 7). This is consistent with previous observations in Alaska in springtime that suggested an ocean influence on the presence of halogens in the coastal atmosphere resulting in higher Hg deposition (Douglas and Sturm, 2004; Landers et al., 1995; Snyder-Conn et al., 1997). We propose that low snowpack Hg concentrations ($<0.5 \text{ ng L}^{-1}$ for Hg_{diss}) are common in inland northern Alaska areas and that the interior arctic snowpacks exhibit lower levels compared to coastal locations that are subjected to a more significant ocean influences and impacts by AMDEs.

To our surprise, no consistent vertical patterns of Hg_{diss} concentrations were found in the snowpack at Toolik (Fig. 2) and along the 200 km transect to the Arctic Coast (Fig. 7). Thus, upper snowpack Hg_{diss} concentrations were not significantly different from those in the deeper layers, which is in contrast to patterns observed in the Sierra Nevada snowpack where strong concentration enhancements (i.e., more than 2 times the average snowpack concentrations (Fain et al., 2011) were observed in the top 3 cm of the snowpack. This is likely due to lower atmospheric dry deposition inputs in this remote tundra atmosphere compared to more industrialized lower latitudes. Indeed, seasonal measurements at Toolik indicate a generic lack of atmospheric gaseous Hg^0 during most of the year and very low amounts of total Hg^0 deposition, i.e., wet aerosols, plus gaseous Hg^0 (Obrist et al., 2017). The lack of significant Hg^0 dry deposition would prevent a Hg enhancement in surface snow and also is consistent with the low pool sizes of Hg in this tundra snowpack. Further support of this notion also includes that fresh snow collected at the surface throughout the arctic winter and spring was not statistically different from snow Hg concentrations contained in the entire snowpack (0.26 ± 0.26 vs $0.17 \pm 0.10 \text{ ng L}^{-1}$, respectively). Yet, another factor to explain a lack of depth gradients in snow Hg concentrations may include that snow layers can be continuously mixed and redistributed by wind gust (e.g., $>5 \text{ m s}^{-1}$ 12% of the time) across the landscape in the Arctic (Cherry et al., 2014).

We observed significant differences in the amount of Hg contained in the snowpacks over the tundra and over the adjacent Toolik Lake. In fact, while Hg_{diss} concentrations were not statistically significantly different between tundra and lake snow (Table S1), snowpack Hg_{diss} loads on the frozen lake were much lower ($6.2 \pm 0.2 \text{ ng m}^{-2}$), i.e., only about 1/4, compared to snowpack Hg_{diss} load on the adjacent tundra ($23.3 \pm 5.0 \text{ ng m}^{-2}$). Two reasons may explain the large discrepancy between lake and tundra snowpack Hg loads: (1) lake would not accumulate the snowpack on open water prior to lake freezing in the early fall; (2) low surface roughness over the lake may prevent settling of snowfall and facilitate remobilization of snow by wind transport (Essery et al., 1999; Essery and Pomeroy, 2004). The implication of this process is a reduction of direct atmospheric deposition over Arctic lakes which is consistent with studies that estimated that annual Hg contribution to lakes via wet deposition is small, generally less than 20% of total deposition (Fitzgerald et al., 2005, 2014). Such spatial redistribution of snow across the tundra landscape further implies that both wet deposition and snow accumulation rates are variable leading to spatial heterogeneity of snowmelt Hg inputs.

Little temporal variation in snowpack Hg concentrations was observed between the early season snowpack evolving mainly under darkness and the late season snowpack exposed to solar radiation (Fig. 2 and Fig. 6) although some temporal differences were evident during March and April when AMDEs were present in the region. Snowpack Hg_{diss} concentrations averaged 0.16 ng L^{-1} both during the completely dark period (i.e., December and January) and after March 1st. Such patterns support measurements of Hg^0_{gas} throughout the winter that indicated the snowpack to be a relatively inert matrix with little oxidoreduction reactions (oxidation of Hg^0_{gas} or reduction of Hg^{II}). An apparent trend in surface snow, however, emerged during springtime when Hg_{diss} concentrations reaching 1.15 ng L^{-1} were temporally measured in surface layers (Fig. 6) in April 2016. This was a period when AMDEs occurred at this site, as evident by depletions of atmospheric Hg^0_{gas} with formation and deposition of oxidized atmospheric Hg^{II} (Obrist et al., 2017; Van Dam et al., 2013). Surface snow Hg concentration enhancements during AMDEs are commonly reported in polar regions, with at times Hg concentration enhancements up to

100-times the base concentration in the Arctic (Lalonde et al., 2002; Lindberg et al., 1998; Nerentorp Mastromonaco et al., 2016; Poulain et al., 2004; Steffen et al., 2002). The presence of AMDEs generally results in increased deposition of Hg to snow and ice surfaces, yet such additional deposition often is short lived due to the photochemical re-emission of Hg^0_{gas} (Kirk et al., 2006). In our study, snow Hg_{diss} in surface snow quickly declined to levels similar to what was observed prior to AMDEs, and no corresponding concentration enhancements were observed deeper in the snowpack. The influence on snow Hg concentrations was therefore small compared to most studies reporting snow Hg enhancement during AMDEs. We attribute this to the large distance to the coast from our study site and the scarcity of AMDEs and O_3 depletion events that occur at this inland arctic location (Van Dam et al., 2013). Hence, minor impacts of AMDEs can be present in the interior arctic tundra as evident by patterns observed at Toolik some 200 km south of the Arctic Ocean.

Fresh surface snow that was collected throughout the season can serve as a proxy for atmospheric wet deposition Hg concentrations and loads (Faïn et al., 2011). Both low concentrations measured in fresh surface snow as well as low pool sizes as discussed above suggest low wet deposition rates during winter at our inland arctic sites. Estimation of deposition loads by snow collection can be compromised by quick re-volatilization losses of Hg from fresh snowfall (within the first few hours, e.g., Faïn et al., 2013), or snowmelt losses, but we do not consider these processes to be important at this site. The low Hg_{diss} concentrations measured in surface snow ($0.26 \pm 0.26 \text{ ng L}^{-1}$) be lower than the 10th percentile of wet deposition Hg concentrations reported for Kodiak Island in Alaska during the same period (National Atmospheric Deposition Program, 2017). For comparison, snowfall Hg_{diss} concentrations measured at Alert were between 100 and 200 times higher than in our measurements (A. Steffen, personal communication). Using median concentrations in the surface snow multiplied by the amount of wet deposition for each snow covered season, we estimated the Hg_{diss} load annually deposited by snowfall to 41.3 and 15.3 ng m^{-2} in the 2014–2015 and 2015–2016, respectively. This is up to 100 times lower than values recently provided from a coastal location 400 km northwest of our study site (Douglas et al., 2017) and up to 200 times lower than long term measurements from Alert between 1998 and 2010 (A. Steffen, personal communication).

4.31.1 Origin of mercury in the interior arctic snowpack

Major cation (Ca^{2+} , K^+ , Mg^{2+} , Na^+ , and NH_4^+) and anion (Cl^- , NO_3^- , and SO_4^{2-}) values are used to assess the chemical composition and potential origins for Hg in the snowpack (Pearson et al., 2015; Table 1). Three main sources of major ions have been identified in snow deposition in North America by several authors (de Caritat et al., 2005; Krnavek et al., 2012; Poulain et al., 2004; Toom Saunty and Barrie, 2002): (1) marine with sea spray (associated with Na^+ and Cl^-); (2) lithogenic with rock and soil dust (associated with Ca^{2+} and Mg^{2+}); and (3) anthropogenic with long range acid pollution (associated with NH_4^+ and SO_4^{2-}). Results of correlation matrices (Table 2b) indicated that Hg_{diss} in the fresh surface snow (i.e., top 3 cm) originated from a mix of natural sources, possibly linked to both mineral dust (Ca^{2+}) and sea spray (Cl^-). The correlation between Ca^{2+} and Cl^- ($\rho = 0.69$), as well as the absence of correlation between Hg_{diss} and Na^+ ($\rho = 0.30$), in surface snow samples likely indicated that a part of Cl^- was originated from mineral dust as CaCl_2 . A minor influence of sea salt was consistent with coastal observations that showed the highest Hg concentrations close to the Arctic Ocean related to bromine

chemistry (Fig. 7; Douglas and Sturm, 2004). In addition, local or regional dust from rock and soil weathering contributed to the wintertime Hg deposition, particularly at the interior sites close to the Brooks Range where higher snow pH reported were from mineral dust that contained carbonates (Douglas and Sturm, 2004). Indeed, the mountain influence was dominant during the two snow-covered seasons at Toolik: 50% of snow events and 80% of dry periods (i.e., periods without snowfall, 90% of the time) coming from the south. Finally, the ternary diagram of major ions showed the highest Hg_{diss} concentrations were measured in snow with the lowest SO_4^{2-} (Fig. 8), indicating that anthropogenic influence from combustion processes was minor or absent for snow Hg deposition. In fact, Alaska generally showed the lowest SO_4^{2-} concentrations among Arctic sites (de Caritat et al., 2005). Norman et al. (1999) also reported relatively small contributions of anthropogenic SO_4^{2-} in snow at Alert (Canada). From this, we propose that the Hg sources in the arctic snowpack is mainly derived from local lithological erosion, and that Arctic Ocean sources are minor contributions.

The lack of consistent statistically significant associations between major ions and Hg_{diss} across the entire snowpack depth (Table 2a) suggests that the original snowfall Hg content was maintained and largely unaltered after deposition, with no clear accumulation or depletion zones as found in other snowpacks (Ferrari et al., 2005; Poulain et al., 2004; Steffen et al., 2014). We found a small, relative enrichment of alkaline earth elements in snowpack samples compared to surface snow, which indicates some additional contributions of local mineral dust, yet this did not result in a measurable increase in snowpack Hg levels. Hence, we suggest no significant additional deposition of Hg (e.g., by dry deposition of gaseous or particulate Hg) to exposed older snow consistent with the lack of correlation to pollution tracers (SO_4^{2-} and NO_3^-). We also suggest largely an absence of re-emission losses or elution losses from snow melt as occurs in temperate snowpacks (discussed in Fain et al. (2013) and Pearson et al. (2015)). Elution losses are unlikely given that no temperatures above freezing were present in the Arctic until May, and atmospheric re-emissions losses of volatile Hg^0_{gas} were not important in this arctic snowpack for most of the season as discussed above.

Water stable isotope signatures in wet deposition indicated that some of the highest concentrations of Hg_{diss} (April 2016) were present when snow showed consistent values of $\delta^2\text{H}$ and $\delta^{18}\text{O}$ averaging -245.8 and -32.0‰ , respectively (Fig. 9). However, similar water isotope signatures were found also when Hg_{diss} concentrations were lower (e.g., November and December 2015), so that no significant associations of isotope signatures with Hg concentrations were found. Neither the origin of precipitation as shown by the wide range of stable isotope ratios, nor the physical conditions that often causes isotopic variation in precipitation (e.g., air temperatures that explain up to 50% of isotopic values via mass effects (Siegenthaler and Oeschger, 1980)), apparently, shaped the Hg concentrations measured in snow the snowpack.

5.4 Conclusions

In this study, we investigated snow Hg dynamics in the interior arctic tundra at Toolik Field Station, Alaska, simultaneously analyzing Hg in: (1) the gas-phase (Hg^0_{gas}) of the atmosphere, interstitial snowpack, and soil pores; and (2) in the solid phase in snow (Hg_{tot} and Hg_{diss}). Gaseous Hg^0 in the atmosphere-snowpack-soil continuum showed consistent concentration patterns

throughout most of the snow season, ~~whereby with~~ the arctic tundra soil ~~servesserving~~ as a continuous sink for Hg^0_{gas} , important to consider in Arctic Hg cycling. To our surprise, photochemical formation of Hg^0_{gas} in the snowpack was largely absent and played a ~~very~~ minor role in the interior tundra largely limited to periods of active AMDEs. These observations are in contrast with strong photochemical formation of Hg^0_{gas} in surface snow observed at temperate sites and along the arctic coast, resulting in significant photochemical losses of Hg^0_{gas} from these snowpacks. This calls for a regional adjustment of photochemical Hg^0_{gas} losses from the snowpack in models, which should ~~be treated differently in~~ have different treatment for the arctic snowpack compared to temperate snowpacks. Small Hg_{diss} enhancements were temporarily observed in surface snow during springtime, when AMDEs were present, reflecting the typical sequence of Hg deposition to the top snowpack followed by fast photochemical volatilization losses of Hg^0_{gas} during that time. At this interior arctic site, AMDEs, however, resulted in negligible deposition loads. Low concentrations of both Hg_{tot} and Hg_{diss} were measured in the snowpack across this northern Alaska region, resulting in a small reservoir of Hg stored in this snowpack available for potential mobilization during snowmelt ($<30 \text{ ng m}^{-2}$ for Hg_{diss}). These low values suggest that wet Hg deposition via snow is not a major source of Hg to this interior arctic site, a notion we previously supported by direct measurements and stable Hg isotopes that showed that two thirds of the Hg source are derived from Hg^0_{gas} deposition. Multielement analysis of ~~fresh~~ surface snow (top 3 cm) indicated that arctic snowpack Hg originated from a mix of diffuse and likely natural sources, including local mineral dust (associated with Ca^{2+} and Mg^{2+}) and, to a lesser extent, regional marine sea spray (associated with Cl^- and Na^+).

Acknowledgements

We thank Toolik Field Station staff for their support in this project over two years, especially Jeb Timm, Joe Franish, and Faye Ethridge, for helping ~~us~~ with snow collection. We also thank Martin Jiskra (Geosciences Environnement Toulouse) and Christine Olson (DRI) for their field support, Christopher Pearson, Olivia Dillon, and Jacob Hoberg (DRI) for their support with laboratory analyses, and Dominique Colegrove and Tim Molnar (University of Colorado) for helping with field work and data processing. We finally thank Alexandra Steffen for providing mercury snow data from Alert. Funding was provided by the U.S. National Science Foundation (NSF) under award (#PLR 1304305) and cooperative agreement from National Aeronautics and Space Administration (NASA EPSCoR NNX14AN24A).

References

Alaska Division of Oil and Gas: Regional geology of the north slope of Alaska, 2008.

Angot, H., Dastoor, A., De Simone, F., Gårdfeldt, K., Gencarelli, C. N., Hedgecock, I. M., Langer, S., Magand, O., Mastromonaco, M. N., Nordstrøm, C., Pfaffhuber, K. A., Pirrone, N., Ryjkov, A., Selin, N. E., Skov, H., Song, S., Sprovieri, F., Steffen, A., Toyota, K., Travníkov, O., Yang, X. and Dommergue, A.: Chemical cycling and deposition of atmospheric mercury in polar regions: review of recent measurements and comparison with models, *Atmospheric Chem. Phys.*, 16(16), 10735–10763, doi:10.5194/acp-16-10735-2016, 2016a.

- Angot, H., Magand, O., Helmig, D., Ricaud, P., Quennehen, B., Gallée, H., Del Guasta, M., Sprovieri, F., Pirrone, N., Savarino, J. and Dommergue, A.: New insights into the atmospheric mercury cycling in central Antarctica and implications on a continental scale, *Atmospheric Chem. Phys.*, 16(13), 8249–8264, doi:10.5194/acp-16-8249-2016, 2016b.
- 5 Atwell, L., Hobson, K. A. and Welch, H. E.: Biomagnification and bioaccumulation of mercury in an arctic marine food web: insights from stable nitrogen isotope analysis, *Can. J. Fish. Aquat. Sci.*, 55(5), 1114–1121, doi:10.1139/f98-001, 1998.
- Barker, A. J., Douglas, T. A., Jacobson, A. D., McClelland, J. W., Ilgen, A. G., Khosh, M. S., Lehn, G. O. and Trainor, T. P.: Late season mobilization of trace metals in two small Alaskan arctic watersheds as a proxy for landscape scale permafrost active layer dynamics, *Chem. Geol.*, 381, 180–193, doi:10.1016/j.chemgeo.2014.05.012, 2014.
- 10 Bergin, M. H., Jaffrezo, J.-L., Davidson, C. I., Dibb, J. E., Pandis, S. N., Hillamo, R., Maenhaut, W., Kuhns, H. D. and Makela, T.: The contributions of snow, fog, and dry deposition to the summer flux of anions and cations at Summit, Greenland, *J. Geophys. Res. Atmospheres*, 100(D8), 16275–16288, doi:10.1029/95JD01267, 1995.
- Brooks, S., Lindberg, S., Southworth, G. and Arimoto, R.: Springtime atmospheric mercury speciation in the McMurdo, Antarctica coastal region, *Atmos. Environ.*, 42(12), 2885–2893, doi:10.1016/j.atmosenv.2007.06.038, 2008.
- 15 Brooks, S. B., Saiz-Lopez, A., Skov, H., Lindberg, S. E., Plane, J. M. C. and Goodsite, M. E.: The mass balance of mercury in the springtime arctic environment, *Geophys. Res. Lett.*, 33(L13812), doi:10.1029/2005GL025525, 2006.
- de Caritat, P., Hall, G., Gislason, S., Belsey, W., Braun, M., Goloubeva, N. I., Olsen, H. K., Scheie, J. O. and Vaive, J. E.: Chemical composition of arctic snow: concentration levels and regional distribution of major elements, *Sci. Total Environ.*, 336(1), 183–199, doi:10.1016/j.scitotenv.2004.05.031, 2005.
- 20 Cherry, J. E., Déry, S. J., Cheng, Y., Stieglitz, M., Jacobs, A. S. and Pan, F.: Climate and hydrometeorology of the Toolik Lake region and the Kuparuk River basin, in *Alaska's changing arctic: ecological consequences for tundra, streams, and lakes*, edited by J. E. Hobbie and G. W. Kling, pp. 21–60, Oxford University Press, New York., 2014.
- Cobbett, F. D., Steffen, A., Lawson, G. and van Heyst, B. J.: GEM fluxes and atmospheric mercury concentrations (GEM, RGM and Hg_p) in the Canadian Arctic at Alert, Nunavut, Canada (February–June 2005), *Atmos. Environ.*, 41(31), 6527–6543, doi:10.1016/j.atmosenv.2007.04.033, 2007.
- 25 Corbitt, E. S., Jacob, D. J., Holmes, C. D., Streets, D. G. and Sunderland, E. M.: Global source-receptor relationships for mercury deposition under present-day and 2050 emissions scenarios, *Environ. Sci. Technol.*, 45(24), 10477–10484, doi:10.1021/es202496y, 2011.
- Craig, H.: Isotopic variations in meteoric waters, *Science*, 133(3465), 1702–1703, doi:10.1126/science.133.3465.1702, 1961.
- 30 Dominé, F. and Shepson, P. B.: Air-snow interactions and atmospheric chemistry, *Science*, 297(5586), 1506–1510, doi:10.1126/science.1074610, 2002.
- Dommergue, A., Ferrari, C. P., Poissant, L., Gauchard, P.-A. and Boutron, C. F.: Diurnal cycles of gaseous mercury within the snowpack at Kuujuarapik/Whapmagoostui, Québec, Canada, *Environ. Sci. Technol.*, 37(15), 3289–3297, doi:10.1021/es026242b, 2003.
- 35 Dommergue, A., Sprovieri, F., Pirrone, N., Ebinghaus, R., Brooks, S., Courteaud, J. and Ferrari, C. P.: Overview of mercury measurements in the Antarctic troposphere, *Atmospheric Chem. Phys.*, 10(7), 3309–3319, doi:10.5194/acp-10-3309-2010, 2010.

- Douglas, T. A. and Sturm, M.: Arctic haze, mercury and the chemical composition of snow across northwestern Alaska, *Atmos. Environ.*, 38(6), 805–820, doi:10.1016/j.atmosenv.2003.10.042, 2004.
- Douglas, T. A., Sturm, M., Simpson, W. R., Brooks, S., Lindberg, S. E. and Perovich, D. K.: Elevated mercury measured in snow and frost flowers near Arctic sea ice leads, *Geophys. Res. Lett.*, 32(4), L04502, doi:10.1029/2004GL022132, 2005.
- 5 Douglas, T. A., Sturm, M., Simpson, W. R., Blum, J. D., Alvarez-Aviles, L., Keeler, G. J., Perovich, D. K., Biswas, A. and Johnson, K.: Influence of snow and ice crystal formation and accumulation on mercury deposition to the Arctic, *Environ. Sci. Technol.*, 42(5), 1542–1551, doi:10.1021/es070502d, 2008.
- 10 Douglas, T. A., Loseto, L. L., Macdonald, R. W., Outridge, P., Dommergue, A., Poulain, A., Amyot, M., Barkay, T., Berg, T., Chételat, J., Constant, P., Evans, M., Ferrari, C., Gantner, N., Johnson, M. S., Kirk, J., Kroer, N., Larose, C., Lean, D., Nielsen, T. G., Poissant, L., Rognerud, S., Skov, H., Sørensen, S., Wang, F., Wilson, S. and Zdanowicz, C. M.: The fate of mercury in arctic terrestrial and aquatic ecosystems, a review, *Environ. Chem.*, 9(4), 321–355, doi:10.1071/EN11140, 2012.
- Douglas, T. A., Sturm, M., Blum, J. D., Polashenski, C., Stuefer, S., Hiemstra, C., Steffen, A., Filhol, S. and Prevost, R.: A pulse of mercury and major ions in snowmelt runoff from a small arctic Alaska watershed, *Environ. Sci. Technol.*, 51(19), 11145–11155, doi:10.1021/acs.est.7b03683, 2017.
- 15 Driscoll, C. T., Mason, R. P., Chan, H. M., Jacob, D. J. and Pirrone, N.: Mercury as a global pollutant: sources, pathways, and effects, *Environ. Sci. Technol.*, 47(10), 4967–4983, doi:10.1021/es305071v, 2013.
- [Enrico, M., Le Roux, G., Heimbürger, L.-E., Van Beek, P., Souhaut, M., Chmieleff, J. and Sonke, J. E.: Holocene atmospheric mercury levels reconstructed from peat bog mercury stable isotopes, *Environ. Sci. Technol.*, 51\(11\), 5899–5906, doi:10.1021/acs.est.6b05804, 2017.](https://doi.org/10.1021/acs.est.6b05804)
- 20 Essery, R. and Pomeroy, J.: Vegetation and topographic control of wind-blown snow distributions in distributed and aggregated simulations for an arctic tundra basin, *J. Hydrometeorol.*, 5(5), 735–744, doi:10.1175/1525-7541(2004)005<0735:VATCOW>2.0.CO;2, 2004.
- Essery, R., Li, L. and Pomeroy, J.: A distributed model of blowing snow over complex terrain, *Hydrol. Process.*, 13(1415), 2423–2438, doi:10.1002/(SICI)1099-1085(199910)13:14/15<2423::AID-HYP853>3.0.CO;2-U, 1999.
- 25 Fäin, X., Grangeon, S., Bahlmann, E., Fritsche, J., Obrist, D., Dommergue, A., Ferrari, C. P., Cairns, W., Ebinghaus, R., Barbante, C., Cescon, P. and Boutron, C.: Diurnal production of gaseous mercury in the alpine snowpack before snowmelt, *J. Geophys. Res.*, 112(D21311), doi:10.1029/2007JD008520, 2007.
- 30 Fäin, X., Ferrari, C. P., Dommergue, A., Albert, M., Battle, M., Arnaud, L., Barnola, J.-M., Cairns, W., Barbante, C. and Boutron, C.: Mercury in the snow and firn at Summit Station, Central Greenland, and implications for the study of past atmospheric mercury levels, *Atmos Chem Phys*, 8(13), 3441–3457, doi:10.5194/acp-8-3441-2008, 2008.
- Fäin, X., Obrist, D., Pierce, A., Barth, C., Gustin, M. S. and Boyle, D. P.: Whole-watershed mercury balance at Sagehen Creek, Sierra Nevada, CA, *Geochim. Cosmochim. Acta*, 75(9), 2379–2392, doi:10.1016/j.gca.2011.01.041, 2011.
- Fäin, X., Helmig, D., Hueber, J., Obrist, D. and Williams, M. W.: Mercury dynamics in the Rocky Mountain, Colorado, snowpack, *Biogeosciences*, 10(6), 3793–3807, doi:10.5194/bg-10-3793-2013, 2013.
- 35 Ferrari, C. P., Dommergue, A., Boutron, C. F., Jitaru, P. and Adams, F. C.: Profiles of mercury in the snow pack at Station Nord, Greenland shortly after polar sunrise, *Geophys. Res. Lett.*, 31(3), L03401, doi:10.1029/2003GL018961, 2004.

- Ferrari, C. P., Gauchard, P.-A., Aspö, K., Dommergue, A., Magand, O., Bahlmann, E., Nagorski, S., Temme, C., Ebinghaus, R., Steffen, A., Banic, C., Berg, T., Planchon, F., Barbante, C., Cescon, P. and Boutron, C. F.: Snow-to-air exchanges of mercury in an Arctic seasonal snow pack in Ny-Ålesund, Svalbard, *Atmos. Environ.*, 39(39), 7633–7645, doi:10.1016/j.atmosenv.2005.06.058, 2005.
- 5 Ferrari, C. P., Padova, C., Fäin, X., Gauchard, P.-A., Dommergue, A., Aspö, K., Berg, T., Cairns, W., Barbante, C., Cescon, P., Kaleschke, L., Richter, A., Wittrock, F. and Boutron, C.: Atmospheric mercury depletion event study in Ny-Ålesund (Svalbard) in spring 2005. Deposition and transformation of Hg in surface snow during springtime, *Sci. Total Environ.*, 397(1–3), 167–177, doi:10.1016/j.scitotenv.2008.01.064, 2008.
- 10 Fitzgerald, W. F., Engstrom, D. R., Lamborg, C. H., Tseng, C.-M., Balcom, P. H. and Hammerschmidt, C. R.: Modern and historic atmospheric mercury fluxes in Northern Alaska: global sources and arctic depletion, *Environ. Sci. Technol.*, 39(2), 557–568, doi:10.1021/es049128x, 2005.
- Fitzgerald, W. F., Hammerschmidt, C. R., Engstrom, D. R., Balcom, P. H., Lamborg, C. H. and Tseng, C.-M.: Mercury in the Alaskan arctic, in *Alaska's changing arctic: ecological consequences for tundra, streams, and lakes*, edited by J. E. Hobbie and G. W. Kling, pp. 287–302, Oxford University Press, New York., 2014.
- 15 Garbarino, J. R., Snyder-Conn, E., Leiker, T. J. and Hoffman, G. L.: Contaminants in Arctic snow collected over Northwest Alaskan sea ice, *Water, Air, Soil Pollut.*, 139(1–4), 183–214, doi:10.1023/A:1015808008298, 2002.
- Gat, J. R.: *Isotope hydrology: a study of the water cycle*, World Scientific, London., 2010.
- King, M. D. and Simpson, W. R.: Extinction of UV radiation in arctic snow at Alert, Canada (82°N), *J. Geophys. Res. Atmospheres*, 106(D12), 12499–12507, doi:10.1029/2001JD900006, 2001.
- 20 Kirk, J. L., St. Louis, V. L. and Sharp, M. J.: Rapid reduction and reemission of mercury deposited into snowpacks during atmospheric mercury depletion events at Churchill, Manitoba, Canada, *Environ. Sci. Technol.*, 40(24), 7590–7596, doi:10.1021/es061299+, 2006.
- Krnavek, L., Simpson, W. R., Carlson, D., Domine, F., Douglas, T. A. and Sturm, M.: The chemical composition of surface snow in the Arctic: Examining marine, terrestrial, and atmospheric influences, *Atmos. Environ.*, 50(Supplement C), 349–359, doi:10.1016/j.atmosenv.2011.11.033, 2012.
- 25 Lalonde, J. D., Poulain, A. J. and Amyot, M.: The role of mercury redox reactions in snow on snow-to-air mercury transfer, *Environ. Sci. Technol.*, 36(2), 174–178, doi:10.1021/es010786g, 2002.
- Landers, D. H., Ford, J., Gubala, C., Monetti, M., Lasorsa, B. K. and Martinson, J.: Mercury in vegetation and lake sediments from the U.S. Arctic, *Water, Air, Soil Pollut.*, 80(1–4), 591–601, doi:10.1007/BF01189711, 1995.
- 30 Lindberg, S. E., Hanson, P. J., Meyers, T. P. and Kim, K.-H.: Air/surface exchange of mercury vapor over forests—the need for a reassessment of continental biogenic emissions, *Atmos. Environ.*, 32(5), 895–908, doi:10.1016/S1352-2310(97)00173-8, 1998.
- Liptzin, D., Williams, M. W., Helmig, D., Seok, B., Filippa, G., Chowanski, K. and Hueber, J.: Process-level controls on CO₂ fluxes from a seasonally snow-covered subalpine meadow soil, Niwot Ridge, Colorado, *Biogeochemistry*, 95(1), 151–166, doi:10.1007/s10533-009-9303-2, 2009.
- 35 Mann, E., Meyer, T., Mitchell, C. P. J. and Wania, F.: Mercury fate in ageing and melting snow: development and testing of a controlled laboratory system, *J. Environ. Monit.*, 13(10), 2695–2702, doi:10.1039/C1EM10297D, 2011.

- Mann, E., Ziegler, S., Mallory, M. and O'Driscoll, N.: Mercury photochemistry in snow and implications for arctic ecosystems, *Environ. Rev.*, 22(4), 331–345, doi:10.1139/er-2014-0006, 2014.
- Mann, E. A., Mallory, M. L., Ziegler, S. E., Tordon, R. and O'Driscoll, N. J.: Mercury in Arctic snow: quantifying the kinetics of photochemical oxidation and reduction, *Sci. Total Environ.*, 509–510, 115–132, doi:10.1016/j.scitotenv.2014.07.056, 2015.
- 5 Monson, R. K., Burns, S. P., Williams, M. W., Delany, A. C., Weintraub, M. and Lipson, D. A.: The contribution of beneath-snow soil respiration to total ecosystem respiration in a high-elevation, subalpine forest, *Glob. Biogeochem. Cycles*, 20(GB3030), doi:10.1029/2005GB002684, 2006.
- Moore, C. W., Obrist, D., Steffen, A., Staebler, R. M., Douglas, T. A., Richter, A. and Nghiem, S. V.: Convective forcing of mercury and ozone in the Arctic boundary layer induced by leads in sea ice, *Nature*, 506(7486), 81–84, doi:10.1038/nature12924, 2014.
- 10 National Atmospheric Deposition Program: (NRSP-3), NADP Program Office, Illinois State Water Survey, University of Illinois, Champaign, IL 61820., 2017.
- Nerentorp Mastromonaco, M., Gårdfeldt, K., Jourdain, B., Abrahamsson, K., Granfors, A., Ahnoff, M., Dommergue, A., Méjean, G. and Jacobi, H.-W.: Antarctic winter mercury and ozone depletion events over sea ice, *Atmos. Environ.*, 129, 125–132, doi:10.1016/j.atmosenv.2016.01.023, 2016.
- 15 Norman, A. L., Barrie, L. A., Toom-Sauntry, D., Sirois, A., Krouse, H. R., Li, S. M. and Sharma, S.: Sources of aerosol sulphate at Alert: apportionment using stable isotopes, *J. Geophys. Res. Atmospheres*, 104(D9), 11619–11631, doi:10.1029/1999JD900078, 1999.
- Obrist, D., Tas, E., Peleg, M., Matveev, V., Faïn, X., Asaf, D. and Luria, M.: Bromine-induced oxidation of mercury in the mid-latitude atmosphere, *Nat. Geosci.*, 4(1), 22–26, doi:10.1038/ngeo1018, 2011.
- 20 Obrist, D., Pokharel, A. K. and Moore, C.: Vertical profile measurements of soil air suggest immobilization of gaseous elemental mercury in mineral soil, *Environ. Sci. Technol.*, 48(4), 2242–2252, doi:10.1021/es4048297, 2014.
- Obrist, D., Agnan, Y., Jiskra, M., Olson, C. L., Colegrove, D. P., Hueber, J., Moore, C. W., Sonke, J. E. and Helmig, D.: Tundra uptake of atmospheric elemental mercury drives Arctic mercury pollution, *Nature*, 547(7662), 201–204, doi:10.1038/nature22997, 2017.
- 25 Oechel, W. C., Vourlitis, G. and Hastings, S. J.: Cold season CO₂ emission from arctic soils, *Glob. Biogeochem. Cycles*, 11(2), 163–172, doi:10.1029/96GB03035, 1997.
- Pearson, C., Schumer, R., Trustman, B. D., Rittger, K., Johnson, D. W. and Obrist, D.: Nutrient and mercury deposition and storage in an alpine snowpack of the Sierra Nevada, USA, *Biogeosciences*, 12(12), 3665–3680, doi:10.5194/bg-12-3665-2015, 2015.
- 30 Poulain, A. J., Lalonde, J. D., Amyot, M., Shead, J. A., Raofie, F. and Ariya, P. A.: Redox transformations of mercury in an Arctic snowpack at springtime, *Atmos. Environ.*, 38(39), 6763–6774, doi:10.1016/j.atmosenv.2004.09.013, 2004.
- Schroeder, W. H. and Munthe, J.: Atmospheric mercury—An overview, *Atmos. Environ.*, 32(5), 809–822, doi:10.1016/S1352-2310(97)00293-8, 1998.
- 35 Schroeder, W. H., Anlauf, K. G., Barrie, L. A., Lu, J. Y., Steffen, A., Schneeberger, D. R. and Berg, T.: Arctic springtime depletion of mercury, *Nature*, 394, 331–332, doi:10.1038/28530, 1998.

- Selin, N. E.: Global biogeochemical cycling of mercury: a review, *Annu. Rev. Environ. Resour.*, 34(1), 43–63, doi:10.1146/annurev.enviro.051308.084314, 2009.
- Seok, B., Helmig, D., Williams, M. W., Liptzin, D., Chowanski, K. and Hueber, J.: An automated system for continuous measurements of trace gas fluxes through snow: an evaluation of the gas diffusion method at a subalpine forest site, Niwot Ridge, Colorado, *Biogeochemistry*, 95(1), 95–113, doi:10.1007/s10533-009-9302-3, 2009.
- Shaver, G. R. and Chapin, F. S.: Production: biomass relationships and element cycling in contrasting arctic vegetation types, *Ecol. Monogr.*, 61(1), 1–31, doi:10.2307/1942997, 1991.
- Siegenthaler, U. and Oeschger, H.: Correlation of ^{18}O in precipitation with temperature and altitude, *Nature*, 285(5763), 314–317, doi:10.1038/285314a0, 1980.
- Simpson, W. R., von Glasow, R., Riedel, K., Anderson, P., Ariya, P., Bottenheim, J., Burrows, J., Carpenter, L. J., Frieß, U., Goodsite, M. E., Heard, D., Hutterli, M., Jacobi, H.-W., Kaleschke, L., Neff, B., Plane, J., Platt, U., Richter, A., Roscoe, H., Sander, R., Shepson, P., Sodeau, J., Steffen, A., Wagner, T. and Wolff, E.: Halogens and their role in polar boundary-layer ozone depletion, *Atmos Chem Phys*, 7(16), 4375–4418, doi:10.5194/acp-7-4375-2007, 2007.
- Snyder-Conn, E., Garbarino, J. R., Hoffman, G. L. and Oelkers, A.: Soluble trace elements and total mercury in arctic alaskan snow, *Arctic*, 50(3), 201–215, 1997.
- ~~Sommerfeld, R. A., Massman, W. J., Musselman, R. C. and Mosier, A. R.: Diffusional flux of CO_2 through snow: spatial and temporal variability among alpine subalpine sites, *Glob. Biogeochem. Cycles*, 10(3), 473–482, doi:10.1029/96GB01610, 1996.~~
- Sprovieri, F., Pirrone, N., Ebinghaus, R., Kock, H. and Dommergue, A.: A review of worldwide atmospheric mercury measurements, *Atmospheric Chem. Phys.*, 10(17), 8245–8265, doi:10.5194/acp-10-8245-2010, 2010.
- St. Louis, V. L., Sharp, M. J., Steffen, A., May, A., Barker, J., Kirk, J. L., Kelly, D. J. A., Arnott, S. E., Keatley, B. and Smol, J. P.: Some sources and sinks of monomethyl and inorganic mercury on Ellesmere Island in the Canadian high Arctic, *Environ. Sci. Technol.*, 39(8), 2686–2701, doi:10.1021/es049326o, 2005.
- Steffen, A., Schroeder, W., Bottenheim, J., Narayan, J. and Fuentes, J. D.: Atmospheric mercury concentrations: measurements and profiles near snow and ice surfaces in the Canadian Arctic during Alert 2000, *Atmos. Environ.*, 36(15–16), 2653–2661, doi:10.1016/S1352-2310(02)00112-7, 2002.
- Steffen, A., Douglas, T., Amyot, M., Ariya, P., Aspmo, K., Berg, T., Bottenheim, J., Brooks, S., Cobbett, F., Dastoor, A., Dommergue, A., Ebinghaus, R., Ferrari, C., Gardfeldt, K., Goodsite, M. E., Lean, D., Poulain, A. J., Scherz, C., Skov, H., Sommar, J. and Temme, C.: A synthesis of atmospheric mercury depletion event chemistry in the atmosphere and snow, *Atmos Chem Phys*, 8(6), 1445–1482, doi:10.5194/acp-8-1445-2008, 2008.
- Steffen, A., Bottenheim, J., Cole, A., Douglas, T. A., Ebinghaus, R., Friess, U., Netcheva, S., Nghiem, S., Sihler, H. and Staebler, R.: Atmospheric mercury over sea ice during the OASIS-2009 campaign, *Atmospheric Chem. Phys.*, 13(14), 7007–7021, doi:10.5194/acp-13-7007-2013, 2013.
- Steffen, A., Bottenheim, J., Cole, A., Ebinghaus, R., Lawson, G. and Leaitch, W. R.: Atmospheric mercury speciation and mercury in snow over time at Alert, Canada, *Atmos Chem Phys*, 14(5), 2219–2231, doi:10.5194/acp-14-2219-2014, 2014.

Sturm, M. and Liston, G. E.: The snow cover on lakes of the Arctic Coastal Plain of Alaska, U.S.A., J. Glaciol., 49(166), 370–380, doi:10.3189/172756503781830539, 2003.

Toom-Sauntry, D. and Barrie, L. A.: Chemical composition of snowfall in the high Arctic: 1990–1994, Atmos. Environ., 36(15–16), 2683–2693, doi:10.1016/S1352-2310(02)00115-2, 2002.

- 5 Uematsu, M., Kinoshita, K. and Nojiri, Y.: Scavenging of insoluble particles from the marine atmosphere over the sub-arctic north Pacific, J. Atmospheric Chem., 35(2), 151–163, doi:10.1023/A:1006219028497, 2000.

US EPA: Method 1631: Mercury in water by oxidation, purge and trap, and cold vapor atomic fluorescence spectrometry, United States Environmental Protection Agency., 2002.

- 10 Van Dam, B., Helmig, D., Burkhardt, J. F., Obrist, D. and Oltmans, S. J.: Springtime boundary layer O₃ and GEM depletion at Toolik Lake, Alaska, J. Geophys. Res. Atmospheres, 118(8), 3382–3391, doi:10.1002/jgrd.50213, 2013.

Table 1: Mean concentration ($\mu\text{g L}^{-1}$), including standard deviation (~~italicized~~), of cations and anions in ~~the collected snow precipitation and both~~ tundra and lake snowpack and in surface snow at Toolik Field Station.

location		Mg ²⁺	Ca ²⁺	Na ⁺	K ⁺	Cl ⁻	NH ₄ ⁺	NO ₃ ⁻	SO ₄ ²⁻
tundra	surface	7.2	453.0	112.6	29.4	228.6	11.3	265.0	191.3
		6.8	530.8	104.6	46.7	232.9	3.9	187.5	130.6
	snowpack	32.1	523.5	58.5	60.8	137.5	13.2	202.8	234.0
		34.7	452.1	38.9	102.3	113.1	5.4	104.5	131.8
lake		27.8	784.1	119.1	23.1	117.5	12.8	270.5	181.2
		21.8	403.7	135.9	28.6	73.4	2.9	94.0	78.1

Table 2: Spearman’s coefficient correlations (ρ , in bold if ≥ 0.5 or ≤ -0.5) between chemical elements (dissolved Hg [Hg_{diss}] and major ions) in the tundra snowpack (a) and surface snow over the tundra (b).

a. Tundra snowpack

	Hg_{diss}	Mg^{2+}	Ca^{2+}	Na^+	K^+	Cl^-	NH_4^+	NO_3^-
SO_4^{2-}	-0.16	0.42	0.32	0.39	0.48	0.47	0.58	0.17
NO_3^-	0.07	0.74	0.83	0.55	0.33	0.59	0.03	
NH_4^+	-0.22	-0.04	0.03	0.15	0.35	0.30		
Cl^-	-0.11	0.41	0.39	0.89	0.72			
K^+	-0.10	0.34	0.33	0.70				
Na^+	0.11	0.47	0.38					
Ca^{2+}	-0.07	0.90						
Mg^{2+}	0.06							

b. Surface snow

	Hg_{diss}	Mg^{2+}	Ca^{2+}	Na^+	K^+	Cl^-	NH_4^+	NO_3^-
SO_4^{2-}	-0.08	0.54	0.14	0.16	-0.08	-0.04	0.74	0.74
NO_3^-	0.14	0.62	0.28	0.08	0.07	-0.20	0.57	
NH_4^+	-0.02	0.45	0.24	0.18	-0.08	-0.04		
Cl^-	0.63	0.35	0.69	0.82	0.86			
K^+	0.62	0.45	0.80	0.78				
Na^+	0.30	0.68	0.56					
Ca^{2+}	0.80	0.39						
Mg^{2+}	0.08							

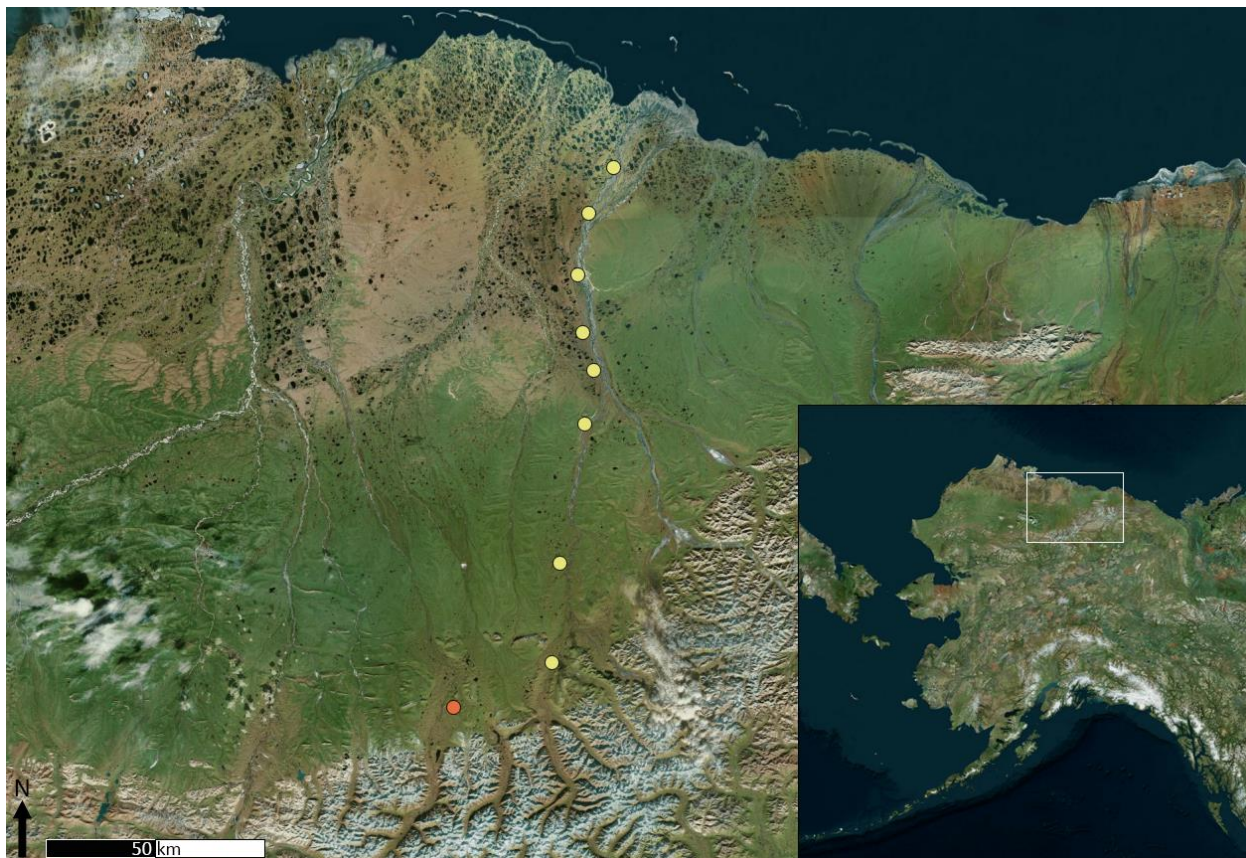


Figure 1: Study area in northern Alaska, including Toolik Field Station (orange bullet point) and the eight transect sites (yellow bullet points). Satellite images are true color images (Earthstar Geographics SIO, 2017).

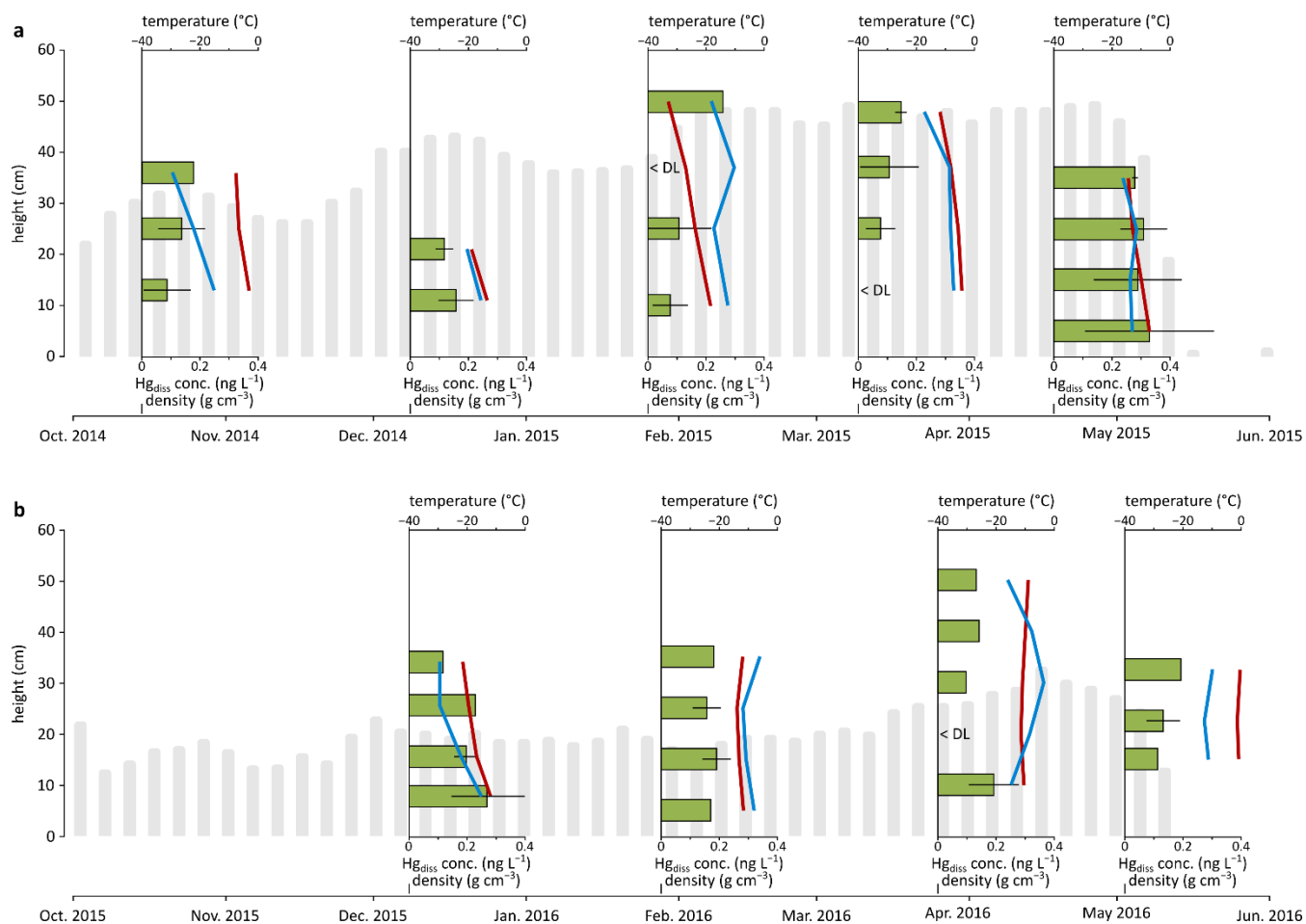


Figure 2: Snowpack temperatures (red lines) and densities (blue lines) and dissolved Hg concentrations (green bars, including mean values and standard deviations) for five snow pits in the 2014–2015 season (a) and four snow pits in the 2015–2016 season (b) over the Arctic tundra at Toolik Field Station. The gray bars illustrate the average snow heights.

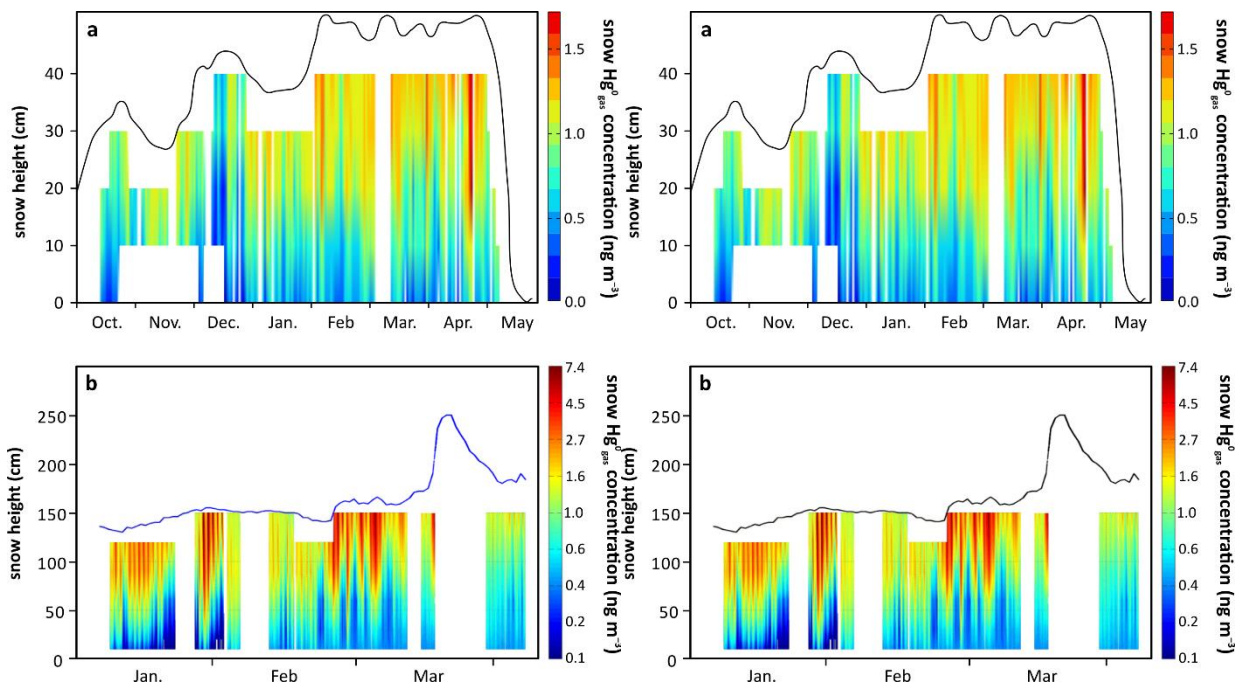


Figure 3: Gaseous Hg^0 concentration profiles in the snowpack interstitial air during the snow-covered season from October 2014 to May 2015 over the Arctic tundra measured at Toolik Field Station based on continuous observations at up to five heights in the snowpack each hour, and interpolation of this data across the entire snowpack (a). For comparison, interpolated Hg^0_{gas} concentration profiles in snowpack interstitial air during the snow-covered season based on similar measurements at Niwot Ridge, Rocky Mountains, Colorado, USA, during the winter of 2009 (b) (adapted with permission; Faïn et al., 2013).

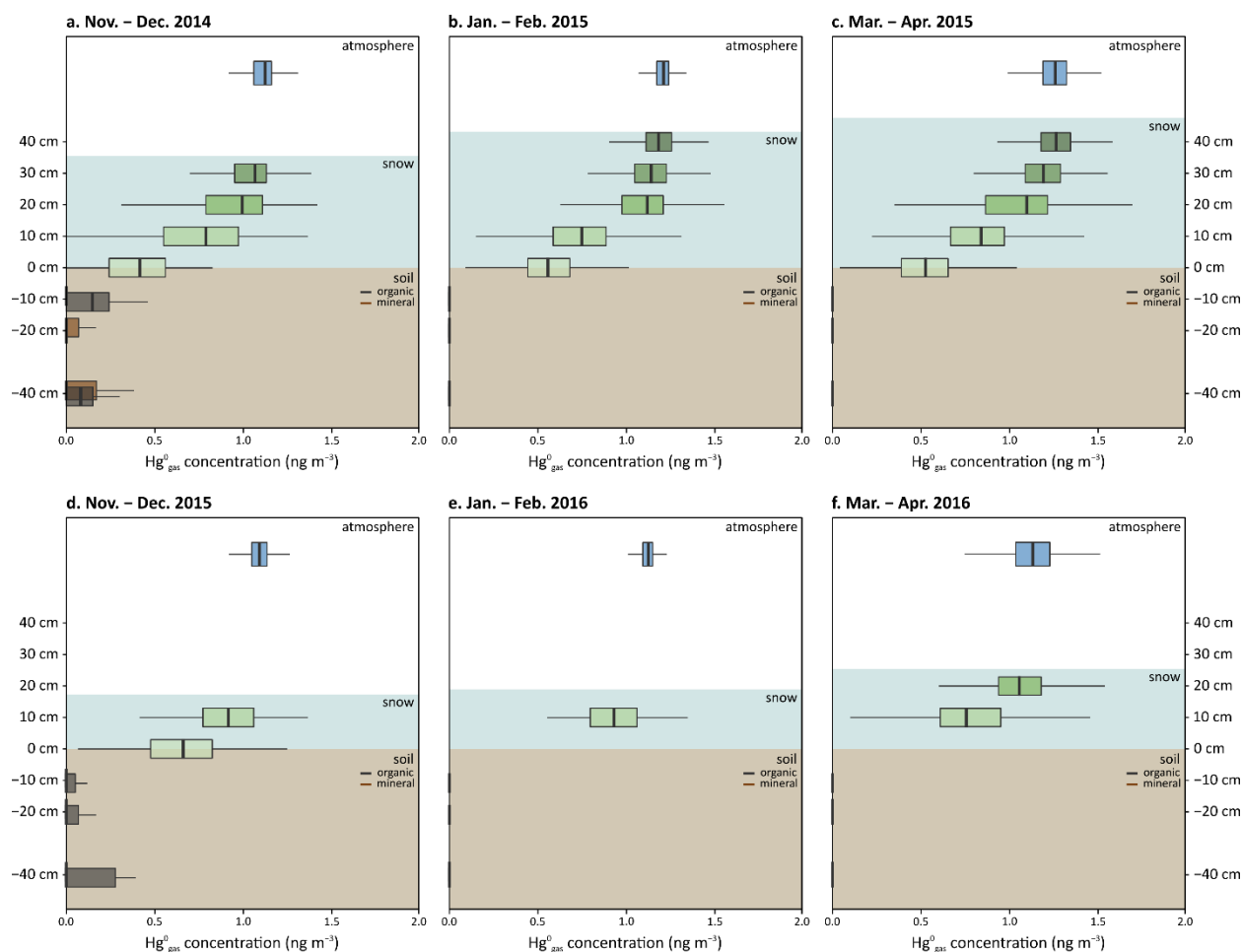


Figure 4: Hg^0_{gas} concentration profiles in the atmosphere, snowpack interstitial air, and soil interstitial air in early winter (from November to December; a and d), in winter (from January to February; b and e), and in early spring (from March to April; c and f) for 2014–2015 (top panels) and 2015–2016 (bottom panels) snow-covered periods over the arctic tundra measured at Toolik Field Station.

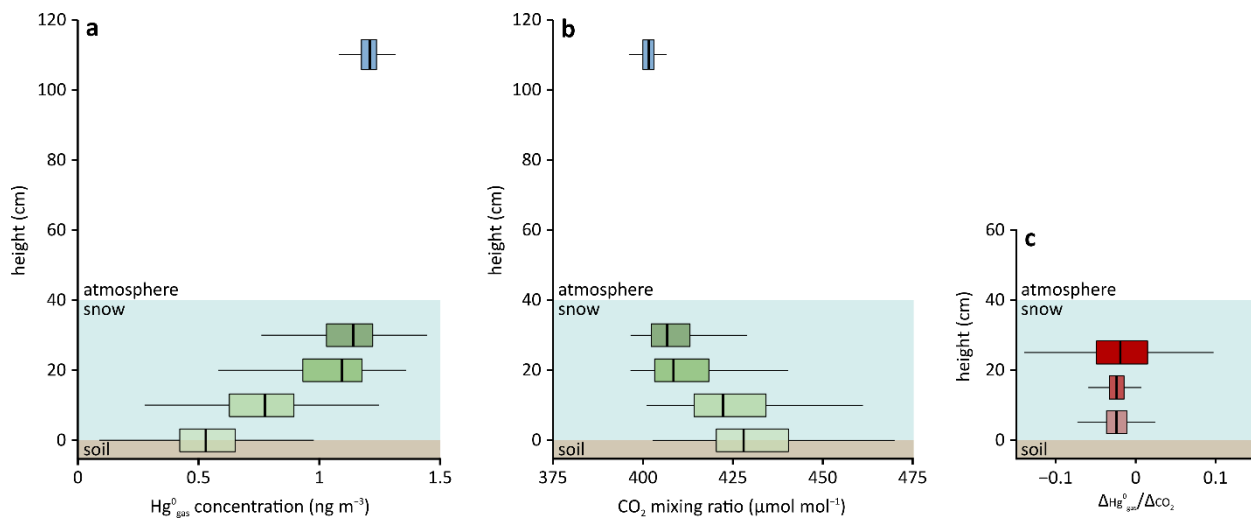


Figure 5: Snow concentration profiles for Hg^0_{gas} (a) and CO_2 (b) concentrations, and $\Delta Hg^0_{gas}/\Delta CO_2$ ratios for 0 to 10 cm, 10 to 20 cm, and 20 to 30 cm snowpack height based on daily averages (c) in January 2015 (snow height averaged 40 cm) over the arctic tundra measured at Toolik Field Station.

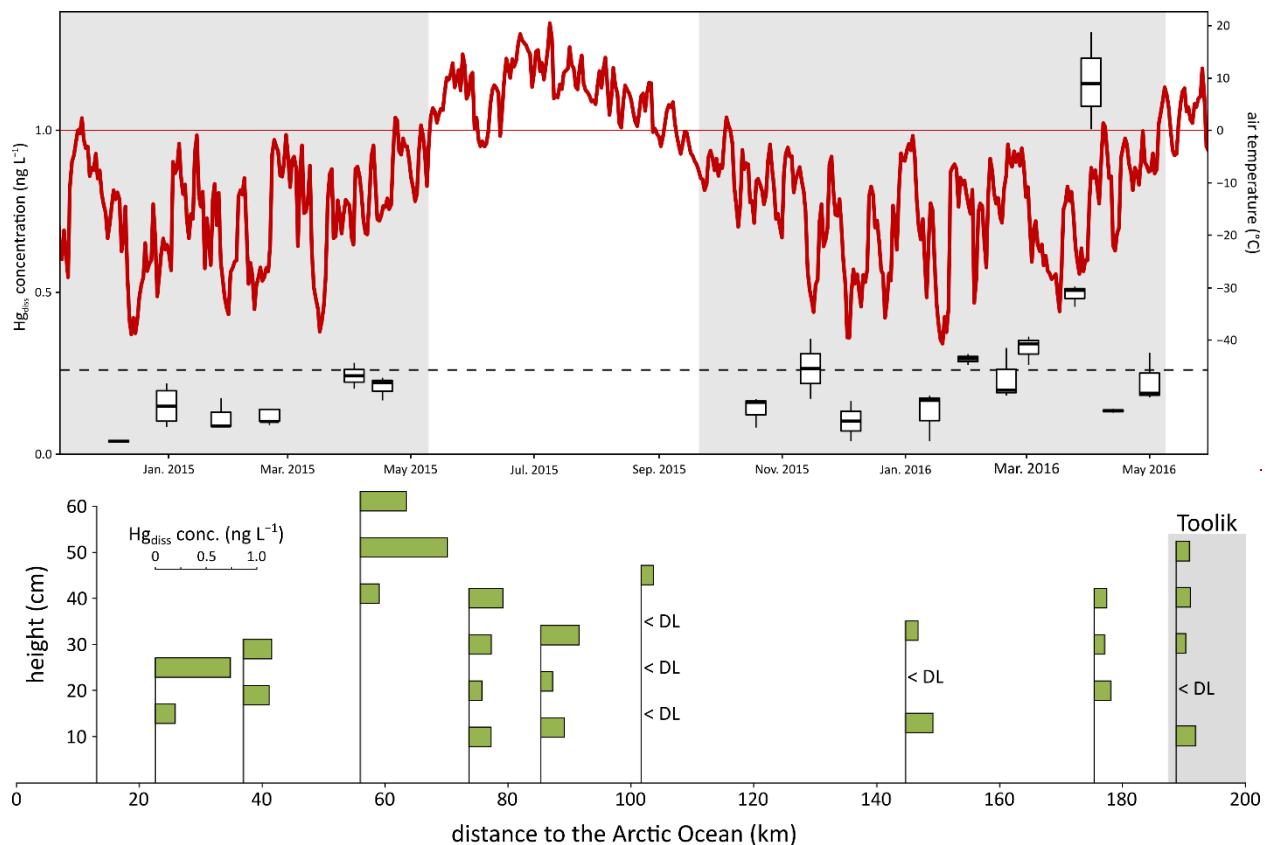


Figure 6: Spatial pattern of dissolved Hg concentrations (Hg_{diss}) in snowpack profiles across the North slope transect on March 27th–28th, 2016, and comparison with Toolik Field Station (gray box) in March 25th, 2016.

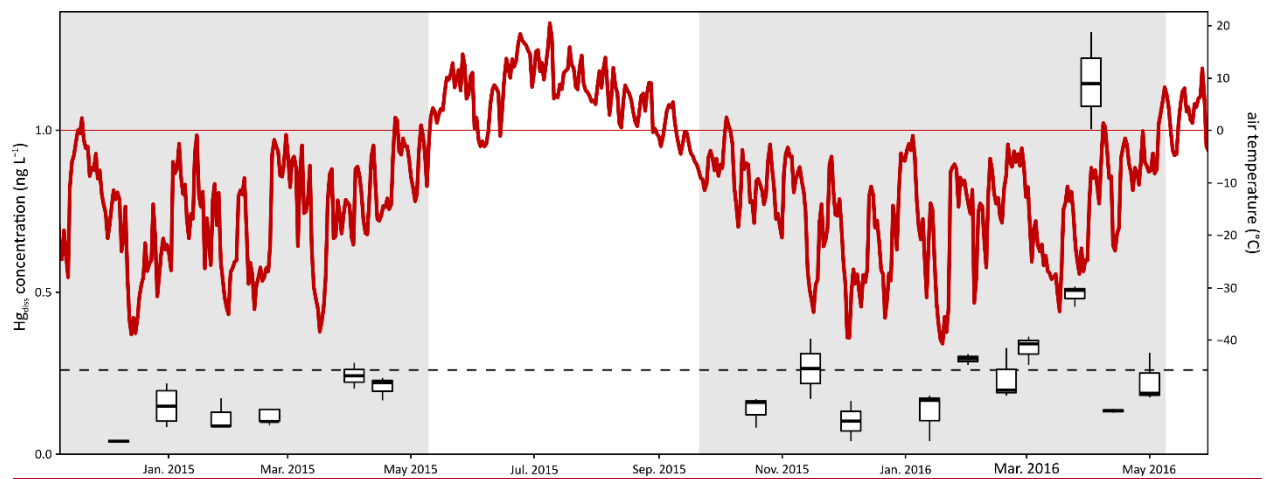


Figure 7: Temporal pattern of dissolved Hg (Hg_{diss}) concentrations in surface snow samples (top 3 cm) throughout the 2014–2015 and 2015–2016 snow-covered seasons (in grey) at Toolik Field Station. The broken line indicates the average surface snow Hg_{diss} concentration (0.26 ng L^{-1}). The red line indicates the daily average air temperature.

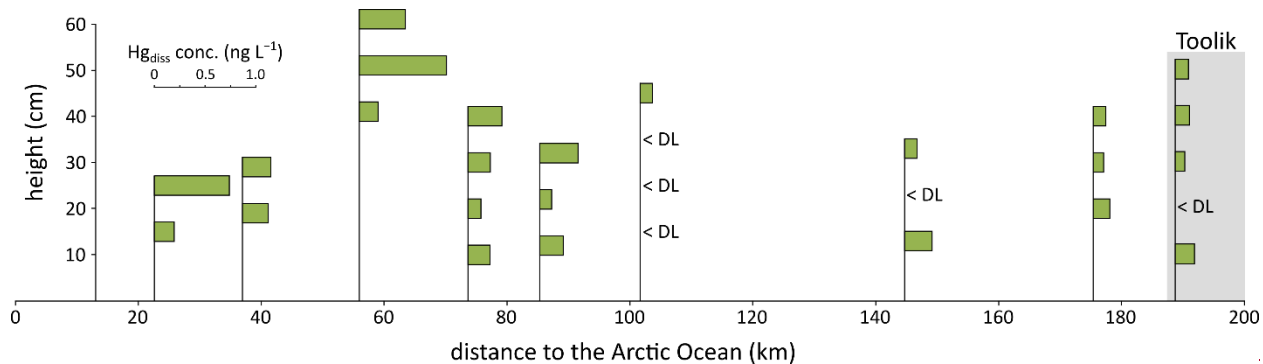


Figure 7: Spatial pattern of dissolved Hg concentrations (Hg_{diss}) in snowpack profiles across the North slope transect on March 27th–28th, 2016, and comparison with Toolik Field Station (gray box) in March 25th, 2016.

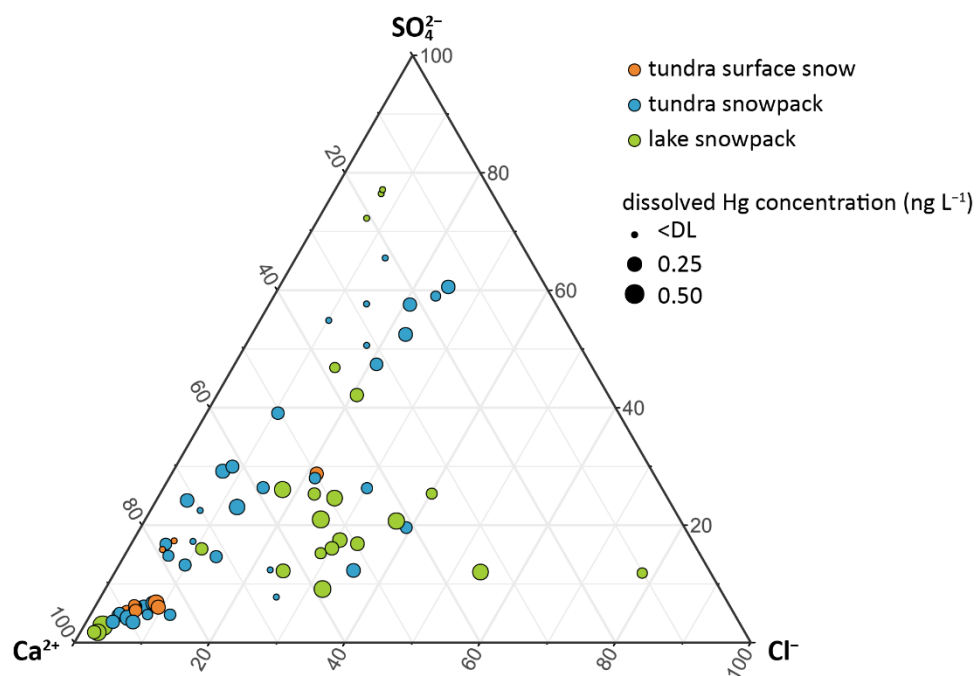


Figure 8: Ternary diagram of tundra surface snow (orange), tundra snowpack (blue), and lake snowpack (green) samples from Toolik Field Station ordered by dissolved Hg concentration between Ca²⁺, Cl⁻, and SO₄²⁻ (proportions based on meq L⁻¹).

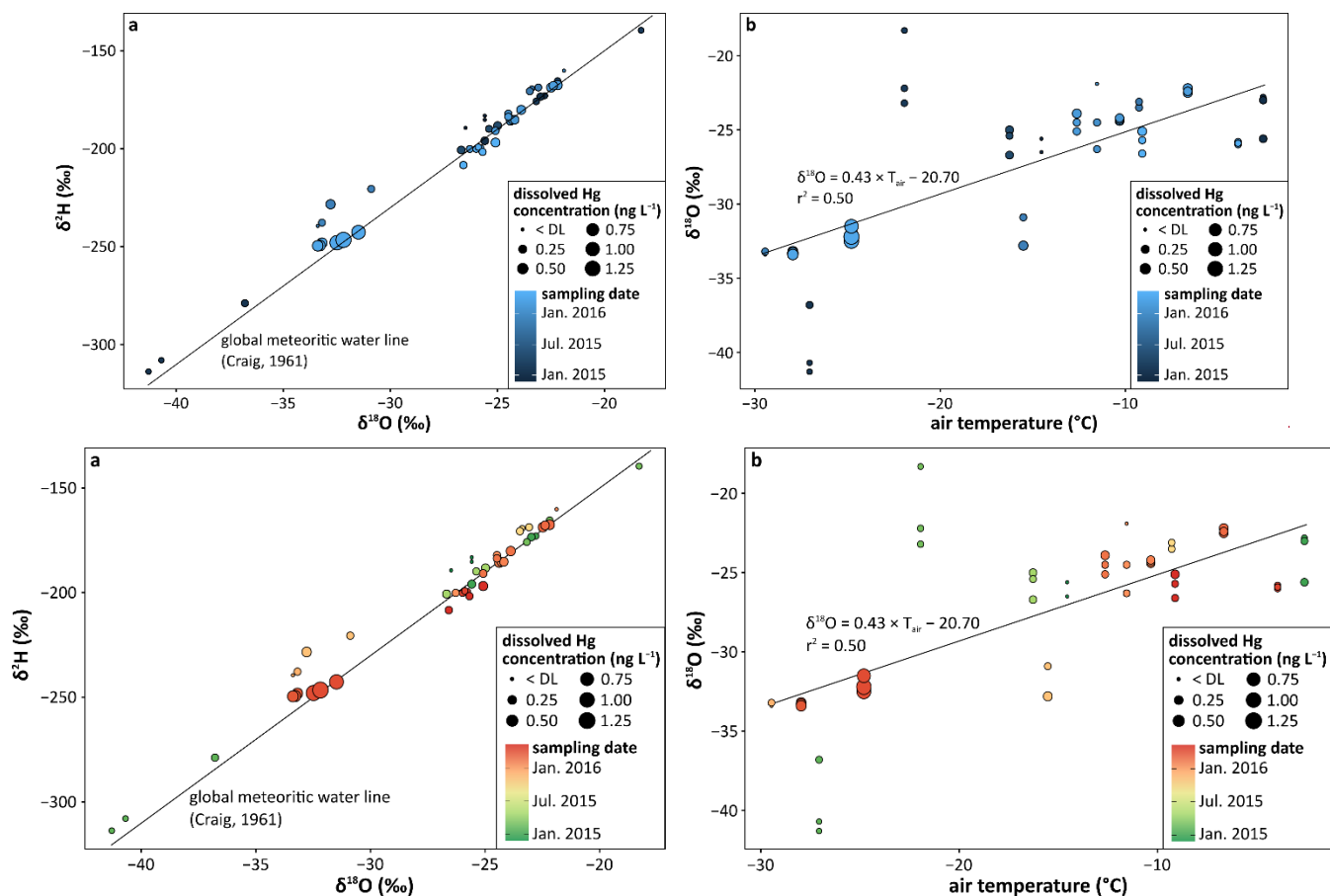


Figure 9: Dissolved Hg concentrations in surface snow samples for 2014 to 2016 in: (a) the $\delta^2\text{H}$ vs $\delta^{18}\text{O}$ diagram and (b) a plot of $\delta^{18}\text{O}$ vs air temperature (T_{air}) during the previous snowfall at Toolik Field Station.